


8-2016

The Impact of Cortical State on Neural Coding and Behavior

Charles Beaman

Follow this and additional works at: http://digitalcommons.library.tmc.edu/utgsbs_dissertations

 Part of the [Cognitive Neuroscience Commons](#), [Computational Neuroscience Commons](#), [Medicine and Health Sciences Commons](#), and the [Systems Neuroscience Commons](#)

Recommended Citation

Beaman, Charles, "The Impact of Cortical State on Neural Coding and Behavior" (2016). *UT GSBS Dissertations and Theses (Open Access)*. 696.

http://digitalcommons.library.tmc.edu/utgsbs_dissertations/696

This Dissertation (PhD) is brought to you for free and open access by the Graduate School of Biomedical Sciences at DigitalCommons@TMC. It has been accepted for inclusion in UT GSBS Dissertations and Theses (Open Access) by an authorized administrator of DigitalCommons@TMC. For more information, please contact laurel.sanders@library.tmc.edu.

THE IMPACT OF CORTICAL STATE ON NEURAL CODING AND BEHAVIOR

by

Charles Bradford Beaman, B.S.M.E.

Approved:

Valentin Dragoi, Ph.D. Advisory Professor

Daniel J. Felleman, Ph.D.

Ruth Heidelberger, M.D., Ph.D.

Harel Shouval, Ph.D.

Caleb Kemere, Ph.D.

Syed Hashmi, M.D., Ph.D.

APPROVED:

Dean, The University of Texas
Graduate School of Biomedical Sciences at Houston

THE IMPACT OF CORTICAL STATE ON NEURAL CODING AND BEHAVIOR

A

DISSERTATION

Presented to the Faculty of
The University of Texas
Health Science Center at Houston
and
The University of Texas
MD Anderson Cancer Center
Graduate School of Biomedical Sciences
in Partial Fulfillment
of the Requirements
for the Degree of

DOCTOR OF PHILOSOPHY

by

Charles Bradford Beaman
Houston, Texas

August, 2016

DEDICATION

~~~

This work is dedicated to my parents,  
who gave me every resource needed to succeed.

~~~

ACKNOWLEDGMENTS

The journey to obtain a doctoral degree in neuroscience cannot be completed in isolation. I wish to thank all the individuals who provided tremendous support to me throughout this process. I would not have made it without them.

First of all, I want to thank my parents. They sacrificed years of their time and energy to prepare me for a life in academia. My father taught me an invaluable, logical approach to problem solving: the ability to break down incredibly complex problems into simple and achievable steps. I use this method every day to probe the mysteries of the brain, likely the most complicated problem known to humankind. My mother prepared me in different, yet equally important, ways. She fostered a creative spirit that is essential to productive scientific exploration. As Albert Einstein once said, “Imagination is more important than knowledge.” I also want to thank my two brothers, Justin and Clark, my sister, Lily, and all of my aunts and uncles, for asking me what I am doing in the lab. I often don’t truly understand a concept until I can explain it clearly to them.

I am extremely grateful for the love and support of my girlfriend, Ashley May. Research can often be a lonely endeavor, but my time spent with her fills any emptiness my brain may contain. She is also, without a doubt, one of the smartest people I have ever met. She pushes me to expand my knowledge into the realms of art, history, and culture, and I am simply a better person with her in my life.

I would also like to thank the members of the Dragoi lab with whom I have shared many stimulating conversations, cups of coffee, lab lunches, and trips to Valhalla. Special thanks to Diego Gutnisky for all of the helpful scientific advice through email. I learned a tremendous amount in our collaboration. He has an uncanny ability to find more analyses that can strengthen an investigation. I want to thank Bryan Hansen

for introducing me to life in a PhD lab. I am grateful to Mircea Chelaru for the stimulating conversations we've had over the years. He helped me think about eastern philosophy, mindfulness, and the importance of maintaining a healthy work/life balance. Thank you Marcello Mulas for welcoming me and making me feel at home in the lab. We played 60+ games of chess over the years and every game was a great challenge! Thank you to Jose Fernandez-Leon for being a good friend and engaging in countless discussions about the resting state of brain. Thank you to Ming Hu for getting me up to speed in visual neuroscience. Thank you to Sorin Pojoga for all of the help in the experiment room. And of course, I want to acknowledge the fellow graduate students who have been there with me the whole time – Ariana Andrei and Neda Shahidi – for the guidance and scientific input along the way. They have helped me become the scientist I am today.

I want to give special thanks to the faculty members that made up my doctoral advisory committee: Drs. Ruth Heidelberger, Daniel Felleman, Harel Shouval, Caleb Kemere, and Syed Hashmi. They pushed me to think critically about my scientific approach. I cherish the rousing debates we had about different methods and techniques to appropriately analyze the data. I understand the pitfalls and limitations of my work much better thanks to this distinguished group. I also want to thank Dr. Behrang Amini for supporting my interest in academic radiology. He let me peer over his shoulder and ask as many questions as I wanted about how radiological diagnoses are made. He also set me up with an interesting clinical project and let me attend intellectually stimulating spine conferences at MD Anderson. In this same vein, I want to thank Dr. Rivka Colen for allowing me to shadow and learn in the neuroradiology suite over the past year. It was an invaluable experience.

I would be remiss to forget to acknowledge the sacrifice made by all of the research animals in our lab. I would have achieved nothing without them. I hope they can swing from the trees some future day in retirement.

I am also grateful for the support of the Vision Training Grant. It supported me financially throughout my time in the PhD program and also allowed me to travel and present my research at several scientific conferences.

Finally, I would like to thank my thesis advisor, Valentin Dragoi. When I entered the lab, I knew very little about the basic mechanisms of neural coding in the brain. The challenge to add worthwhile knowledge to the field seemed overwhelmingly daunting at first. Yet, he fostered my academic growth, helped me find novel questions, and gave me the academic freedom to pursue questions that I found truly interesting.

ABSTRACT

THE IMPACT OF CORTICAL STATE ON NEURAL CODING AND BEHAVIOR

Charles Bradford Beaman, B.S.M.E.

Advisory Professor: Valentin Dragoi, Ph.D.

The brain is never truly silent – up to 80% of its energy budget is expended during ongoing activity in the absence of sensory input. Previous research has shown that sensory neurons are not exclusively influenced by external stimuli but rather reflect interactions between sensory inputs and the ongoing activity of the brain. Yet, whether fluctuations in the state of cortical networks influence sensory coding in neural circuits and the behavior of the animal are unknown. To shed light on this issue, we conducted multi-unit electrophysiology experiments in visual areas V1 and V4 of behaving monkeys. First, we studied the impact of neural population spiking before stimulus presentation on orientation discrimination in the primary visual cortex. We found that when neuronal populations are in a low firing state, they have a higher capacity to discriminate stimulus features despite an overall reduction in evoked responses. Importantly, behavioral performance was significantly improved in the low firing network state. Next, we conducted recordings in the visual cortical area V4 while animals participated in a natural image orientation discrimination task to determine whether fluctuations in local population synchrony during wakefulness play any role in modulating network and behavioral performance. We found that populations of cells exhibit rapid fluctuations in synchrony of ongoing activity ranging from desynchronized responses, indicative of high alertness, to more synchronized responses, indicative of drowsiness. These state fluctuations control the variability in the accuracy of population

coding and behavioral performance across trials in a visual discrimination task. When the local population activity is desynchronized, the correlated variability between neurons is reduced, and network and behavioral performance are improved. Lastly, we controlled the state of cortical networks by manipulating the animal's behavioral state from wakefulness to rest. Thus, we analyzed population recordings from area V4 while the animals participated in an orientation discrimination task, which was immediately followed by a brief resting period of 20-30 minutes, and lastly, by a second task period (Task – Rest – Task). We found that cortical networks were desynchronized after rest such that behavioral performance was improved relative to the pre-rest condition. Altogether, the findings in this thesis demonstrate that the variability in spontaneous cortical activity is not simply noise but rather contains a dynamic structure which controls how incoming sensory information is optimally integrated with ongoing processes to guide network coding and behavior.

TABLE OF CONTENTS

DEDICATION.....	iii
ACKNOWLEDGMENTS	iv
ABSTRACT.....	vii
TABLE OF CONTENTS.....	ix
LIST OF FIGURES	xi
LIST OF ABBREVIATIONS	xiii
CHAPTER I: INTRODUCTION	1
General visual processing and visual area V1	2
Visual area V4	3
Spontaneous cortical activity	5
Synchrony and behavioral state in visual networks	8
Restorative effects of rest.....	9
Goals.....	11
Structure of this dissertation.....	15
CHAPTER II: Spontaneous fluctuations in V1 impact network and behavioral performance.....	16
Introduction	17
Methods	19
Results	23
Discussion.....	45

CHAPTER III: Population synchrony in cortical networks modulates network and behavioral performance	49
Introduction	50
Methods	51
Results	58
Discussion	73
CHAPTER IV: Rest Desynchronizes Cortical Networks and Improves Behavioral Performance	75
Introduction	76
Methods	77
Results	79
Discussion	92
CHAPTER V: Conclusions and Future Directions.....	94
Implications of synchronous fluctuations in V4 impacting behavioral performance ...	96
Control of cortical states	98
Future directions.....	99
REFERENCES	102
VITA.....	132

LIST OF FIGURES

Figure II-1. Experimental setup and firing rate difference by pre-stimulus state.	24
Figure II-2. Neural stability over the recording session.	26
Figure II-3. Distribution of mean firing rates in the low and high pre-stimulus periods for the neurons recorded in the behavioral experiments.	27
Figure II-4. Ongoing activity of individual cells in correlated to the population activity. .	28
Figure II-5. Ongoing activity influences behavioral performance in an orientation discrimination task.	33
Figure II-6. Ongoing activity influences behavioral performance in an orientation discrimination task with fixed delay period.	35
Figure II-7. Ongoing activity influences behavioral performance in an orientation discrimination task for each monkey.	38
Figure II-8. Ongoing activity influences behavioral performance in an orientation discrimination task with random delay period.	38
Figure II-9. Pre-target activity influences behavioral performance.	39
Figure II-10. Fisher linear discriminant (FLD) analysis from an example session.	41
Figure II-11. Population d' analysis and noise correlations.	43
Figure III-1. Trial-by-trial fluctuations in population synchrony in V4.	59
Figure III-2. Additional examples of population activity in desynchronized and synchronized trials.	61
Figure III-3. Cortical state impacts the ability of the population of cells to extract sensory information.	64
Figure III-4. Population synchrony impacts behavioral performance.	66

Figure III-5. Behavioral performance is higher in desynchronized trials for each monkey.	68
Figure III-6. Percent performance difference between desynchronized and synchronized trials using different trial separation criteria.....	69
Figure III-7. Using LFP power to characterize the functional impact of population synchrony.	72
Figure IV-1. Design for rest experiment and orientation discrimination task.	80
Figure IV-2. Single unit and population firing rates in two example time periods.	81
Figure IV-3. LFP Power Ratio and population synchrony rise during rest period.....	82
Figure IV-4. Behavioral performance is improved following rest.	84
Figure IV-5. Population synchrony decreases following rest.....	85
Figure IV-6. Spontaneous firing rates are increased following rest.	86
Figure IV-7. Evoked firing rates in the test period are increased following rest.....	87
Figure IV-8. Spontaneous correlations are decreased following rest.	89
Figure IV-9. Neural discrimination performance is improved following rest.....	91

LIST OF ABBREVIATIONS

V1	Primary Visual Cortex
V2	Secondary Visual Cortex
V4	Extrastriate Visual Cortex Area V4
DP	Dorsal Prelunate Area
FEF	Frontal Eye Field
FST	Fundus of the Superior Temporal Sulcus
LFP	Local Field Potential
LIP	Lateral Intraparietal Area
LGN	Lateral Geniculate Nucleus
MST	Middle Superior Temporal Sulcus
MT	Middle Temporal Area
PIP	Posterior Intraparietal Area
TE	Cytoarchitectonic area TE in anterior temporal cortex
TEO	Cytoarchitectonic area TEO in posterior inferior temporal cortex
VIP	Ventral Intraparietal Area
fMRI	Functional Magnetic Resonance Imaging

CHAPTER I: INTRODUCTION

To gaze is to think.

-Salvador Dalí

General visual processing and visual area V1

The visual system evolved over millions of years to assist in the survival and reproduction of organisms that depend on an effective understanding of the surrounding environment. The essential activities of life – finding food and shelter, avoiding predators, and sexual reproduction – all benefit from an accurate extraction and processing of visual information that comes from light emitted or reflected by objects in the 3-dimensional world¹. This 3-dimensional visual information in the form of light is first converted by the retina in the back of the eyes into 2-dimensional information that is passed to the lateral geniculate nucleus (LGN) and subsequently to the primary visual cortex (visual area V1, located in the calcarine sulcus of the visual cortex). Eventually, all visual information must be reconstructed back into a 3-dimensional representation in real-time (albeit with a small delay on the order of 100's of ms) by the cerebral cortex to create the rich and dynamic visual experience necessary for survival².

In the mid-20th century, Hubel and Wiesel first discovered that the primary visual cortex was organized into approximately 1mm x 1mm hypercolumns responsible for processing orientation stimuli in the brain³⁻⁶. These seminal early findings created a strong interest to elucidate the fundamental mechanisms responsible for orientation tuning in the visual cortex. How could neurons in V1 respond strongly to lines or edges of a particular orientation but not to a perpendicular orientation? A feedforward processing model was initially championed by Hubel and Wiesel and was supported by several different studies. Spike-triggered averaging of simultaneous recordings (a tool meant to characterize the response properties of neurons using spikes caused by time-varying stimuli) from the LGN and V1 demonstrated that ON subfields of simple cells in

V1 are excited by ON-centered LGN relay cells (as well as OFF to OFF)⁷. In addition, groups of LGN cells projecting to an orientation column in V1 (an organized region of neurons that are excited by line stimuli or certain angles) create a simple-like receptive field that is aligned to the V1 column's preferred orientation⁸. Hubel and Wiesel also discovered complex cells (making up to 75% of the cells in V1), which were thought to receive input from several simple cells with similar receptive field orientations but different positions⁶. This feedforward model explains some of the properties of complex cells such as motion-sensitive receptive fields, nonlinear responses, position insensitivity, and large receptive fields². However, a purely feedforward model likely fails to fully account for the complexity of responses in the visual cortex. Observed properties such as cross-orientation suppression and contrast invariance of orientation tuning width have invoked new models relying on lateral inhibition and cortical feedback, but there is still considerable debate on how necessary these mechanisms are to orientation tuning⁹.

Despite the decades of visual research, it is apparent that new studies will be needed to fully understand the fundamental mechanisms underlying orientation selectivity in V1. The contribution of cortical layers, feedback control, and the role of spontaneous activity on orientation tuning (addressed in this thesis) will help us develop a more comprehensive model of stimulus coding in the primary visual cortex.

Visual area V4

The macaque visual area V4 is an extrastriate region located primarily on the prelunate gyrus of the visual cortex (the lunate and superior temporal sulci and parts of

the occipitotemporal gyrus are associated with V4 as well)¹⁰. V4 is a mid-tier cortical area that is strongly associated with color and shape perception¹¹. Anterograde and retrograde tracers have identified that V4 has **feedback** (modulatory) connections to V2 and V3, **intermediate type** connections (not fully feedforward or feedback) to DP, MT, VIP, FEF, and PIP and **feedforward** (driving) connections to LIP, FST, MST, TEO, TE, and TF^{12,13}. Investigations using fMRI have shown that macaque and human V4 are homologous, but more work will be needed to fully understand the neurophysiological comparisons between the two species^{10,14,15}.

V4 is classically associated with object recognition in the ventral processing pathway, and the area is known to encode a diverse set of stimuli including color¹⁶⁻¹⁹, depth²⁰⁻²³, motion^{24,25}, and shape²⁶⁻²⁸. We do not currently understand the complete functional role of area V4, but it has been suggested that the area is essential to figure-ground separation, attentional and contextual modulation, and behavioral performance¹⁰. V4 likely implements low-level visual features such as lines and edges from the primary visual cortex to construct more complicated features associated with object recognition, which are then passed toward decision and emotion areas in the cortex¹⁰.

In my thesis, I focus on the orientation coding of natural stimuli by neurons in V4. Several studies have found prominent orientation selectivity in V4 cells²⁹⁻³³, particularly in the interglob cells^{11,16}, which are interleaved between color-selective glob cells¹⁶. It is likely that orientation domains in V4 do not simply process lines or edges but rather encode higher-order visual features such as polar and hyperbolic gratings, angled contours, and combinations of color and shape^{11,28,34}. In experiments pertaining to

thesis chapters III and IV, we present oriented natural images – containing a wide range of edges and contours – in order to elicit robust neural responses in V4.

Spontaneous cortical activity

Spontaneous cortical activity is defined as the firing of neurons in the cerebral cortex in the absence of any external sensory input. In the 20th century, the canon in neuroscience was to label seemingly random spikes of spontaneous activity as “noise” in the brain, devoid of any significance. In this paradigm, the evoked spikes that arrive from the retina, via the LGN, are added to the noisy spontaneous spikes of the visual cortex, and then the higher regions of the cerebral cortex must decode the true signal from the noise³⁵. However, in the past 10-15 years, neuroscientists have begun to realize that the ongoing activity in the brain cannot be dismissed so easily. In the primary visual cortex, only 5-10% of excitatory synaptic input to layer 4 comes from feed-forward thalamic signals. A small portion of synaptic input arises from long-range feedback inputs, but the vast majority of cortical synapses originate from sources within the local network^{36,37}. This suggests that intracortical circuitry may play a dominant role in how external stimuli are processed.

The first major finding that challenged the previous dogma was that spontaneous cortical activity is highly structured in space and time³⁸. Using a diversity of recording tools – voltage-sensitive dyes^{39,40}, two-photon calcium imaging⁴¹, multi-electrode arrays⁴², and fMRI⁴³⁻⁴⁵ – researchers observed that spontaneous neural activity is correlated across regions of cortex and on different timescales^{46,47}. Further efforts demonstrated that spontaneous firing rates of individual cells were correlated to firing rates of the local network⁴⁸. In addition, the level of variability in spontaneous

firing rates was found to be similar in magnitude to the variability of evoked responses to high-contrast visual stimuli⁴⁹. The importance of spontaneous neural activity was further strengthened by the unexpected finding that orientation maps exist even in the absence of external stimulation⁵⁰. Each of these findings support the notion that ongoing activity is not simply “noise,” but rather reflects the underlying structural organization of the brain⁵¹⁻⁵⁴.

The structure of ongoing neural activity is clearly important; however, a critical question remains: does spontaneous cortical activity functionally impact cortical processing? There are two proposed models by which the brain could operate in regards to spontaneous activity. In one scenario, the spikes created by external visual stimulation functionally erase the spontaneous spikes in the visual cortex to create an entirely new representation of the visual world⁵⁵. In the alternative model, feed-forward spiking from external stimuli *modulates* a highly organized spontaneous network, which updates an existing representation of the visual world that is continually reverberating in the ongoing cortical activity^{38,56}. Recent research has overwhelmingly supported the latter hypothesis. A seminal study by Arieli et al.⁵⁷ demonstrated that the variability of evoked responses to repeated stimuli could largely be explained by the fluctuations of ongoing activity prior to the stimulation. Further evidence comes from the finding that evoked response patterns of the cerebral cortex are similar to firing patterns of the spontaneous network^{51,58}. Importantly, it was found that the strength of incoming stimuli guides the interaction between ongoing and evoked neural activity. With high contrast stimuli, feed-forward thalamic drive dominates neural activity in the visual cortex, and conversely, with low contrast stimuli, the structure of feedback and locally controlled spontaneous activity plays the dominant role^{36,59}.

This collection of evidence clearly supports a pivotal role for spontaneous cortical activity in stimulus processing, but what factors modulate the baseline activity in the brain? The main synaptic input to the visual cortex, apart from feed-forward LGN signals, arises from feedback control from higher cortical regions to the superficial and deep layers of the cortex. Several studies have reported that cognitive factors such as attention and expectation of task-related stimuli can modulate ongoing firing rates by top-down control⁶⁰⁻⁶². Importantly, this modulation of ongoing firing rates may be critically important for behavioral performance. A study by Super et al. demonstrated that increased spontaneous firing rates and correlations in the primary visual cortex of macaques prior to stimulus presentation resulted in improved performance on a figure-ground detection task⁶³. However, it is currently unclear if this finding was detection task-specific or representative of a more general feature in cortical processing. Indeed, a previous study conducted in our lab suggests the former⁶⁴. We found that when neurons in a low firing state immediately preceding a stimulus, the cortical network has a greater capacity to discriminate between disparate orientation stimuli. That is, in the low pre-stimulus firing state, the tuning of orientation stimuli was non-linearly sharpened compared to the high pre-stimulus firing state⁶⁴. These findings suggest that the level of ongoing activity before stimulus presentation may ultimately be important for the discrimination performance of the animal. We will directly test this hypothesis in chapter II.

Synchrony and behavioral state in visual networks

Behavioral state varies along a continuum ranging from a highly synchronized state in slow-wave sleep or deep anesthesia to a highly desynchronized state in the alert and actively behaving animal^{65,66}. In sleep or anesthesia, cortical networks fluctuate between periods of generalized population firing (“on periods” or “up periods”) and periods of generalized silence (“off periods” or “down periods”)^{67,68}. The cyclical on and off periods generate large amplitude synchronous waves of electrical activity oscillating at frequencies between 0.5 and 4 Hz, called Delta waves, that can be observed on EEG⁶⁹. Along with Delta waves, sleeping animals experience reduced muscle tone and rolling eye movements⁷⁰. As an animal wakes up from sleep or anesthesia, the amplitude of Delta waves diminish, muscle tone increases, eye movements become behaviorally relevant, and the cortex becomes more desynchronized^{70,71}.

However, cortical state does not simply exist in bimodal form (synchronized vs. desynchronized), but rather varies continuously, even within the waking state. In alert and behaving animals, neural firing is highly desynchronized, but in quiescent and awake animals, neural firing fluctuates in synchronous oscillations^{51,72-75}. It should also be noted that the oscillations in awake animals are much less regular than those observed during deep sleep or anesthesia. The amplitude and frequency of the up and down periods change erratically over time⁷¹.

Two clear questions emerge from these findings: 1) Do synchronous oscillations significantly impact neural coding properties? 2) Do these oscillations impact behavioral performance? The answer to the first question has been shown to be a decisive **‘yes’**

in research conducted on a wide range of **anesthetized** animals. Firing rates, single unit variability and correlated variability have all been shown to be affected by synchronous fluctuations^{51,71,73,76-78}. However, much less is known about how synchronous fluctuations might impact neural coding in the awake state and even less is known about their impact on behavioral performance. In chapters III and IV, I will attempt to thoroughly address these questions for the first time.

Restorative effects of rest

Rest is known to play a critical role in information processing and learning in the brain. Previous work has shown that humans demonstrate improvements in learning, memory, and perceptual performance following short daytime naps ranging from 10 to 90 minutes⁷⁹⁻⁸⁵. In two separate studies, human subjects increased their performance on declarative memory tasks following naps as short as 6 minutes^{86,87}. In addition, human subjects who experienced short periods of light sleep (stages 1 and 2) increased their performance on visual discrimination tasks when compared to non-resting control subjects^{80,81}, further demonstrating the efficacy of light sleep to improve behavioral performance.

Sleep research in animals has the potential to elucidate the neural mechanisms contributing to improved performance following rest. Yet, an important limitation in previous rodent research is the paucity of appropriate sleep staging. In human studies, it is customary to divide NREM sleep into light sleep (stages 1 and 2) and slow wave sleep (stages 3 and 4). However, in rodent work, the term “slow wave sleep” is commonly used to describe all of NREM sleep⁸⁸. Moreover, rodents are primarily

nocturnal and experience polyphasic, fragmented daytime sleep^{89,90}, making useful comparisons to human sleep stages difficult. In this regard, non-human primates have the potential to fill the gap between rodent and human investigations of sleep and behavioral performance. The rhesus monkey (*Macaca mulatta*), in particular, is known to have consolidated nighttime sleep and exhibit daytime napping with human-like sleep stages, making it an ideal animal model to study the effects of resting periods on performance^{91,92}.

It is likely simplistic to say that stages 3-4 are “better” than stages 1-2, or vice versa. Most experts theorize that the separate stages of sleep accomplish different goals for the brain. For example, stages 1-2 are likely more important for active memory consolidation. Sleep spindles (prominent in stages 1-2) are oscillations in the thalamocortical network that increase following learning sessions compared to baseline and are thought to be critical for active memory consolidation^{93,94}. In addition, sharp wave ripples (also more prominent in stages 1-2) are large bursts of hippocampal activity thought to be important for bidirectional information transfer between the cortex and hippocampus during sleep, likely needed for active consolidation of memories^{88,95}. Recent work demonstrated that disrupting slow wave sleep (stages 3-4) and REM sleep, while preserving light sleep, did not impair memory performance in a word-pair learning task, providing further evidence that stage 2 sharp wave ripples and sleep spindles might play a primary role in declarative memory⁹⁶. Functional magnetic resonance imaging and intracranial electroencephalography studies have demonstrated that corticocortical connectivity decreases as humans transition from stages 1-2 to stages 3-4 of sleep (as measured by coherence in LFP signals)⁹⁷⁻⁹⁹. Increased global connectivity in lighter stages of sleep has been proposed to further

promote reorganization of memory traces through the cortex and hippocampus to improve declarative memory⁸⁸. Alternatively, the disconnected networks in stages 3-4 of sleep may be necessary for important homeostatic mechanisms such as synaptic downscaling^{100,101}. In this hypothesis, slow wave sleep renormalizes synaptic weights to enable efficient neural encoding following sleep. Indeed, suppression of stage 3-4 sleep has been shown to negatively affect learning and memory performance^{102,103}, and the amount of stage 3-4 sleep in humans correlated positively with memory performance on a face-location association task¹⁰⁴.

From this previous research, it is clear that short periods of rest have the potential to enhance perceptual performance and the underlying function of cortical networks. In chapter IV, I test the ability of monkeys to improve neural and behavioral discrimination performance following short naps of 20-30 minutes.

Goals

Until recently, our understanding of neural coding in the brain has been driven by the study of evoked spiking activity in sensory networks. However, the role of spontaneous neural activity, which consumes up to 80% of the energy of the brain, has often been overlooked^{105,106}. Several research groups have identified that the brain can fluctuate between a continuous range of cortical states that have the potential to impact neural coding and behavior^{73,76,107}. It has also been demonstrated that responses of sensory neurons are not exclusively influenced by sensory inputs but rather reflect interactions between external stimuli and the ongoing activity of the brain⁵⁷; yet, we still

know very little about how spontaneous cortical activity influences population coding and perceptual performance of behaving animals.

The insertion of multiple recording electrodes into the visual cortex allows for high temporal and spatial resolution investigations of network interactions in cortical circuits. We record in the receptive fields of neurons in the visual cortex that correspond to stimuli presented on a computer screen in behaving animals. In this way, we can relate neural activity of small populations of cells (approximately 10-20 neurons) to perceptual performance on a trial-by-trial basis.

My research seeks use these tools to elucidate the impact of spontaneous neural activity on information processing in the visual cortex areas V1 and V4 and behavioral performance of monkeys (*Macaca mullata*). Orientation discrimination tasks of gratings and natural stimuli will be used to determine: **whether and how the state of cortical networks before stimulus presentation, as measured by level of spontaneous activity and population synchrony, influences the ability of neurons to encode incoming orientation stimuli; whether and how behavioral performance of the animals is affected by spontaneous neural activity; and whether a period of rest can desynchronize the cortical state and improve neural coding and behavioral performance.** To test these hypotheses, the following specific aims will be implemented:

Specific Aim 1: To determine the impact of pre-stimulus spontaneous neural activity on neural coding and behavior in primary visual area V1: Little is known about whether and how pre-stimulus firing rates impact network coding and perceptual performance in behaving animals. To address this, I analyze two

large data sets recorded in the macaque primary visual cortex V1 while the animals undergo an orientation discrimination task of sinusoidal gratings. **Our hypothesis is that the distribution of ongoing states of a network of cells can shape the accuracy of population coding and impact the behavioral performance of the monkey.** Specifically, we expect that when neuronal populations are in a 'low' pre-stimulus state, they will have a higher capacity to discriminate stimulus features, such as orientation, despite their overall reduction in evoked response. In addition, we expect that behavioral performance will be improved in the low pre-stimulus state.

Specific Aim 2: To determine the impact of trial-by-trial synchronous state on neural coding accuracy and behavior in visual area V4: Synchronous waves of spontaneous activity are known to exist during rest and during anesthesia. Whether fluctuations in local population synchrony during wakefulness play any role in modulating the accuracy of sensory encoding and behavioral performance is currently unknown. I analyze two data sets in V4 to determine if synchronous neural activity impacts neural coding and perceptual performance in awake, behaving monkeys. **Our hypothesis is that local state fluctuations in the awake animal can control trial-by-trial variability in the accuracy of population coding and behavioral performance across trials in a visual discrimination task.** Specifically, we expect that when the local population activity is desynchronized, the correlated variability between neurons will be reduced, and the network and behavioral performance will be enhanced.

Specific Aim 3: To determine the impact of brief resting periods on the synchronous state of the brain, neural coding, and behavior in visual area V4:

Brief resting periods have been shown to improve perceptual performance in animals, but little is known about their impact on population synchrony and neural coding. I analyze two data sets recorded in V4 while monkeys participate in a natural image orientation task. The animals are then allowed to rest for 20-30 minute periods, before undergoing a second task period. **Our hypothesis is that a short resting period will desynchronize neural networks and lead to improved behavioral performance in subsequent tasks.**

Structure of this dissertation

This dissertation is organized into 5 chapters:

Chapter I (current chapter) provides an introduction to spontaneous neural activity in the visual cortex, as well as the research hypothesis and specific aims implemented to address my hypothesis.

Chapter II focuses on experimental findings related to fluctuations of pre-stimulus cortical activity in visual area V1 and their impact on neural coding and behavior.

Chapter III focuses on experimental findings related to fluctuations in population synchrony in visual area V4 and their impact on neural coding and behavior.

Chapter IV provides the results of my research related to rest, neural synchrony, and behavioral performance based on recordings from visual area V4.

Chapter V provides a summary and general conclusions of the dissertation research. In addition, a discussion is provided on future research directions.

CHAPTER II: Spontaneous fluctuations in V1 impact network and behavioral performance

Introduction

Note: This chapter is based upon: Gutnisky D*, Beaman CB*, Lew S, and Dragoi V. Optimal network states for perceptual discrimination. *denotes equal contribution. This manuscript is in preparation for submission (Gutnisky and Dragoi recorded the data. I conducted the analysis.).

Despite the fact that spontaneous activity consumes more than 80% of the energy budget of the brain, its function remains a long-standing mystery in neuroscience^{106,108}. Indeed, most systems neuroscience studies focus on examining task-related changes in neuronal activity, thus ignoring the component that consumes most of the brain's energy: spontaneous activity. However, it is well known that waves of ongoing population activity continuously sweep across the cortex in various directions to potentially influence stimulus coding and behavioral performance. Research in recent years has shown that correlated spontaneous activity can change the state of neuronal populations involved in stimulus processing to impact behavioral performance. Yet, most of these investigations have been conducted using electroencephalogram (EEG), magnetoencephalogram (MEG), and fMRI techniques in humans^{63,109-121}. The definition of population activity includes the aggregate activity of millions of cells of a wide diversity of stimulus tuning and coding properties, possibly including subthreshold activity, with heterogeneous contributions from local and long-range circuits. In addition, a separate series of investigations has been conducted to elucidate the single cellular and population mechanisms contributing to spontaneous neural activity^{74,76,78,122-126}. These studies have collectively demonstrated that ongoing activity can fluctuate rapidly in time to impact neural coding. Despite the clear

importance of this previous work, the relationship between single neuron and network spontaneous activity with behavioral performance continues to remain elusive.

Intracellular studies have shown that the membrane potential can dynamically change to produce fluctuations in spontaneous activity to adaptively enhance neurons' sensitivity to synchronous inputs while decreasing the sensitivity to temporally uncorrelated inputs¹²⁷. In addition, theoretical and experimental evidence has shown that increasing the background synaptic input and neuronal conductance can decrease the response gain of *in vitro* and model neurons, without changing the variability of membrane potential fluctuations and spike responses¹²⁸. More recent work has demonstrated that individual cells can rapidly shift between various states of excitability to influence stimulus processing, raising the possibility that the state of neuronal populations in cerebral cortex can fluctuate rapidly to influence sensory coding and possibly behavior^{48,53,57,105,122,123,129}. In previous research from our group⁶⁴, we found that ongoing neural activity in fixating animals can modulate stimulus coding at the network level in a non-linear manner. We demonstrated that when neurons are in a *low* firing pre-stimulus state, they have a greater capacity to discriminate orientation stimuli. Nevertheless, it is still unclear whether and how ongoing activity impacts neural coding of large networks of cells in a behaving animal.

To determine if *low* cortical activity preceding stimulus onset leads to improved neural and behavioral performance, we recorded multiple single-units in primary visual cortex of awake, behaving monkeys. Specifically, we examined the effects of pre-stimulus activity on neural coding of orientation responses in the primary visual cortex (V1). Briefly, we tested the relationship between the ongoing activity before stimulus

presentation, the population response, and behavioral performance in an orientation discrimination task. Our goal was to determine if ongoing activity of nearby neurons influences the ability of cortical networks to process orientation signals. In summary, we demonstrate that the level of cortical activity across a network of cells impacts both neuronal and behavioral performance.

Methods

Behavioral Experiments:

All experiments in this manuscript were conducted in accordance with protocols approved by the National Institutes of Health and the Institutional Animal Care and Use Committee at The University of Texas Health Science Center at Houston. Three male monkeys (*Macaca mulatta*) were trained in a fixed delayed-match-to-sample task in which they had to indicate whether the orientation of two successively presented 4 deg circular sine-wave gratings had the same or different orientation. A fourth monkey was also trained in the randomized delay experiment. In the fixed-delay task, after the monkeys maintained fixation for 100 ms, a target stimulus was flashed for 400 ms. The possible target orientations ranged from 0 to 135° in 45° intervals. During a delay of 1050 ms the screen remained blank and monkeys maintained fixation. In half of the trials, the test stimulus had the same orientation as the target ('match' condition). In the other half of the trials, the target stimulus was randomly chosen within $\pm 5^\circ$ or $\pm 10^\circ$ of the target ('non-match' condition) and flashed for 200-400 ms. In the randomized delay task, the stimulus expectation effect is diminished (delay was randomized between 250-750 ms). We also increased the length of the fixation period to 400ms to be able to compare the effects of the pre-target response state in the behavioral performance

(Fig. 3E and Fig. 9). All analyses were performed by dividing trials into two groups, low spiking and high spiking ongoing activity trials, contingent on whether the neuronal activity during the pre-stimulus period (200 ms) was above or below the median pre-stimulus firing rate (this enables analysis on an equal number of trials in the two categories). For all of the recorded neurons, we determined the pre-stimulus activity and evoked response magnitude. In addition, we computed the change in performance on a session-by-session basis to eliminate potential bias. The number of possible combinations of subpopulation of size 1 to n for each session increases with the growth rate of a factorial function. As population size increases (e.g., $n=13$), sessions with larger numbers of cells would bias the results as they would weigh more into the pooled results. For this reason, we decided to average our results across sessions, and hence prevent the bias from individual sessions.

In all monkey experiments, eye position was monitored using an infrared eye tracking system operating at 1KHz (Eyelink Inc.). We examined whether pre-stimulus states are associated with changes in the quality of fixation (standard deviation of eye position, eye movement velocity, etc.) on the vertical and horizontal axes during the pre-stimulus interval, but found that eye movements were not statistically different in the low and high pre-stimulus states ($P > 0.1$, paired t-test). We examined whether correct and incorrect behavioral responses were associated with changes in eye movements, but failed to detect a significant relationship ($P > 0.1$, Wilcoxon signed-rank test, by comparing the standard deviation of horizontal and vertical eye movements for correct and incorrect responses).

Electrophysiological recordings:

All experiments were conducted by Sorin Pojoga and Valentin Dragoi using a combination of in-house or Crist-grid electrode arrays (up to 6 electrodes) and laminar electrodes (Plextrode® U-Probe, Plexon Inc) with 16 equally spaced contacts (100 μm inter-contact spacing). They recorded at cortical depths between 200 and 400 μm (monkey V1) with the electrode grid and from all depths with the linear electrode array. They recorded cells with orientation preferences spanning the entire orientation range (between 0-180°). Stimulus presentation was controlled by the Experimental Control Module (ECM, FHC Inc.). Neuronal and behavioral events were recorded using the Plexon system (Plexon Inc.).

Real-time neuronal signals were amplified, recorded, and stored digitally with Multichannel Acquisition Processor system (MAP, Plexon Inc) at a sampling rate of 40Khz. Units were identified by visual inspection in an oscilloscope and also listened to through a speaker. Waveforms that crossed a user-specified threshold (typically ~4sd of the noise) were stored for further offline analyses. The spike waveforms were manually sorted using Plexon's offline sorter software (with waveform clustering using parameters such as principle component analysis, spike amplitude, timing, width, valley and peak).

Pearson correlation:

The Pearson correlation $R(x,y)$ of two time series $x(n)$, $y(n)$, $n = 1,2,\dots,N$ is given by:

$$R(x, y) = \frac{\sum_{n=1}^N [x(n) - \bar{x}][y(n) - \bar{y}]}{\sigma_x \sigma_y} ;$$

where \bar{x} and \bar{y} are the means of x and y , respectively, and σ_x and σ_y are the standard deviations of x and y , respectively. We used the MATLAB function *corrcoef* to compute the Pearson correlation.

Fisher linear discriminant analysis:

Fisher linear discriminant (FLD) is a method to reduce the dimensionality of the data and to assess the neural classification performance in the low and high pre-stimulus conditions. We calculated the most discriminant dimension w^* as:

$$w^* = S_w^{-1}(u_1 - u_2)$$

where u_1 and u_2 represent the mean vectors of spikes for all cells in the target and test condition, respectively. S_w^{-1} represents the inverse of the total scatter matrix defined by:

$$S_w^{-1} = (S_1 + S_2)^{-1}$$

Where S_1 and S_2 represent the scatter matrices for target and test, respectively.

$$S_1 = (n - 1) * cov(x_1) \quad \text{and} \quad S_2 = (n - 1) * cov(x_2)$$

x_1 and x_2 represent the matrices of spikes for the target and test stimuli, respectively.

This analysis allowed us to find the optimal line direction w^* on which to project our data. We then plotted histograms in this dimension and fit a normal distribution using the *fitdist* function in MATLAB. To compute the “difference in FLD means” in Fig. 5D, we calculated the difference between the means in the fitted distributions. To compute the “FLD pooled σ ”, we calculated the square root of the average variance of the fitted distributions.

The discriminability between two multivariate distributions using the FLD weight vector can be quantified with the multivariate generalization of d^2 ^{35,130,131} given by:

$$d^2 = \Delta\mu^T Q^{-1} \Delta\mu;$$

Where $\Delta\mu$ is the vector difference in mean responses between the target and test orientation and Q is the pooled covariance matrix. Probability of correct classification (“With correlations”) is given by:

$$\text{erfc}(-\sqrt{d^2})/2$$

“Without correlations” represents the probability of correct classification while ignoring the effect of noise correlations using:

$$d_{shuffled}^2 = \Delta\mu^T Q_d^{-1} \Delta\mu$$

where Q_d is the diagonal covariance matrix obtained by zeroing the off-diagonal elements corresponding to correlations between neurons. The quantity measures the information in a dataset of uncorrelated neural response and can be smaller or larger than d^2 ³⁵.

Results

We performed multiple-electrode recordings in primary visual cortex (V1) of behaving monkeys using custom-made electrode grids and linear arrays (U-Probe¹³²). To test whether pre-stimulus fluctuations in ongoing activity are functionally significant for behavior, monkeys were trained to discriminate the orientation of sinusoidal gratings by deciding whether two successive stimuli (target and test) had the same or different orientations (Fig. 1A). After the monkey maintained fixation for 100 ms, a target stimulus was flashed for 400 ms and was followed, after a 1050 ms delay, by a test

stimulus of random orientation (within 5° or 10° of the target), which was briefly flashed for 200-400 ms.

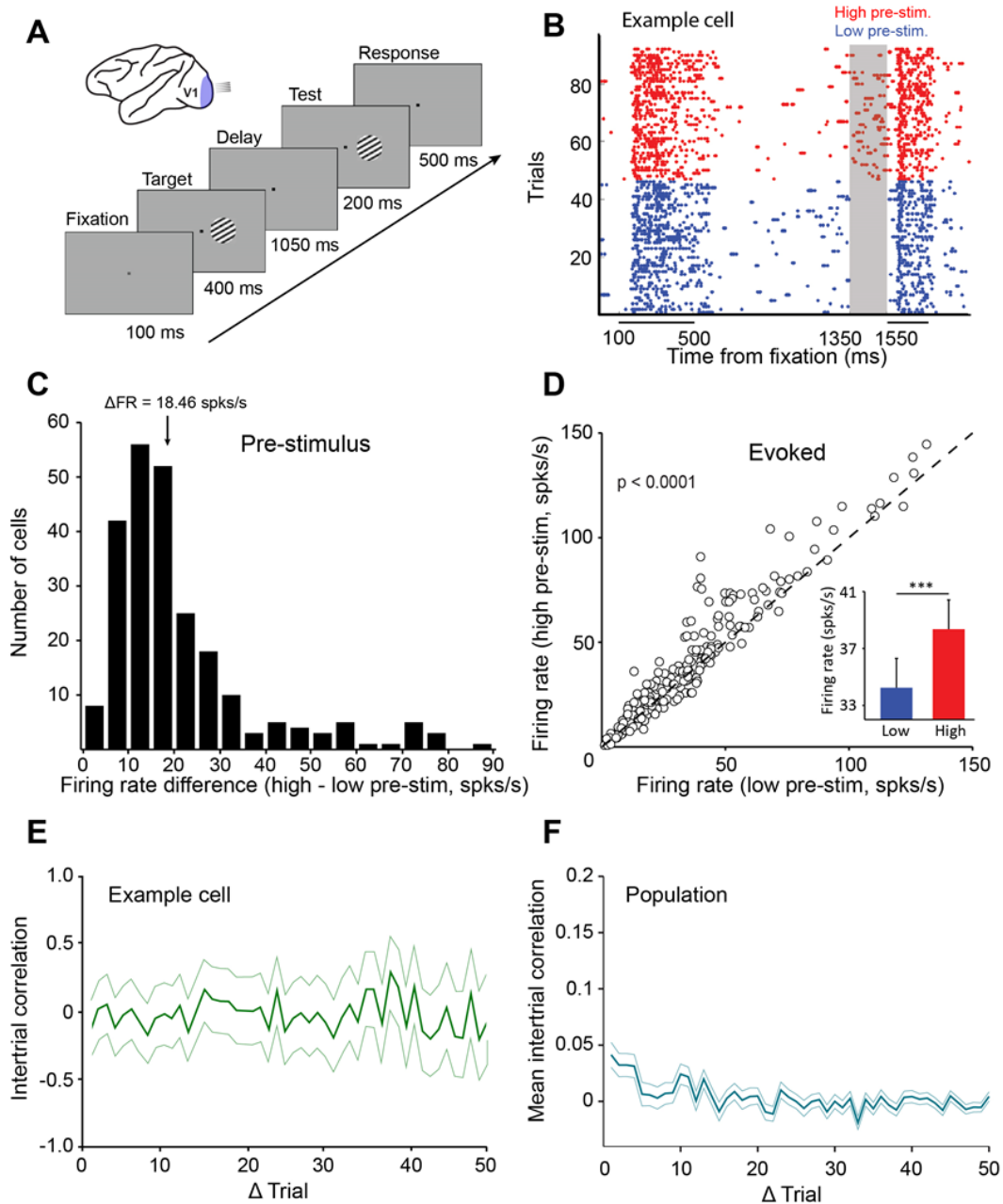


Figure II-1. Experimental setup and firing rate difference by pre-stimulus state.

(A) Schematic representation of the experimental setup. **(B)** Neuronal activity during the delayed-match-to-sample orientation discrimination task. The gray shaded area indicates the interval used to classify trials into low and high pre-stimulus state trials.

The colored dots represent the firing of an example neuron in the low (blue) and high pre-stimulus trials (red). **(C)** Histogram of firing rate change between the two pre-stimulus states. The median difference in firing rate between the two states was 18.46 ± 1.04 spks/s (arrow marks bin). **(D)** Evoked firing rate of the high pre-stimulus plotted as a function of the evoked firing rate in the low pre-stimulus state. Evoked firing rate was significantly greater in the high pre-stimulus state ($p < 0.0001$, paired t-test). **(E)** Auto-correlation of pre-stimulus firing rates for one example cell showing no significant correlation in trial-by-trial pre-stimulus firing rates (green shadow represents the 95% confidence intervals). **(F)** Mean correlation in pre-stimulus firing rates between trials for the entire population of cells (correlation values are near chance level) (error bars represent SEM).

Overall, we recorded up to 13 neurons per recording session and analyzed a total of 263 stimulus-responsive cells. Examples of single-unit responses and stability are shown in Fig. 2. To assess the impact of spontaneous activity on behavior, trials were divided into low and high pre-stimulus state trials based on the median ongoing activity (in the 200-ms interval before the test stimulus presentation) of the neurons recorded simultaneously within the same session (Fig. 1B shows an example of a cell recorded during the behavioral task in different pre-stimulus response states; see Fig. 3 for statistics of firing rates during the pre-test period). We found that the median change in firing rate between the two pre-stimulus states was 18.46 ± 1.04 spks/s (Fig. 1C). We also confirmed previous findings that the evoked firing rate is correlated to the pre-stimulus firing rate^{46,48,64}. As expected, the evoked firing rate was significantly greater in the high pre-stimulus state (Fig. 1D) (38.36 ± 2.17 spks/s vs. 34.24 ± 1.93 spks/s; $P < 0.0001$, paired t-test). Next, to determine if the ongoing activity state corresponds to a general state of excitability in the network, we investigated whether the pre-stimulus firing rate was correlated across trials. To this end, we computed the auto-correlation of the pre-stimulus firing rates across trials for each cell in our population and found that correlation levels not significantly different from chance level

($P < 0.05$, Wilcoxon rank-sum) (Figs. 1E-F), suggesting that the network undergoes seemingly random fluctuations in pre-stimulus activity through time.

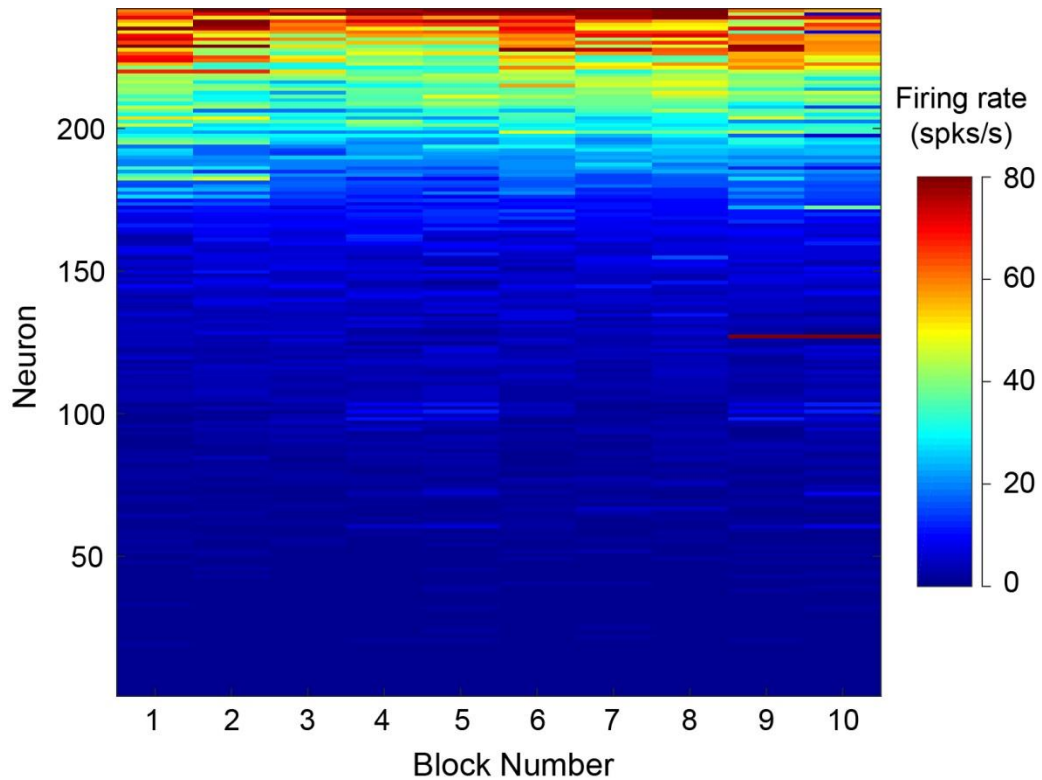


Figure II-2. Neural stability over the recording session.

After dividing each session into ten blocks, we calculated the mean firing rate during the delay period. We observed that 99% of cells exhibited stable firing rates throughout the recording session ($P > 0.05$, Pearson correlation of each neuron over the ten trial blocks).

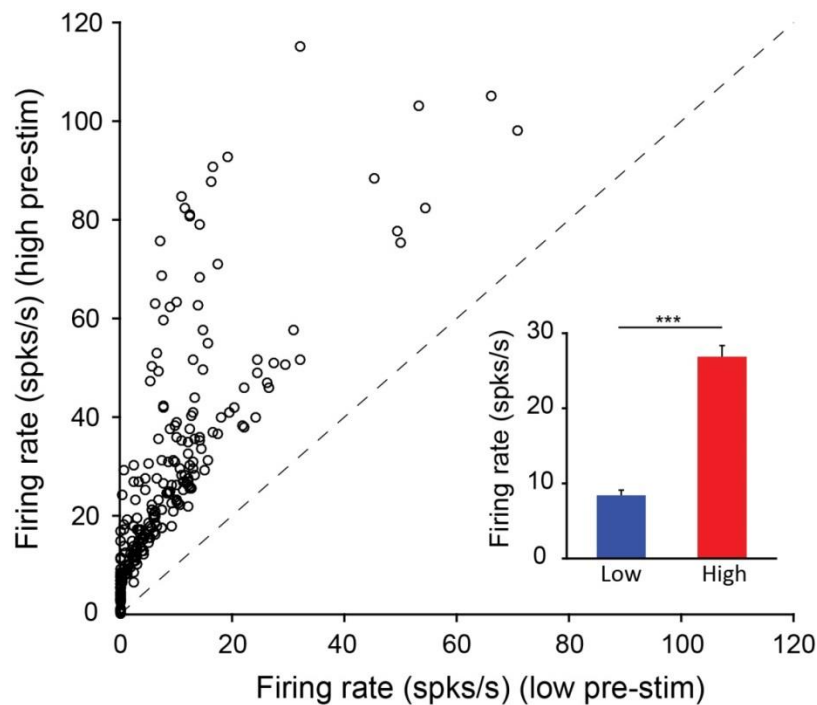


Figure II-3. Distribution of mean firing rates in the low and high pre-stimulus periods for the neurons recorded in the behavioral experiments.

(A) Mean firing rate in the high pre-stimulus state plotted as a function of the mean firing rate in the low pre-stimulus state. (inset) Mean firing rate for low and high pre-stimulus conditions ($P < 0.0001$, Paired t-test).

We determined that the pre-stimulus state of individual neurons is difficult to predict in time, yet, it is still unknown whether spontaneous activity is correlated among neurons in our population. To explore this question, we removed each cell from our simultaneously recorded population and computed the probability that individual cells share the same pre-stimulus state as the remaining population (Fig. 4). That is, for each neuron, we first normalized the firing rate between 0 (minimum firing rate) and 1 (maximum firing rate; independently for each neuron). Then, we computed the median firing rate for each cell and categorized the cell into the low pre-stimulus state if the firing rate was below the median, or alternatively, into the high pre-stimulus state, if the firing rate was above the median. We next performed a similar analysis to find the

mean normalized rate of the remaining population (i.e. for each cell of the population, we normalized the activity between 0 and 1 and then calculated the mean normalized activity) (Fig. 4A).

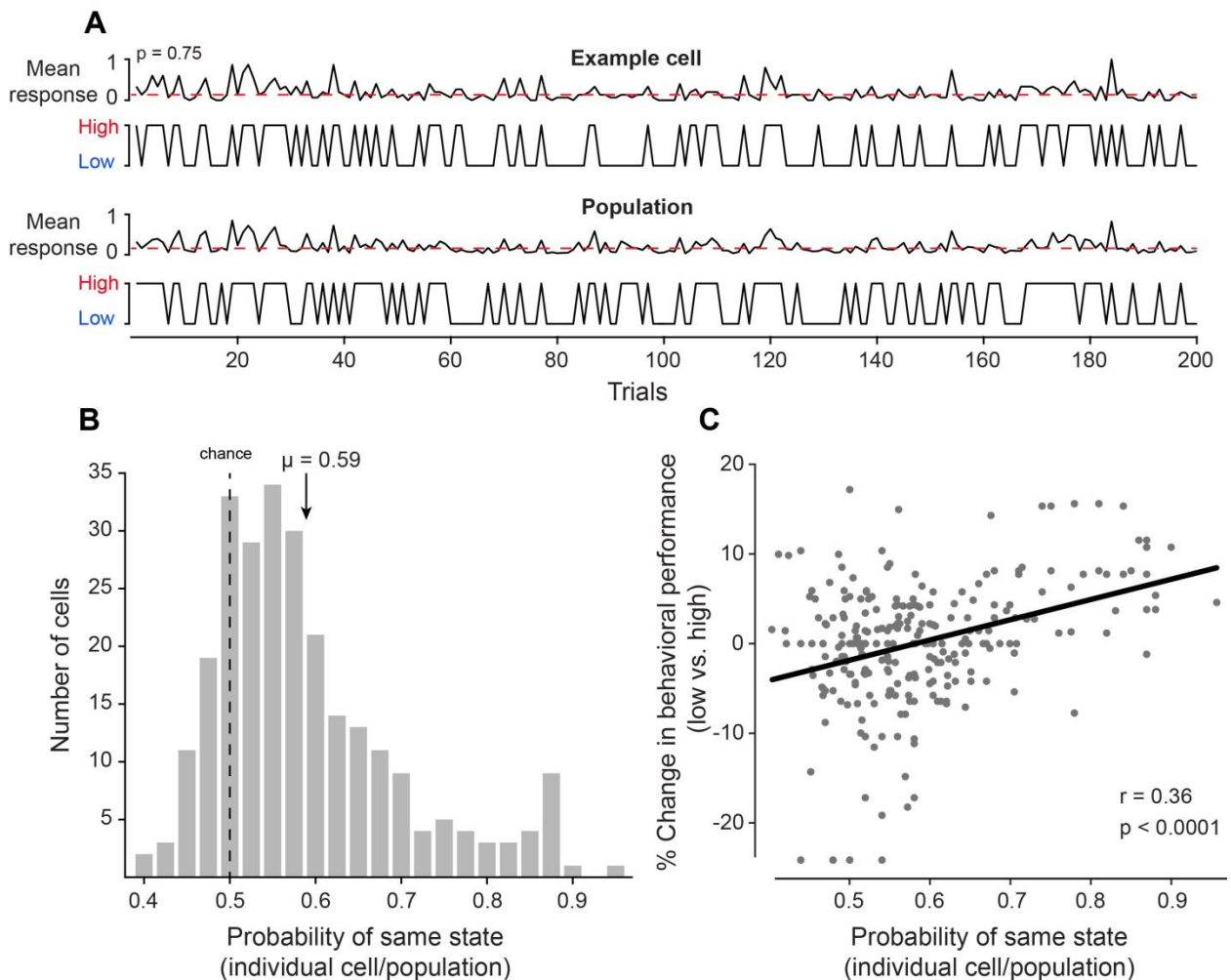


Figure II-4. Ongoing activity of individual cells in correlated to the population activity.

(A) (Top) The firing rate of one example cell normalized between 0 and 1 for 200 trials. The red dotted line represents the median normalized firing rate. Trials with firing rates below the median are placed in the low pre-stimulus firing rate group and trial above the median are placed in the high pre-stimulus category. **(Bottom)** The mean firing rate of the remaining simultaneously recorded population of cells (excluding the example cell) for this example session, normalized between 0 and 1. Trials with firing rates below the median are placed in the low pre-stimulus firing rate group and trial above the median are placed in the high pre-stimulus category. For this example cell, the probability of sharing the same pre-stimulus state with the remaining population is $p = 0.75$. **(B)** Histogram of the probability of same state for the entire set of cells for all sessions. The dotted line represents the chance probability level of 0.5 for a cell to

share the same pre-stimulus state as the population. The mean probability is $\mu=0.59$, which is significantly greater than chance ($P<0.0001$, Wilcoxon rank-sum). **(C)** Percent change in behavioral performance (low pre-stimulus state vs. high pre-stimulus state) plotted against the probability of same pre-stimulus state for each neuron. The two variables are significantly correlated ($r = 0.36$, $P < 0.0001$, Pearson correlation). The black line represents a simple linear regression ($R^2 = 0.13$).

Then, we determined the probability of each cell being in the same pre-stimulus state as the population across trials. It can be appreciated that some cells are highly correlated to the population, while other cells are less correlated, in agreement with previous literature¹³³. Overall, the mean probability of same state for the entire data set was $\mu=0.59$, which was significantly greater than chance level (Fig. 4B) ($P < 0.0001$, Wilcoxon rank-sum), thus demonstrating that spontaneous state is significantly correlated among neurons. In previous work¹³³, it has been shown that neighboring neurons can differ greatly in their coupling to the population, but whether the relationship of individual cells to population activity is predictive of behavioral performance remains unknown. To address this question, we compared the behavioral performance in the low vs. high pre-stimulus states to the probability for each cell of sharing the same state as the population. For each cell, we divided the trials into two groups, low and high pre-stimulus, based on whether the pre-stimulus firing rate was below or above the median pre-stimulus firing rate across trials. We then analyzed the animals' behavioral performance in the low and high trials and compared the % change in performance (low vs. high) to the probability of each cell being in the same state as the population. As demonstrated in Fig. 4C, we found a significant relationship between behavioral performance and how tightly coupled individual neurons were to the population ($r = 0.36$, $P < 0.0001$, Pearson correlation).

Behavioral performance improves in the low pre-stimulus condition

To further explore the impact of spontaneous activity on behavioral performance, we analyzed our population data in terms of the number of cells used to determine the pre-stimulus state. For each session, we analyzed all possible combinations of neuronal subpopulations of size 1 to n (n is the number of simultaneously recorded cells within a session). For instance, for a population of three cells – A, B, and C – there are three possible sets of individual cells (A, B, and C), three possible sets of two cells (i.e., AB, AC, BC), and one set of three cells (ABC) (Fig. 5A). For each set of neurons, we calculated the mean normalized pre-stimulus activity across all the cells within each set (independently for different population sizes) and divided trials into low and high pre-stimulus activity, as described previously in this chapter. Subsequently, we compared the behavioral performance for low and high pre-stimulus states as a function of population size.

Given previous evidence that spontaneous cortical activity influences neuronal response gain and network performance in fixating animals^{64,128}, we tested whether *behavioral performance* would be impacted by the level of ongoing activity before stimulus presentation. First, we determined that orientation discrimination performance was improved in the low pre-stimulus state when the relative difference between the target and test ($\Delta\theta$) was $\pm 5^\circ$ (pooling the positive and negative angles) in N=11 sessions (we excluded 4 sessions with performance in non-match trials lower than 50% correct responses; $P < 0.0001$, Wilcoxon rank-sum at highest population level; $F(1,103)=23.3$; $P < 0.0001$; two-way repeated measures ANOVA). Similar results were observed when $\Delta\theta$ was $\pm 10^\circ$ in 29 sessions ($P < 0.0001$, Wilcoxon rank-sum at highest population level; $F(1,425)=104.4$; $P < 0.0001$, two-way repeated measures ANOVA) (Fig. 6; see also Fig. 7 for individual animal performance). Next, we investigated if the

modulation of behavioral performance by pre-stimulus activity could be explained by top-down anticipation of the test stimulus. That is, could the animals learn the fixed delay duration and optimize their cortical activity just before stimulus presentation (200ms before onset) to improve discrimination performance? To address this question, we modified our experimental approach by randomizing the target-test delay interval (between 250 and 750 ms) (Fig. 8A). We found that behavior was improved in the low pre-stimulus condition for both the $\pm 5^\circ$ ($P < 0.05$, Wilcoxon rank-sum at highest population level; $F(1,259)=42.14$, $P<0.0001$; two-way repeated measures ANOVA) and the $\pm 10^\circ$ discriminations ($P < 0.005$, Wilcoxon rank-sum at highest population level; $F(1,251)=55.7$; $P < 0.0001$, two-way repeated measures ANOVA) (Fig. 8B-D). These findings likely indicate that the modulation of neuronal responses and behavioral performance by ongoing activity cannot be entirely explained by top-down effects, such as expectation or attention^{33,134,135}.

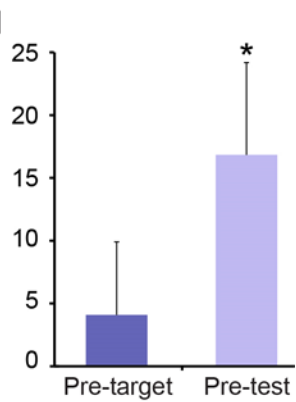
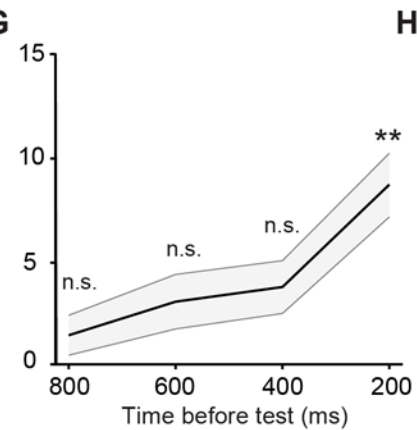
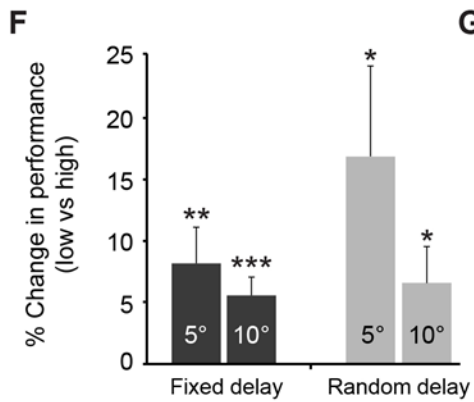
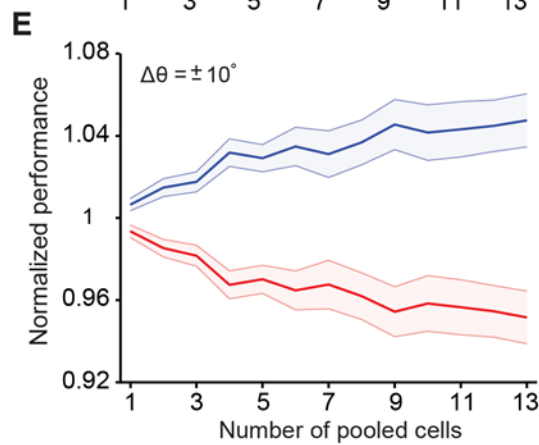
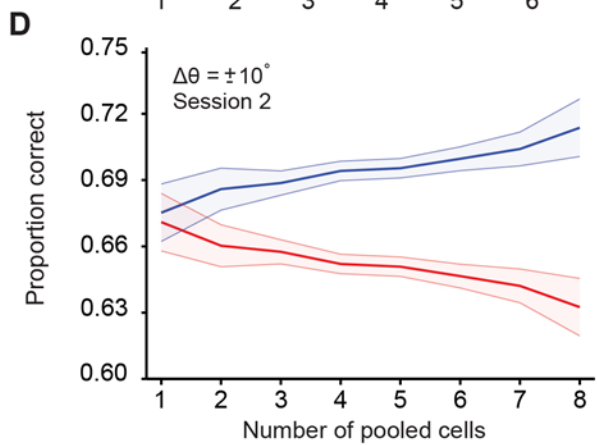
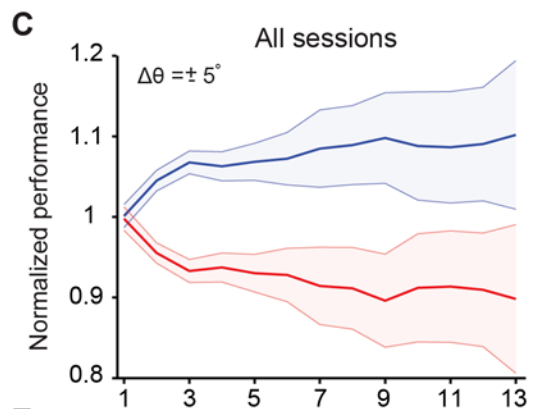
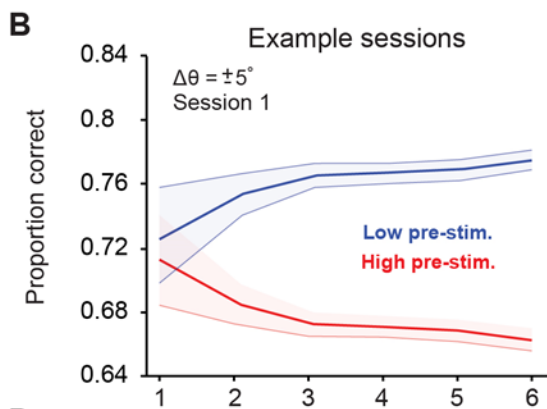
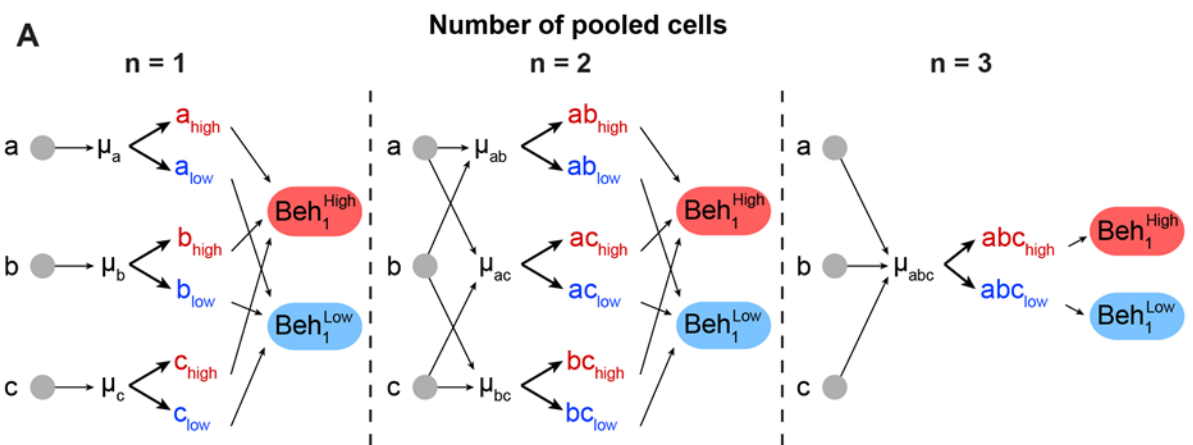


Figure II-5. Ongoing activity influences behavioral performance in an orientation discrimination task.

(A) A diagram depicting the analysis method for an example population of 3 cells. For $n=1$, we computed the mean pre-stimulus firing rate individually for each neuron (μ_A , μ_B , and μ_C) and then calculated the average behavioral performance in the low and high pre-stimulus trials, averaged across the three cells for each group (Beh_1^{low} and Beh_1^{high}). For $n=2$, we computed the mean normalized pre-stimulus activity for each cell pool of size 2 (μ_{AB} , μ_{AC} , and μ_{BC}), divided the trials into high and low groups based on each pool, and then calculated the average performance in the low and high pre-stimulus trials (Beh_2^{low} and Beh_2^{high}). For $n=3$, we computed the mean normalized response for all three cells (μ_{ABC}) and then split the trials to compare behavioral performance the low and high pre-stimulus groups (Beh_3^{low} and Beh_3^{high}). **(B-E)** Behavioral performance is modulated by the ongoing activity state; a single session (panels **B** and **D**); all sessions (panels **C** and **E**). The behavioral performance associated with each ongoing activity state in each session was normalized by dividing the performance in each state by the average session performance (i.e. irrespective of pre-stimulus state). The pre-stimulus state was determined based on the pooled activity of neural populations of varying size (conducted using the method depicted in panel A). The difference in discrimination performance between low and high pre-stimulus states was greater when the population size increases. Figs. 2A and 2B correspond to orientation differences between target and test of $\pm 5^\circ$; Panels 2C and 2D correspond to orientation differences between target and test of $\pm 10^\circ$. “All sessions” in Fig. 2B includes data from monkeys 1 and 2 ($N = 24$ sessions). “All sessions” in Fig. 2D represents data from monkeys 1, 2, and 3 ($N = 42$ sessions). Error bars represent s.e.m of session performance for each population size. In examples B and D, full population sizes of $n=7$ and $n=9$ were removed from the examples distributions ($\pm 5^\circ$ and $\pm 10^\circ$, respectively) for clarity. **(F)** Behavioral improvement in the low vs. high pre-stimulus conditions is consistent in both the fixed delay and random delay conditions at $\pm 5^\circ$ and $\pm 10^\circ$ orientations (* $P < 0.05$, ** $P < 0.01$, *** $P < 0.001$; Wilcoxon signed-rank test). Results in F-H were conducted at a population of 5 to include most sessions in the analysis **(G)** Behavioral improvement in the low vs. high pre-stimulus state for different pre-stimulus periods. The x-axis represents the time relative to the onset of the test stimulus. Pre-stimulus state was assessed based on the pre-stimulus interval in 200 ms steps (during the delay period). The improvement in discrimination performance in the low pre-stimulus state occurs only when assessing the 200 ms period before test presentation. (** $P < 0.01$; n.s. = non-significant; Wilcoxon signed-rank test). Error bars represent s.e.m. **(H)** Pre-test influences the behavior more than pre-target. The low pre-test behavioral performance was significantly better than the high pre-test condition ($P < 0.05$, paired t-test). Behavioral performance was higher in the low pre-target state, but overall, the difference was not significant. $N = 13$ sessions from random delay data. Fixed delay data was included because we only had 100 ms fixation before target presentation.)

Due to the fact that fixed and random delay results were similar, we pooled the data sets together for the remaining analyses. In summary, we found that behavior was

significantly improved in the low pre-stimulus state in N=24 sessions ($P < 0.0001$, Wilcoxon rank-sum at highest population level; $F(1,355)=56.1$, $P < 0.0001$, two-way repeated measures ANOVA) (Fig. 3B-C); similar results were observed when $\Delta\theta$ was $\pm 10^\circ$ (N=42 sessions; $P < 0.0001$, Wilcoxon rank-sum at largest population level; $F(1,697)=164.6$, two-way repeated measures ANOVA, $P < 0.0001$) (Fig. 5D-E). We next determined that increasing the population size (in order to obtain better estimates of networks' pre-stimulus state) yields a larger difference between the behavioral performance in the low and high pre-stimulus states (Figs. 5B-E). That is, the difference in discrimination performance in the low vs. high pre-stimulus activity conditions was amplified when the number of cells used to measure the network pre-stimulus state was increased ($r=0.84$, $P < 0.0001$; Pearson correlation for $\pm 5^\circ$ and $r=0.93$, $P < 0.0001$; Pearson correlation for $\pm 10^\circ$), possibly due to a better estimation of the 'true' cortical state in larger pools of neurons. A summary of the results for each behavioral condition can be observed in Fig. 5F (Wilcoxon signed-rank, population N=5 is displayed to include most sessions in the analysis).

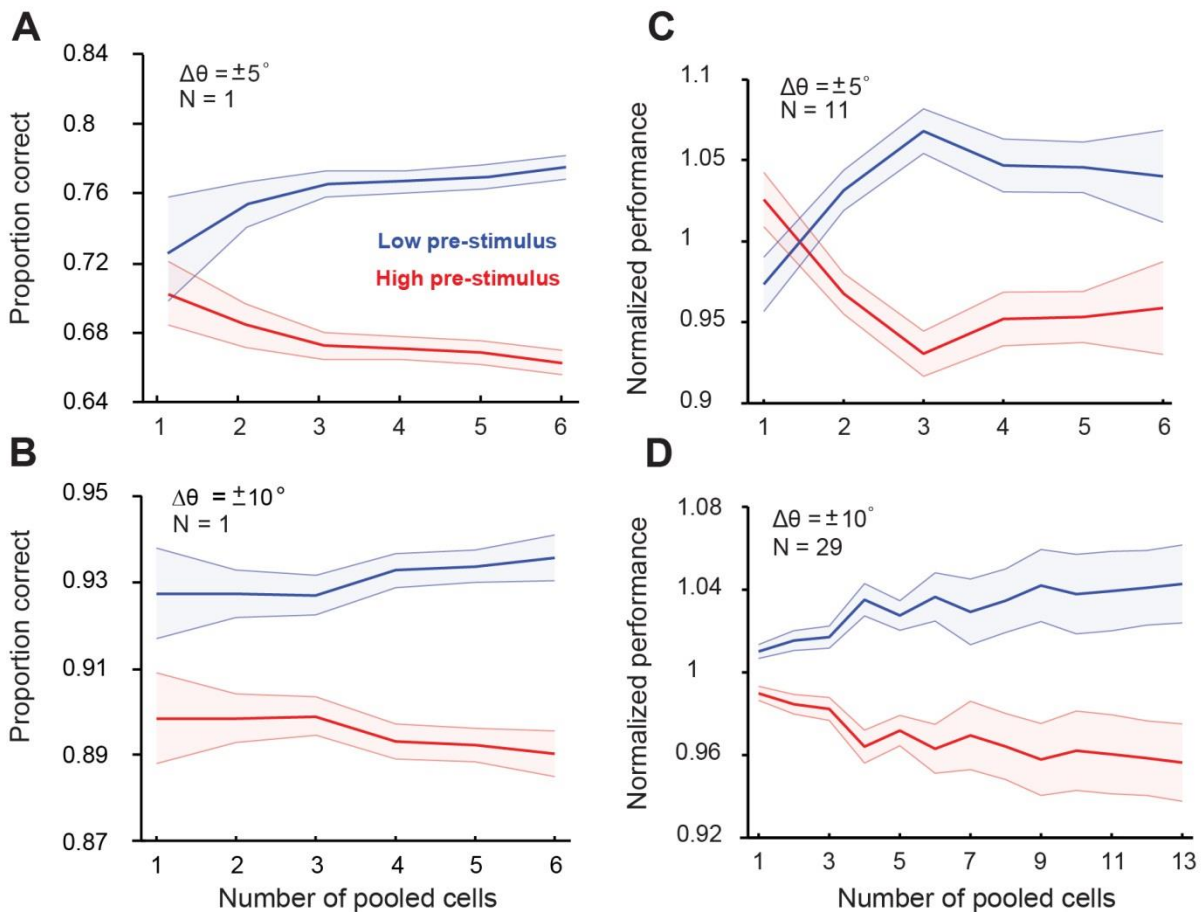


Figure II-6. Ongoing activity influences behavioral performance in an orientation discrimination task with fixed delay period.

Three monkeys were trained in a behavioral task as noted in Fig. 1A. Behavioral performance is modulated by the ongoing activity state; single sessions (panels **A-B**); all sessions (panels **C-D**). Upper panels in **A** and **C** correspond to orientation differences between target and test of $\pm 5^\circ$; lower panels correspond to orientation differences between target and test of $\pm 10^\circ$. Behavioral performance was higher in the low spontaneous group ($P < 0.0001$, Wilcoxon rank-sum at highest population level; $F(1,103)=23.3$; $P < 0.0001$; two-way repeated measures ANOVA) for $\pm 5^\circ$ discrimination. Similar results were found for the $\pm 10^\circ$ discrimination experiment ($P < 0.0001$, Wilcoxon rank-sum at highest population level; $F(1,425)=104.4$; $P < 0.0001$, two-way repeated measures ANOVA). The 5 degree orientation panel **C** includes data from monkeys 1 and 2. The 10 degree panel **D** represents data from monkeys 1, 2, and 3. Error bars represent s.e.m of session performance for each population size.

We further analyzed whether the difference in behavioral performance could be predicted based on pre-stimulus neural activity further from the test presentation (i.e.

400, 600, and 800 ms prior to the stimulus). As shown in Fig. 5G, we found that only the ongoing activity immediately preceding the test stimulus presentation was able to predict behavioral performance – analyzing the pre-stimulus period beyond 200 ms did not provide information about behavioral performance. The results described above demonstrate that we can predict a monkey’s response based on the ongoing activity preceding the test stimulus. This raises the issue of whether this prediction occurs only in relation to the presentation of the stimulus closest in time to the behavioral response (i.e., the test stimulus) or is common to both the target and test stimuli. In principle, since behavioral decisions in the discrimination task are likely made based on a temporal comparison between neuronal responses to the target and test, we reasoned that analyzing the ongoing activity preceding the target will likely demonstrate similar results. We examined this issue by conducting a complementary analysis of behavioral performance in relation to neuronal firing 200 ms before *target* presentation (conducted with random delay data that included a longer 300 ms fixation window). We found a significant difference between behavioral performance in the low versus high pre-test conditions ($P < 0.05$, Wilcoxon signed-rank), but not for the pre-target condition. To further explore this question, we repeated the analyses associated with Figs. 5B-E at all population levels and found (Fig. 9) that behavioral performance was not significantly higher in the low pre-target state when the relative difference between the target and test ($\Delta\theta$) was $\pm 5^\circ$ ($P = 0.40$, Wilcoxon rank-sum at highest population level). We also did not find a significant difference between the high and low pre-target states when $\Delta\theta$ was $\pm 10^\circ$ ($P = 0.09$, Wilcoxon rank-sum at highest population level). Taken together, these results suggest that fluctuations in ongoing activity before the presentation of stimuli that are more remote with respect to decision making have a

diminished effect on behavioral performance. In addition, the target stimulus did not rotate across trials, so the animals may have made a direct categorization of the test stimulus to accomplish the behavioral task.

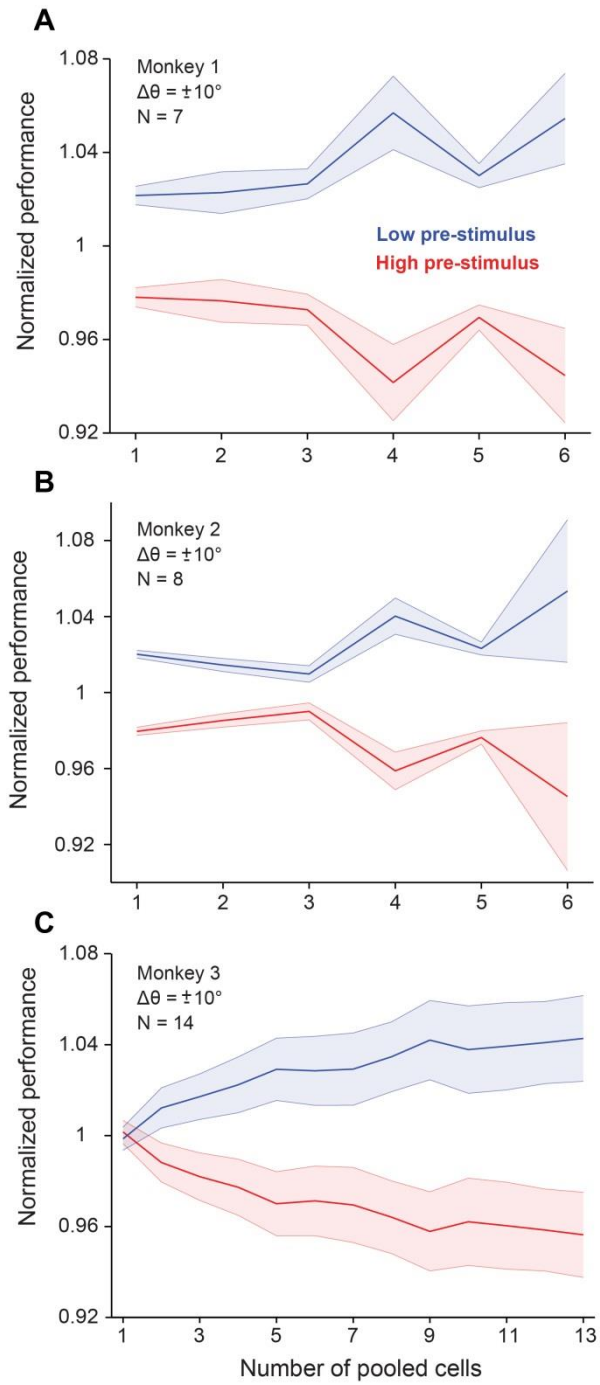


Figure II-7. Ongoing activity influences behavioral performance in an orientation discrimination task for each monkey.

The low pre-stimulus group performs significantly better than the high pre-stimulus group in each monkey ($P < 0.005$, Wilcoxon rank-sum at highest population level, $F(1,65)=63.7$; $P < 0.0001$, two-way repeated measures ANOVA; $P < 0.0001$, Wilcoxon rank-sum at highest population level, $F(1,79)=75.8$; $P < 0.001$, two-way repeated measures ANOVA; $P < 0.005$, Wilcoxon rank-sum at highest population level, $F(1,279)=47.9$; $P < 0.0001$; two-way repeated measures ANOVA, respectively). Each session is from the fixed delay recordings. Error bars represent s.e.m.

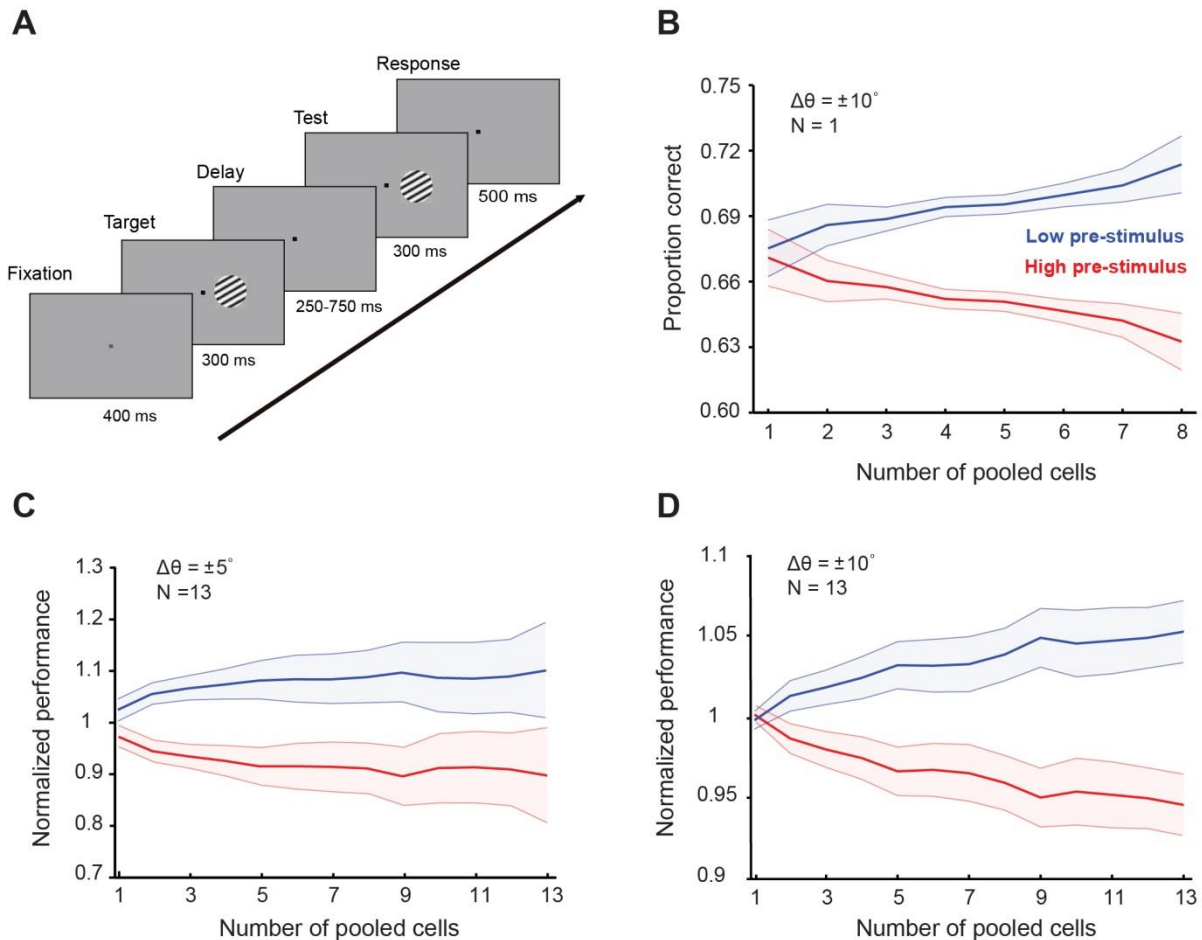


Figure II-8. Ongoing activity influences behavioral performance in an orientation discrimination task with random delay period.

(A) One monkey was trained in an orientation discrimination task with a random delay between target and test presentation (in the 250-750 ms range). Behavioral performance is modulated by the pre-stimulus response state before test presentation. Example of a single session **(B)** and normalized behavioral performance for all recorded sessions for $\pm 5^\circ$ **(C)** and $\pm 10^\circ$ **(D)** discrimination. The responses of each neuron were grouped depending on the level of pre-stimulus activity into ‘low’ and ‘high’

groups. Behavioral performance was higher in the low spontaneous group for $\pm 5^\circ$ discrimination ($P < 0.05$, Wilcoxon rank-sum at highest population level; $F(1,259)=42.14$, $P < 0.0001$; two-way repeated measures ANOVA). Similar results were found for the $\pm 10^\circ$ discrimination experiment ($P < 0.005$, Wilcoxon rank-sum at highest population level; $F(1,251)=55.7$; $P < 0.0001$, two-way repeated measures ANOVA). We analyzed 103 neurons. This figure represents data from monkey 4 of our study. Error bars represent the s.e.m. of session performance for each population size.

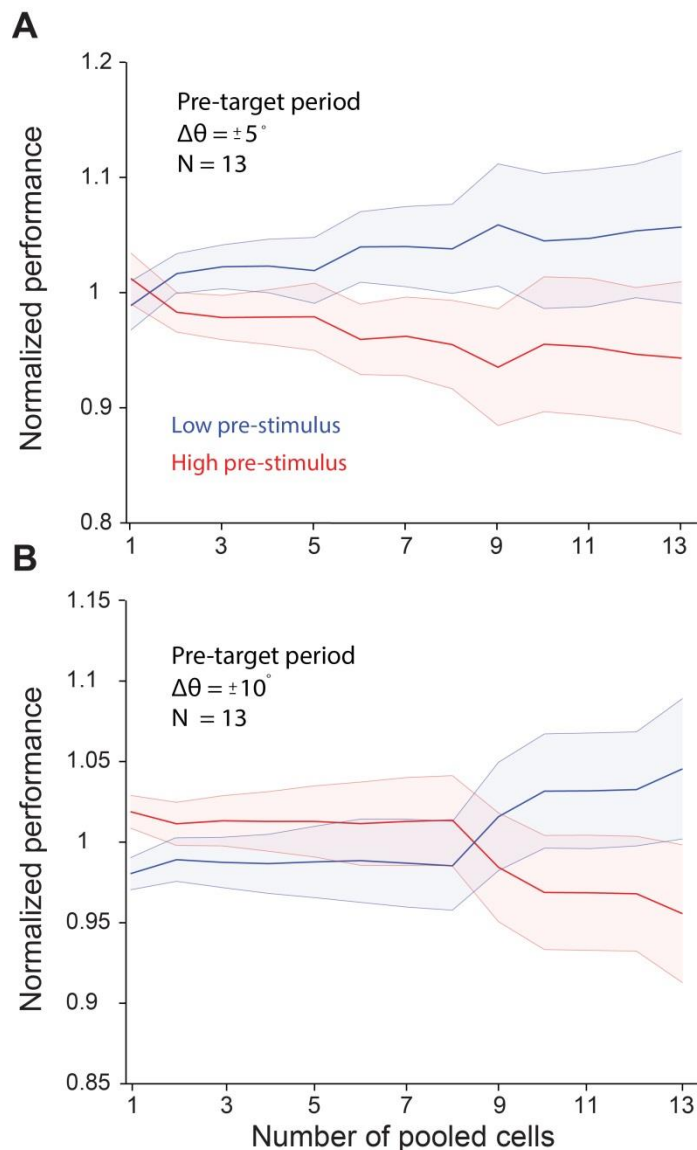


Figure II-9. Pre-target activity influences behavioral performance.

Behavioral performance was higher in the low pre-target state when the relative difference between the target and test ($\Delta\theta$) was 5° ($P = 0.40$, Wilcoxon rank-sum at highest population level). We did not find a significant difference when $\Delta\theta$ was 10° ($P = 0.09$, Wilcoxon rank-sum at highest population level). The 5 degree orientation data

includes data from monkeys 1 and 2. The 10 deg data represents data from monkeys 1, 2 and 4. Error bars represent s.e.m.

Neural discrimination is improved in the low pre-stimulus condition

We demonstrated that behavioral performance was increase in the low pre-stimulus state; thus, we reasoned that if the animals pool the activity in the primary visual cortex to make decisions, then fluctuations in the network information should also be improved in the low pre-stimulus state. To assess the ability of our recorded network to discriminate orientations, we conducted an optimal linear classification, Fisher linear discriminant (FLD), by finding the optimal multi-dimensional projection of the data (number of dimensions equal to number of simultaneously recorded neuron in a session) into one-dimensional space^{35,136} that best separates the two different stimuli. The FLD projection maximizes the distance between the means of two groups of data while minimizing the variance within each group¹³⁷. In our case, we sought to analyze the separation between the target and test stimuli separately, in both the low and high pre-stimulus conditions (see Methods). Fig. 10 represents data from one example session with 13 simultaneously recorded neurons (Fig. 10A). We have displayed the number of spikes of one pair of cells in all trials for both the target and test stimuli (Fig. 10B). The axes of the histograms are plotted perpendicular to the dimensions that maximize the separability between target and test stimuli (green lines), and the solid curves represent one-dimensional Gaussian fits for the target and test distributions. In this way, one can observe the maximum linear separation between the target and test distributions for the low and high pre-stimulus states in a 2-cell example. Fig. 10C represents the same FLD analysis conducted for the entire population of 13 cells. In this example session, you can appreciate that there is greater separability between the

target and test stimuli in the low pre-stimulus condition vs. the high pre-stimulus condition, in accordance with our behavioral results.

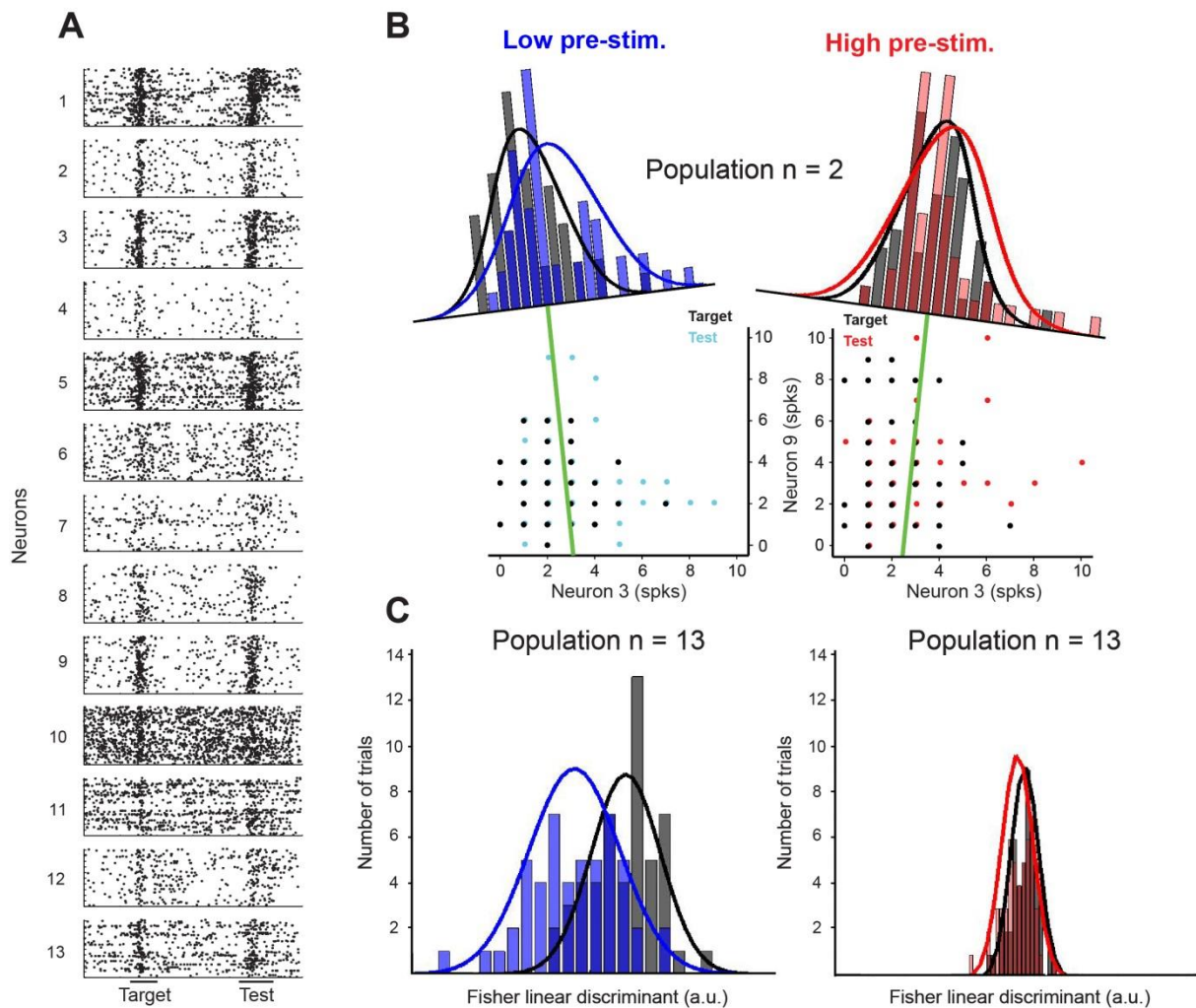


Figure II-10. Fisher linear discriminant (FLD) analysis from an example session.

(A) Raster plots for 13 cells recorded simultaneously in the session. Each dot represents an action potential. Horizontal bars at the bottom represent stimulus duration for target and test. The random delay period has been truncated to align the test responses. **(B)** Example FLD of one cell pair (Neuron 3 and 9). Each circle represents the total number of spikes elicited during the target or test stimulus. Each histogram is plotted on the fisher linear discriminant axis which maximizes the difference between target and test relative to the variance of the responses. The black and blue (black and red for the high pre-stimulus condition) curves represent one-dimensional Gaussian fits for the target and test distributions, respectively. The green line represents the decision boundary. **(C)** Example FLD for the full population of 13 cells. You can appreciate that there is a greater difference between the distributions in the low pre-stimulus trials vs. the high pre-stimulus trials.

The population discriminability between two multivariate distributions using the FLD method can be quantified by a single variable, d^2 :

$$d^2 = (\bar{\mathbf{x}}_A - \bar{\mathbf{x}}_B)^T Q^{-1} (\bar{\mathbf{x}}_A - \bar{\mathbf{x}}_B) \quad 35$$

Where $\bar{\mathbf{x}}_A$ and $\bar{\mathbf{x}}_B$ represent the vector of mean spikes in all trials for target and test, respectively, and Q^{-1} represents the inverse of the pooled covariance matrix. The probability of correct classification (PCC) is directly related to d^2 by the complementary error function (see Methods for further details). We computed the PCC for each session at all population sizes for both the low and high pre-stimulus conditions (Fig. 11A) and found that PCC was significantly greater in low spontaneous activity trials ($P < 0.05$; paired t-test computed at the highest population level for each session). We also compared the difference between decoder performance at small ($N = 2$) and large ($N = 12$) population sizes and discovered that the performance difference was greater at large population sizes ($P < 0.05$, Bootstrap significance test) (Fig. 11A inset).

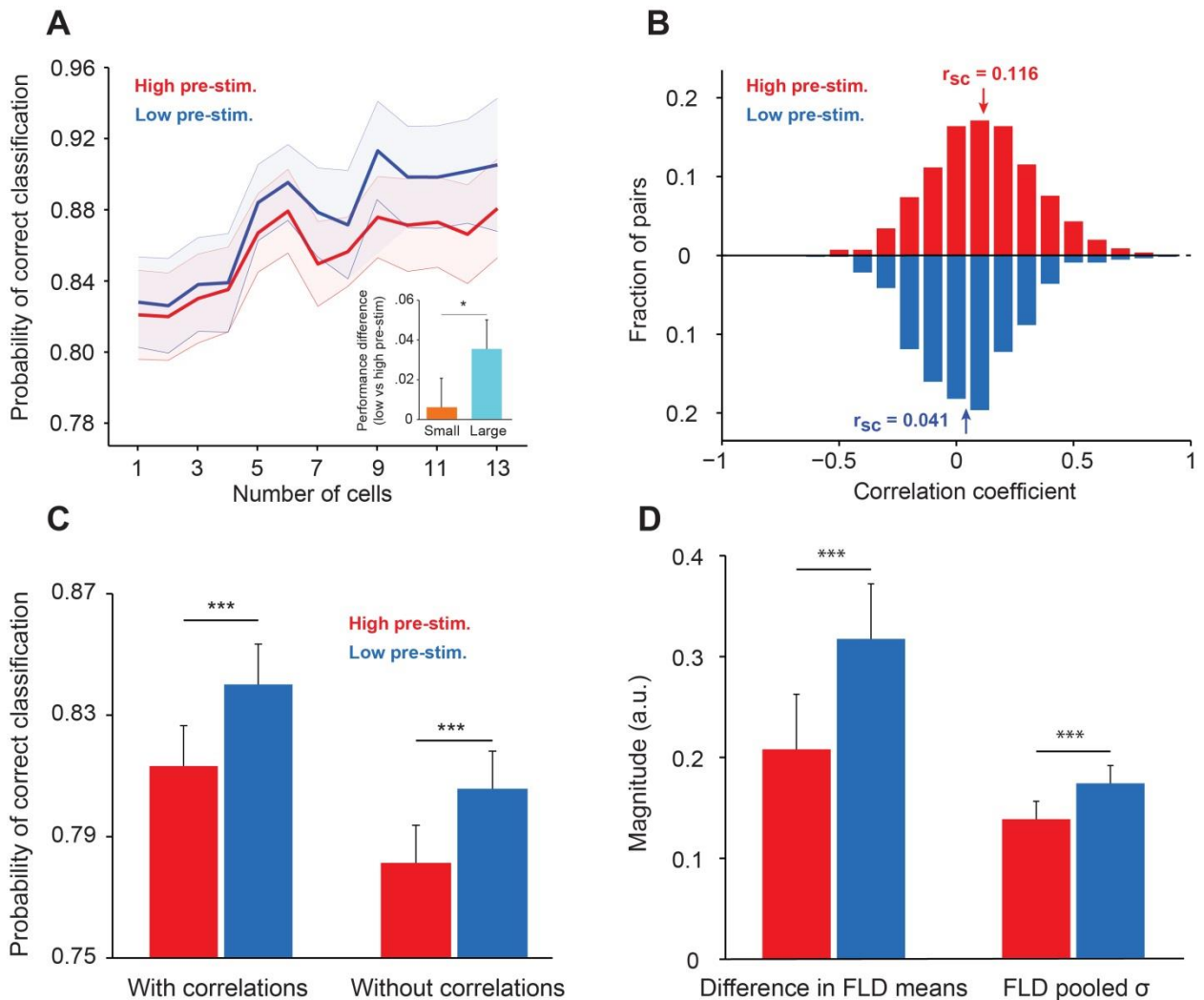


Figure II-11. Population d' analysis and noise correlations.

(A) The probability of correct classification (PCC) as a function of population size. The PCC was significantly higher in the low pre-stimulus case ($F(1,164)=9.32$; $P < 0.005$; two-way repeated measures ANOVA). **(inset)** The difference in classification performance between low and high at a *small* population of $n=2$ (orange) and at a *large* population of $n = 12$ (blue). The performance difference was greater for the large population ($P < 0.05$, bootstrap significance test) **(B)** Noise correlations of the high and low pre-stimulus states. Noise correlations were significantly higher in the high pre-stimulus state ($P < 0.05$; paired t-test). **(C)** Probability of correct classification between the high and low pre-stimulus states. “With correlations” represents data using the following equation: $d^2 = \Delta\mu^T Q^{-1} \Delta\mu$; Probability of correct classification = $erfc(-\sqrt{d^2})/2$ (Averbeck and Lee 2006). “Without correlations” represents the probability of correct classification when ignoring the effect of noise correlations using, $(d_{shuffled}^2 = \Delta\mu^T Q_d^{-1} \Delta\mu)$, where Q_d is the diagonal covariance matrix. In each condition, there was a statistically significant difference between high and low pre-stimulus conditions (* $P < 0.05$; paired t-test). **(D)** The magnitude of the difference in FLD means (left) and the magnitude of the pooled standard deviation (σ) of the FLD (right). In the low pre-stimulus condition, the difference in means was significantly greater ($P < 0.0001$; paired

t-test). The average variance was also higher in the low pre-stimulus condition ($P < 0.0001$; paired t-test), but this had less impact on the population d' overall. Analysis in this figure was conducted on all cells recorded at $\pm 5^\circ$.

There are three possible explanations for improved neural discrimination in the low pre-stimulus state that we wished to explore: change in correlated variability, higher difference in the mean responses in the FLD dimension, or decreased variance in the FLD dimension. First, because information about orientation depends on each neuron's response profile and also on the correlated activity among neurons⁴⁷, we analyzed noise correlations in both the high and low pre-stimulus state. One might postulate that noise correlations would be larger in the high pre-stimulus state due to a higher evoked firing rate (Fig. 1D)¹³⁸ and provide a possible explanation for decreased behavioral performance in the animals^{130,139,140} and indeed, we found a significant difference in correlations between the two states (0.116 ± 0.013 vs. 0.041 ± 0.011 , high vs. low pre-stimulus) (Fig. 11B, $P < 0.05$, paired t-test). We next repeated our decoder analysis at the full population level for each session using the previously applied method, "with correlations," along with a new analysis to determine the amount of information that would be extracted from our population of neurons using a decoding algorithm that ignored correlations, "without correlations." We found that destroying correlations decreased the probability of correct classification, but against our expectations, the difference in classification performance between low and high pre-stimulus states remained ($P < 0.05$; paired t-test) (Fig. 11C, right). Population d' can be deconstructed into the difference in mean responses in the most discriminant dimension (FLD) divided by the square root of the average variance in the same dimension³⁵. In this way, we could observe whether the decoder performance was greater in the low pre-stimulus condition due to a greater difference in FLD means or a smaller FLD pooled standard

deviation. In our data, we found that classification performance was better in the low pre-stimulus condition due to a greater difference in FLD means ($P < 0.0001$; paired t-test) (Fig. 11D). The FLD pooled standard deviation was larger in the low pre-stimulus condition, but ultimately, this difference had a smaller total impact on discrimination performance than the difference in FLD means.

Discussion

We have demonstrated that fluctuations in pre-stimulus ongoing activity can impact neural and behavioral discrimination performance. Altogether, our results indicate that in order to correctly discriminate or recognize a stimulus, cortical networks have to be in an appropriate state of excitability, possibly representing levels of network 'preparedness' to facilitate the processing of incoming stimuli. Our work builds on the growing body of literature dedicated to spontaneous cortical activity by examining the impact of low and high pre-stimulus states on population coding in behaving animals.

The fact that spontaneous waves of cortical activity exhibit similar spatio-temporal characteristics as the stimulus-evoked response has recently made researchers wonder if ongoing activity can modulate behavioral performance. Previous studies examining this topic were performed in human subjects using electroencephalograms EEG: ^{111,112,115,117-119,141}, magnetoencephalograms MEG: ^{114,116,120,121,142}, and functional magnetic resonance imaging fMRI: ^{110,113,143,144}. The most important limitation of these studies is the low spatial and temporal resolution of the techniques used to assess the functional role of ongoing activity. A separate series of important efforts was conducted to investigate single-unit and network coding and its

relationship to spontaneous cortical activity^{74,76,78,122-126}. Even though these studies have collectively concluded that pre-stimulus activity modulates behavioral performance in a variety of tasks, the dynamics of ongoing activity at the single neuron and population level and their impact on behavior have remained unknown. Our study demonstrates that spontaneous neural activity is correlated among neurons along a continuum. We found that neurons that covary strongly with the population are more predictive of behavioral performance compared to neurons that fire more independently. We also demonstrate that decoding the population response before stimulus presentation can be used to predict subsequent neuronal performance and that a large proportion of behavioral variance can be attributed to the internal state of the local circuit. Importantly, the prediction of the behavioral response was not altered when the animal was unable to estimate the timing of occurrence of the test stimulus. Thus, top-down stimulus expectation does not seem to play a dominant role in altering local ongoing activity to impact behavioral performance. However, future research will elucidate whether the relationship between fluctuations in ongoing activity, network coding, and behavioral performance is a solely a characteristic of primary sensory areas or whether this represent a general coding strategy of the brain.

Our behavioral results demonstrated the greatest difference between low and high pre-stimulus states at the largest population sizes. Thus, we chose to focus our neural analysis on well-known population coding techniques, namely, Fisher linear discriminant (FLD) and population d' ^{35,136}, which had the potential to elucidate the neural correlates for our behavioral results. Using these methods, we were able to show that even though the population of neurons exhibited lower evoked firing rates in the low pre-stimulus state, they were able to transmit more information about stimulus

orientation to increase network discrimination accuracy. FLD analysis computes the axes that maximize the separation between these two classes of data, a task which the brain must similarly accomplish to receive reward. We explored the three main components of linear discriminant analysis which can lead to improved neural discrimination: changes in correlated variability, increased difference in mean response, and decreased variance in response³⁵. It has long been reported that correlated firing between neurons can serve to constrain the schemes by which the cortex encodes and decodes information in incoming sensory stimuli^{139,145-147}. We provided an estimate of the effect of correlated trial-to-trial response on information encoding by computing the information that would be contained in our neural population if the cells were uncorrelated, $d_{shuffled}^2$. Through this measure, we determined that the information in the uncorrelated networks was decreased for both the low and high pre-stimulus states, yet the difference in the probability of classification between the states remained (Fig. 11C). Thus, we discovered that higher correlations did not preferentially affect network performance in the high pre-stimulus state (Fig. 11C). In addition, we demonstrated that a greater difference in the mean response in the most discriminant dimension (FLD) led to improved neural discrimination in the low pre-stimulus state. This result in behaving animals is in accordance with theoretical work¹²⁸ and our previous work in fixating animals demonstrating an increase in response gain and neural discrimination in the low pre-stimulus state⁶⁴. The results suggest that neural populations in primary visual cortex fluctuate randomly between various states of excitability and become “optimized” for discrimination when cortical activity is low. That is, when pre-stimulus activity is low in

V1, neurons transmit more information about the stimulus orientation to improve neural and behavioral performance.

In conclusion, our work represents the first effort to examine the effect of pre-stimulus firing rates on population coding and behavior in the primary visual cortex. We found that networks in a low pre-stimulus state have improved discrimination performance that correlates with improved behavioral performance. Future work should further examine the structure of spontaneous activity and if it similar correlates to performance in higher cortical areas.

CHAPTER III: Population synchrony in cortical networks modulates network and behavioral performance

Introduction

Note: This chapter is based upon: Beaman CB, Eagleman SL, and Dragoi V. Population synchrony in the cortex modulates network and behavioral performance. This manuscript is in preparation for submission (Eagleman SL recorded the data. I conducted the analysis).

The dynamics and responsiveness of populations of brain cells in alert animals vary widely across different behavioral contexts^{74,125,148-150}. Thus, even in the absence of external stimulation, the state of the brain can fluctuate between synchronized activity in quiescent animals and highly desynchronized activity during alertness^{75,123,151}. Although the large changes in brain activity and transitions between sleep and waking have been well characterized^{73,76,152}, the functional impact of local fluctuations in population activity during alertness has remained elusive. Indeed, even though global fluctuations in brain state induced by factors such as arousal or attention have been documented^{71,153}, whether and how rapid changes in local population activity during alertness influence both the capacity of networks of neurons to encode sensory information and the behavior of the animal have remained unknown. How do fluctuations in the synchrony of local population spiking activity impact the variability in sensory coding and perceptual performance? To investigate this relationship, we conducted recordings in area V4 of primates participating in a match-to-sample orientation discrimination task (Fig. 1A). Two monkeys performed an image orientation discrimination task (n=28 sessions) while multiple neurons (up to 17) were recorded simultaneously. In each trial, two identical natural scenes (target and test) were flashed

for 367 ms each, and were separated by a 1250 ms delay (**Fig. 1a**). The test image was rotated by 0° (match condition), or 2°, 3°, 5°, 10°, or 20° (non-match condition) with respect to the target. Our strategy was to quantify the rapid fluctuations in ongoing population activity during the delay period, and then examine whether these fluctuations help identify the optimal network states for signal discrimination task performance. We reasoned that the operating mode of cortical circuits would be optimized in the more alert, desynchronized state, reflecting improved neural coding and behavioral performance.

Methods

The experimental approval protocol and surgical procedure was conducted as in Chapter II, but in this case, the recording chamber was cemented over area V4 (using MRI for localization).

Behavioral task:

Two male rhesus monkeys (*Macaca mulatta*) were trained in a delayed-match-to-sample task in which they had to indicate whether two successively presented natural images had the same or different orientation (Fig. 1A; n = 28 sessions). After monkeys fixated for 400 ms, a target stimulus was flashed for 367 ms, and after a delay period of 1250 ms, was followed by a test stimulus flashed for 367 ms. In approximately half of the trials, the test stimulus had the same orientation as that of the target ('match' condition). In the other half of the trials, the test orientation was rotated from the target by 2°, 3°, 5°, 10°, or 20° ('non-match' condition). Match and non-match trials were

randomly interleaved. Animals were trained to release a bar on match trials and hold the bar on non-match trials in order to receive a juice reward.

To calibrate our measure of population synchrony, in a subset of sessions (n=6) we allowed the animals to rest quietly in the dark for 20-30 minutes following the behavioral task, while electrophysiological recordings continued. During this rest period, a white background noise was played on a speaker to prevent external sounds from arousing the animals. We monitored eye position using the eye tracker and night vision video monitoring. The timing of rest was carefully controlled such that monkeys began the rest at approximately 2 pm, which is around the time when monkeys naturally take daytime naps¹⁵⁴.

Visual stimuli:

Gray-scale natural stimuli (e.g., deer eating grass, water buffalo, jungle scenes) were generated with Psychophysics Toolbox using MATLAB and presented on a 19" CRT color video monitor (60 Hz refresh rate). Only one image was presented in each session. Stimuli ranged in size from 8 to 10 degrees, and were presented at 3-10 degrees of eccentricity. Stimulus location and size were optimized in each session such as to stimulate the largest number of simultaneously recorded cells. Stimulus presentation was recorded and synchronized with the neural data using the Experiment Control Module programmable device (ECM, FHC Inc.)

Eye movement control analyses:

On each trial, monkeys were required to fixate on a central point (0.4 deg in size) within a 2° fixation window. Eye position was continuously monitored by using an

eye tracker system operating at 1 kHz (EyeLink II; SR Research). Eye position was calibrated at the beginning of each experiment with a 5-point calibration procedure. We examined whether states of population synchrony were associated with changes in the quality of fixation by measuring the mean eye position, standard deviation of eye position, and eye movement velocity along the horizontal and vertical axes during the delay period. We found that eye movements were not statistically different between the synchronized and desynchronized cortical states ($P > 0.1$).

Electrophysiological recordings:

Single unit electrophysiological recordings were conducted as described in Chapter II of this thesis.

Raw LFPs were collected at 1 KHz sampling frequency and a second-order notch filter was implemented to remove the 60 Hz line noise. The LFP power was then computed for each recording channel independently using the MATLAB R2015b function *bandpower*, which calculates the average power via a rectangle approximation of the integral of the Power Spectral Density estimate. The power was then z-scored across trials. The mean z-scored power was taken across channels for each band in the synchronized and desynchronized trials such that the mean of the combined groups should always be zero. The smallest frequency used to compute LFP power was 2 Hz due to the 1-second inter-stimulus window limitation. A rolling window band of 5 Hz was moved in 1 Hz steps to generate **Fig. 4a**. Physiologic bands were used to construct **Fig. 4b** (Delta = 2-4 Hz, Theta = 4-8 Hz, Alpha = 8-12 Hz, Beta = 12-30 Hz, Gamma = 30-100 Hz). Power ratio was computed as the LFP power in the low band (2-10 Hz) divided by the LFP power in the high band (10-100 Hz). Trials were split into two

groups based on the median power ratio. One session was removed from the analysis due to corrupted LFP signal.

Population synchrony index:

The population synchrony index (PSI) was calculated in each trial by using the coefficient of variation of the ongoing population spike count across 100 windows of $T = 10 \text{ ms}$ ^{78,126}:

$$PSI = Cv = \frac{\sigma_{pop\ sc}}{\mu_{pop\ sc}}$$

The analysis period constituted one second of data during the delay preceding the test stimulus presentation (Fig. 1). For analyses pertaining to **Figs. 2-3**, we separated all trials into two groups, synchronized and desynchronized, depending on whether the PSI in the delay period was above or below the median PSI across all trials. In **Fig. 3f**, we recomputed PSI for the delay period using 20 windows of 50-ms duration, and 10 windows of 100-ms duration. We then calculated behavioral and decoder performance in the newly defined synchronized and desynchronized trials for each separate window size.

Fano factor:

To assess firing rate variability, we computed the Fano Factor (FF) for each neuron, defined as the spike count variance divided by the spike count mean. Spike counts were summed in a 50-ms window starting at the onset of the test stimulus (plus

a delay of 70 ms to account for the latency of V4 neurons, as observed in the recordings). For each neuron, FF was calculated for each test stimulus separately and then averaged across conditions. In a separate analysis, we slid the 50-ms window in 10-ms steps across the duration of the trial for comparisons with previous work¹⁵⁵.

Noise correlations:

Correlated variability was computed for each pair of neurons using the Pearson correlation coefficient $R(x,y)$ given by:

$$R(x, y) = \frac{\sum_{n=1}^N [x(n) - \bar{x}][y(n) - \bar{y}]}{\sigma_x \sigma_y}$$

where N is the number of trials, \bar{x} and \bar{y} are the means of x and y , respectively, and σ_x and σ_y are the standard deviations of x and y , respectively^{156,157}. We used the MATLAB function *corrcoef* to compute the correlation coefficient.

Linear classifier:

We decoded the neural activity by implementing a linear classifier which fits a multivariate normal density with a pooled estimate of covariance using the MATLAB function, *classify*. 50% of the data was used to train the classifier and determine an optimal decision boundary. The accuracy of the decoder was then evaluated on the remaining testing set of data. This process was repeated 100 times and classification performance was averaged across repeats. Data was analyzed separately for the synchronized and desynchronized trials of each session.

Behavioral threshold:

We divided the trials in two halves based on the median PSI and then fitted the psychometric curve of the behavioral response for the synchronized and desynchronized trials in each session to a Weibull function in order to obtain the discrimination threshold¹⁵⁸. The Weibull function was normalized by the false alarm rate, $P_{weib}(0)$. We implemented the following equations:

$$P_{weib}(\Delta\theta) = 1 - (1 - P_{weib}(0)) \cdot k \left(\frac{\Delta\theta}{\tau}\right)^b$$

$$k = \frac{1 - P_{weib}(\tau)}{1 - P_{weib}(0)}$$

$$d'(\Delta\theta) = z(\Delta\theta) - z(0) \Rightarrow z(\tau) = 1 + z(0)$$

$$P_{weib}(\tau) = z^{-1}[z(\tau)]$$

where τ is the discrimination threshold, $P_{weib}(\tau)$ is the proportion of correct responses corresponding to $d' = 1$, z is the z-transform, and b is the slope of the Weibull function.

Cell dropping procedure:

For each session, we sequentially removed neurons from the population synchrony analysis and then recomputed the behavioral and decoder performance using all combinations of the remaining neurons. For example, in a population of 10 neurons, we started by removing 1 neuron. Then, we recomputed the % difference in behavioral and decoder performance for the desynchronized and synchronized trials

assessed after computing PSI based on the remaining 9 neurons. We repeated this procedure for all combinations of 9 neurons and then averaged the results across samples. In the case of 9 neurons we would have $N = 10$ different combinations. The number of combinations is calculated using the formula: $v!/k!(v-k)!$, where k is the combination size and v is the number of total neurons in the pool. We next removed 2 neurons from the total pool of 10 neurons and computed the % difference in behavioral and decoder performance for the desynchronized and synchronized trials assessed after computing PSI based on the remaining 8 neurons. In this case, we would have 45 different combinations of 8 neurons. This was repeated until we removed all but 1 neuron from the total population. The final results were averaged across sessions and plotted based on the number of neurons removed from the population.

Statistics:

When the paired t-test was implemented, a Kolmogorov-Smirnov test was used to test the null hypothesis that the samples had a normal distribution ($p > 0.05$). When the data was not normally distributed, non-parametric tests were implemented, as noted in the main text.

False discovery rate is a method to correct for multiple comparisons and is defined as the expected proportion of rejected hypotheses that are mistakenly rejected. We implemented the method outlined by Benjamini and Yekutieli (2001)¹⁵⁹ that is guaranteed to be accurate for any test dependency structure. The false discovery rate was set at $q = 0.05$ for our analysis.

The Bonferonni correction is a more conservative approach to multiple-hypothesis testing. The procedure is conducted by simple dividing the significance

value α (0.05) by the number of observations. In Fig. 2C, we conducted 150 different comparisons and thus used $\alpha = 0.05/150$ for each statistical test¹⁶⁰.

Results

To analyze population synchrony across trials, we examined the single-unit spiking activity (up to 17 neurons per session) in a 1-second window preceding the test stimulus onset (Fig. 1B). We observed that even during actively engaged behavior, many trials were associated with strong fluctuations in cortical activity, characteristic of the synchronous state (Fig. 1C-F and Fig. 2). To quantify the degree of synchrony in each trial, we calculated the population synchrony index (PSI)^{78,126} during the delay period between the target and test stimuli (Fig. 1B). PSI is defined as the coefficient of variation (standard deviation divided by mean) of the average population firing rate (Fig. 1) in a given time interval using 10-ms bins (small bins can better capture rapid fluctuations in the population response). PSI has clear advantages over other methods of synchrony analysis, such as pairwise correlations, because it relies on the entire population, not just two cells, and can be computed in each trial. If the cells' responses are synchronous, the standard deviation of the binned mean population response will increase (because the mean firing rate of the population will fluctuate between low and high response states, Fig. 1F), and PSI will increase. If, on the other hand, cells are desynchronized, the standard deviation of the binned population response will decrease (the difference between the low and high states of the mean population response will decrease in amplitude, Fig. 1E), which causes PSI to decrease.

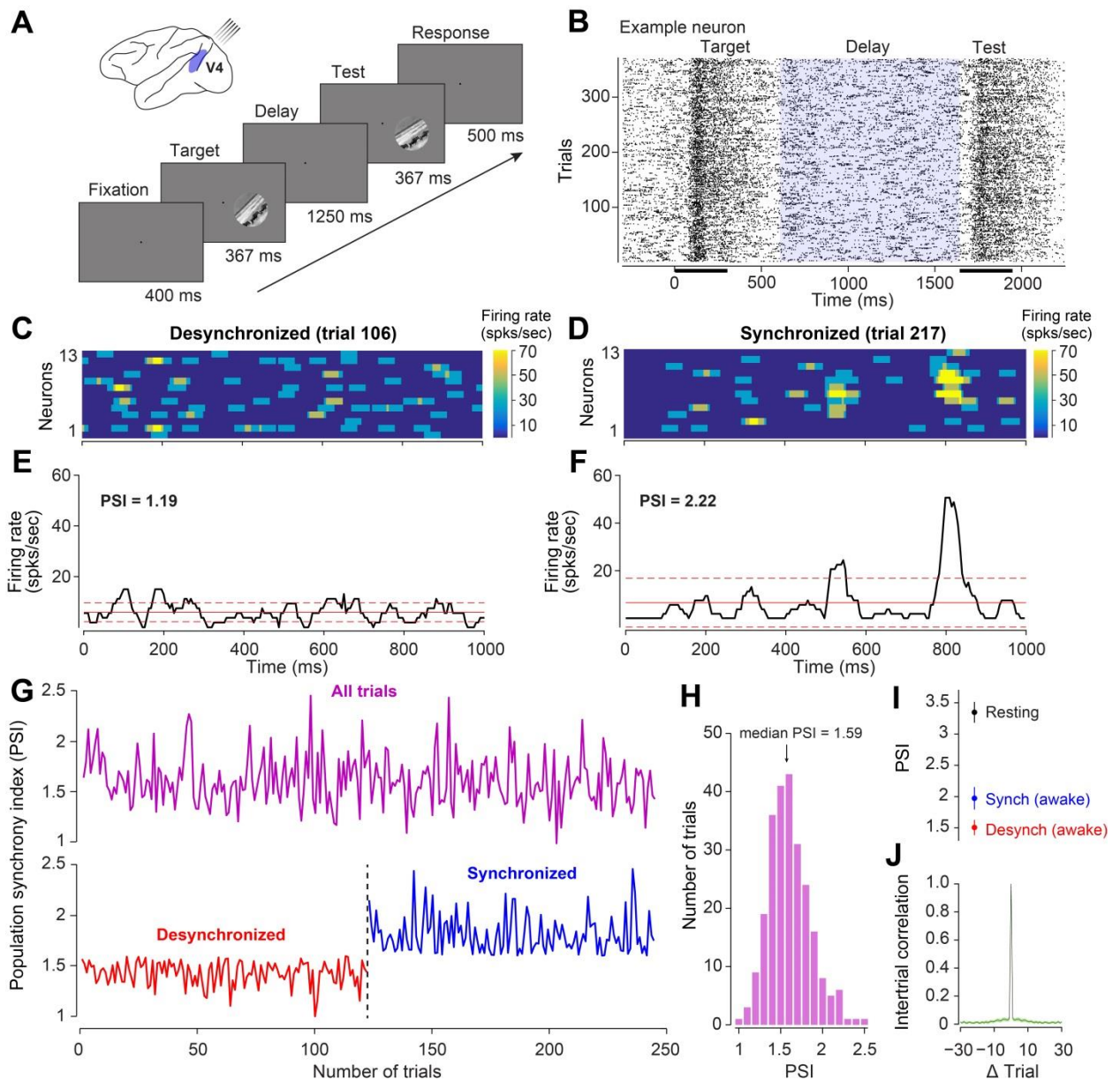


Figure III-1. Trial-by-trial fluctuations in population synchrony in V4.

(A) Schematic of the recording site and experimental design. Animals were trained to report whether two briefly flashed successive natural scenes (target and test) were identical or different. **(B)** Raster plot of one example neuron. The blue shaded inter-stimulus delay period was used to measure population synchrony in each trial. The black bars under the x-axis mark the time intervals when the two stimuli are presented. **(C-D)** Population response measured in individual trials from the same session – the neural population is desynchronized in trial 106 (panel C) and synchronized in trial 217 (panel D). **(D-F)** Population firing rate as a function of time for the example trials in panels C and D. The population of cells is desynchronized in trial 106 (PSI=1.19, panel E) and synchronized in trial 217 (PSI=2.22, panel F). The solid red line indicates the population mean firing rate; the red dotted lines indicate 1 standard deviation (s.d.) from this mean. **(G)** Top: Trial-by-trial population synchrony index (PSI) for the example session from panels C-F. Bottom: Trial-by-trial PSI after dividing the session into

desynchronized (PSI below median) and synchronized trials (PSI above median). **(H)** PSI histogram for the example session in panels C-G. **(I)** Average PSI across sessions for desynchronized (red) and synchronized trials (blue). These PSI values are compared to the mean PSI when animals rest for a 20 to 30-min period (black). Error bars represent standard error. **(J)** The mean autocorrelation function (across sessions) of trial-by-trial PSI.

Individual trials differed widely in their degree of synchrony of the ongoing population response (Fig. 1G, top). Since our goal was to examine the impact of these fluctuations in synchrony on the information encoded in population activity and on behavior, we separated trials into two groups, desynchronized and synchronized, based on whether PSI was lower or higher than the median PSI in each session (Fig. 1G, bottom). PSI values in each session were normally distributed rather than reflecting a bimodal distribution (Fig. 1H). However, our strategy to divide the trials by the median PSI enabled us to compare the network and behavioral performance between two equally-sized data sets. During wakefulness, PSI was significantly lower, both in the desynchronized and synchronized states, compared to the resting state when animals were sitting quietly in the dark with their eyes closed (desynchronized: $P < 0.0005$; synchronized: $P < 0.01$, Wilcoxon rank-sum, Fig. 1I). The autocorrelation of the trial-by-trial PSI values revealed that across sessions the state of synchrony fluctuates randomly during wakefulness ($r < 0.05$ for all trial intervals, Fig. 1J).

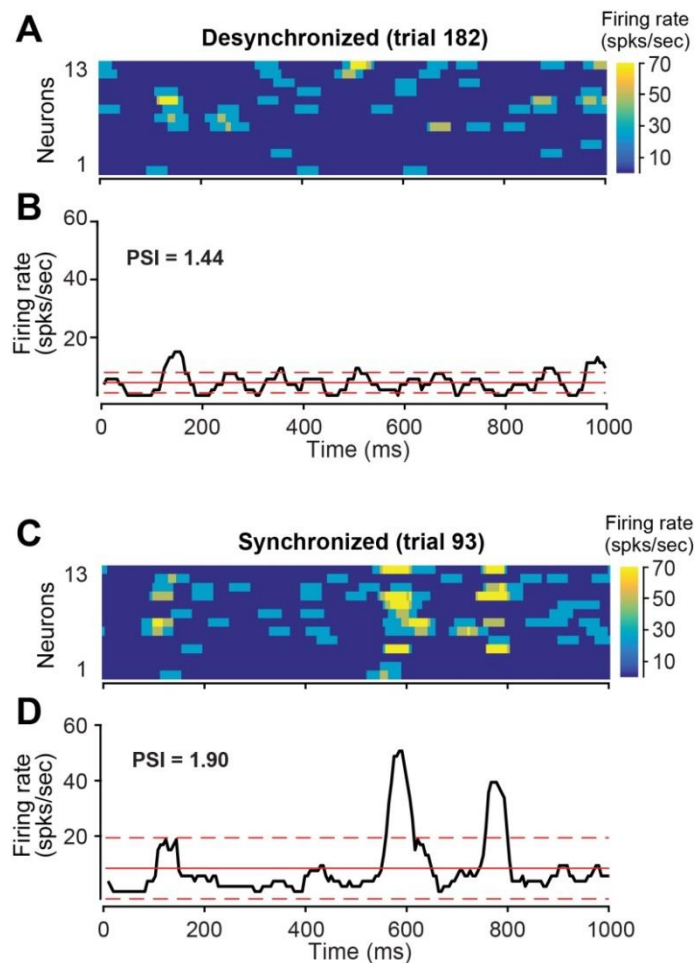


Figure III-2. Additional examples of population activity in desynchronized and synchronized trials.

(A) One example desynchronized trial with 13 simultaneously recorded neurons. The heat map represents the population firing rate for each neuron (40 ms rolling window, 5 ms step). **(B)** The average population firing rate plotted as a function of time for the trial displayed in panel A. Population synchrony index (PSI, see Methods) is denoted. The solid red line indicates the population mean firing rate for the trial, and the red dotted lines indicate 1 standard deviation from this mean. **(C)** One example synchronized trial with 13 simultaneously recorded neurons. **(D)** The average population rate plotted as a function of time for the trial displayed in A. Two periods of synchronized firing can be seen in this trial.

We further assessed the impact of fluctuations in cortical state on the neurons' firing rates and correlated variability as these variables have been shown to influence the available information in a population of cells^{156,161,162}. While previous studies have shown that anesthesia and sleep decrease firing rates and increase

correlations^{73,76,78,107,124}, whether these measures are influenced by fluctuations in the state of cortical populations during wakefulness is unknown. As shown in Fig. 3A, by comparing the ongoing firing rates for all the neurons during the delay period, we found a significantly increased firing rate in desynchronized trials ($P < 0.0001$). In contrast, even though we expected pre-stimulus activity to be correlated to stimulus evoked activity^{57,64}, there was no significant difference in evoked firing rates across the two states ($P = 0.903$). We further calculated the neurons' firing rate variability^{155,163,164}, or Fano factor (FF), for all the neurons in the synchronized and desynchronized trials, but found no significant difference between the two groups (Fig. 3B, $P = 0.23$). We also noticed a stimulus-driven decline in variability for both the synchronized and desynchronized trials (Fig. 3C), in agreement with previous work demonstrating widespread decline in variability immediately after stimulus onset¹⁵⁵.

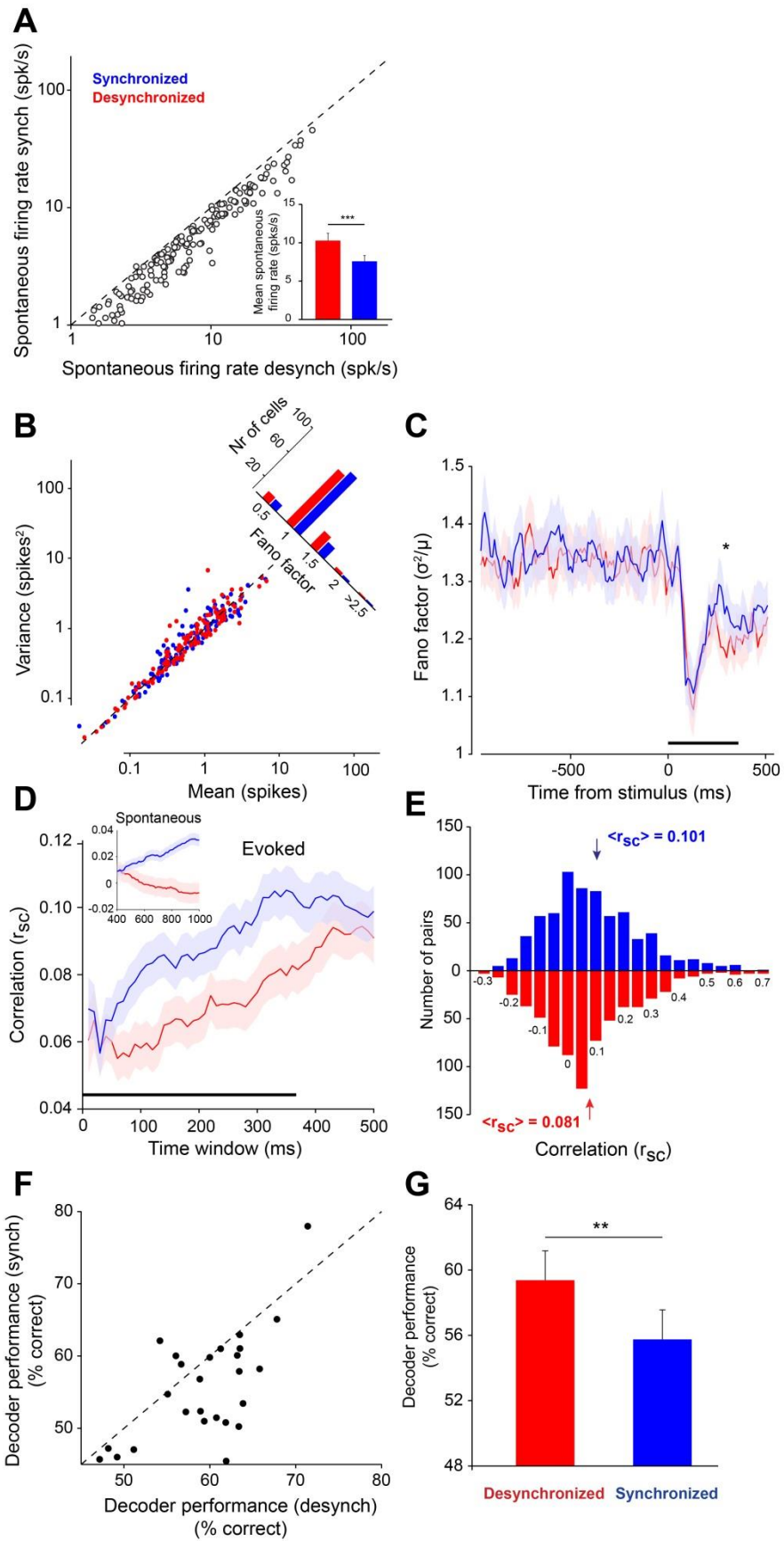


Figure III-3. Cortical state impacts the ability of the population of cells to extract sensory information.

(A) Firing rates are higher in the desynchronized cortical state. The scatter plot pools data across sessions (each circle represents one neuron). Inset: Mean firing rates of neurons in desynchronized and synchronized trials ($***P < 0.0001$). **(B)** Variance of spike counts vs. mean spike counts (computed in 50 ms bins) for the entire population of neurons in the desynchronized (red) and synchronized trials (blue). Top right, histogram of the Fano factor (variance/mean) for the entire population of cells in the two cortical states. **(C)** Fano factor plotted in a 50-ms sliding window (step size 10 ms) from 1-second before test stimulus presentation (black bar) to 500 ms past stimulus onset. **(D)** Pairwise correlation coefficient (r_{sc}) as a function of increasing window size during stimulus presentation (marked by the black line) for synchronized and desynchronized trials (blue and red lines, respectively). Shaded error represents standard error. Inset: correlation coefficient for the spontaneous neural activity represented as an increasing time window during the delay period (cell pairs were the same as in main figure). **(E)** Histogram of the evoked correlation coefficients for the synchronized and desynchronized trials. The arrows represent the mean $\langle r_{sc} \rangle$ for each group. **(F)** Scatter plot of decoder performance (% correct classification) in the synchronized vs. desynchronized state. Each circle represents a session. **(G)** Average decoder performance was significantly higher in the desynchronized state ($**P < 0.005$). Error bars represent standard error.

Prior studies have demonstrated that cortical state can strongly influence pairwise correlations in the anesthetized state^{76,78}, but little is known about how fluctuations in synchronized population activity during wakefulness impact correlations. We thus examined whether population synchrony impacts trial-by-trial fluctuations in correlated variability, or “noise correlations”, in the synchronized and desynchronized trials. We first analyzed the ongoing activity before stimulus presentation and found that correlations were higher in the synchronized state (Fig. 3D, inset, $P < 0.0001$), which is expected based on the increased population co-fluctuations in that state⁷⁸. We next compared stimulus evoked correlations during the stimulus period (Fig. 3D-E) and found significantly higher correlations in the synchronized state ($P < 0.001$). These results raise the possibility that trial fluctuations in cortical state may influence the accuracy with which the population of cells can decode stimulus orientation. To this

end, we used the neurons' responses to the target and test stimuli to train an optimal linear classifier to discriminate between the two stimuli, exactly as the animals were required to do in the task. We found that the network of cells performed significantly better in desynchronized trials, characterized by lower correlations ($P < 0.005$, Fig. 3F-G). Altogether, these results indicate that trial-by-trial fluctuations in network synchrony significantly influence correlated variability and the amount of information in population activity.

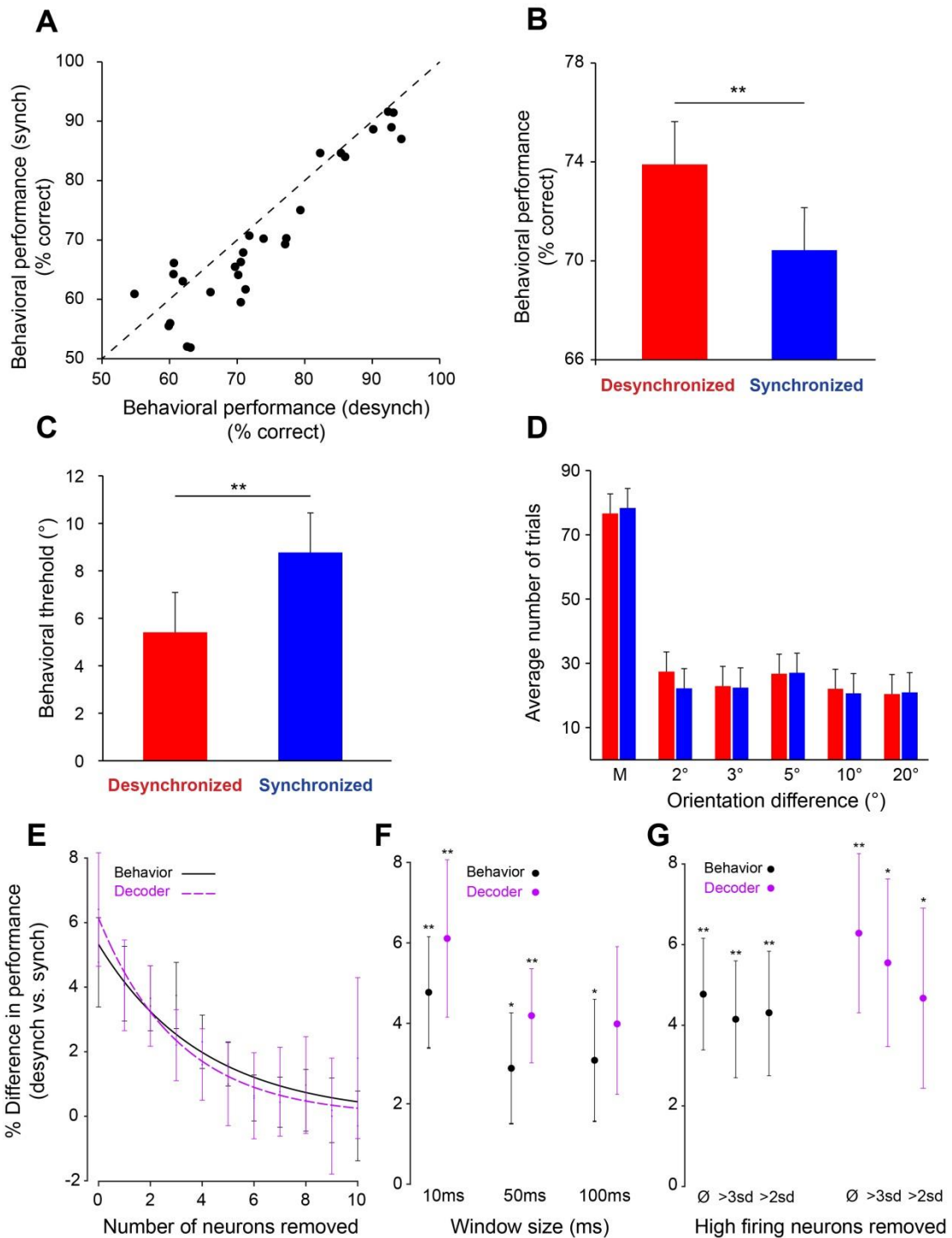


Figure III-4. Population synchrony impacts behavioral performance.

(A) Scatter plot of the behavioral performance (% correct responses) in synchronized vs. desynchronized trials. Each point represents one session. **(B)** Mean behavioral performance is significantly higher in desynchronized trials (** $P < 0.001$). Error bars represent standard error. **(C)** Average behavioral performance threshold is significantly lower in desynchronized trials (** $P < 0.005$). **(D)** Average number of trials (across sessions) corresponding to each test orientation difference for synchronized and

desynchronized trials. 'M' stands for 'match' condition (0° orientation difference). **(E)** Percent difference in behavioral and decoder performance between the desynchronized and synchronized trials using the cell-dropping procedure (behavior: black; decoder: purple). The two curves represent exponential fits. Error bars represent standard error. **(F)** Percent difference in behavioral and decoder performance between desynchronized and synchronized trials for different window sizes to define PSI (**P < 0.005, *P < 0.05). **(G)** Percent difference in behavioral and decoder performance between desynchronized and synchronized trials after removing the high firing rate (outlier) neurons from the population. \emptyset represents no neurons removed, >3 s.d. and >2 s.d. represents removing neurons with average spontaneous firing rates > 3 s.d. and 2 s.d. above the population mean (**P < 0.005, *P < 0.05).

Based on the results of the decoder analysis, we further hypothesized that the higher accuracy with which the network of cells encodes sensory information in the desynchronized cortical state may be correlated with an increase in behavioral performance in the discrimination task. Indeed, our analysis confirmed this hypothesis – behavioral performance (percentage of correct responses) was significantly higher in desynchronized trials (Fig. 4A-B; see also Fig. 5 for individual animal performance; $P < 0.001$). Another measure of performance, the orientation discrimination threshold (obtained by fitting the psychometric curve of the behavioral response to a Weibull function), was also significantly lower in the desynchronized state (Fig. 4C, synchronized: 8.76 ± 1.32 ; desynchronized: 5.41 ± 1.10 , $P < 0.005$). Furthermore, we found even larger differences in behavioral performance between the two network states when comparing the top third (vs. bottom third), or top quarter (vs. bottom quarter), most synchronized and desynchronized trials (Fig. 5). One potential confound when interpreting our behavioral results is that animals might have discriminated stimuli better in the desynchronized cortical state simply because those trials were associated with less difficult test orientations (our range of orientations was 2-20°). However, that was not the case – when we compared the average number of trials associated with each cortical state we found no significant difference across orientations (Fig. 4D, $P >$

0.05), indicating that our results were not due to differences in task difficulty. These results provide the first demonstration that trial-by-trial fluctuations in population synchrony during wakefulness modulate behavioral performance.

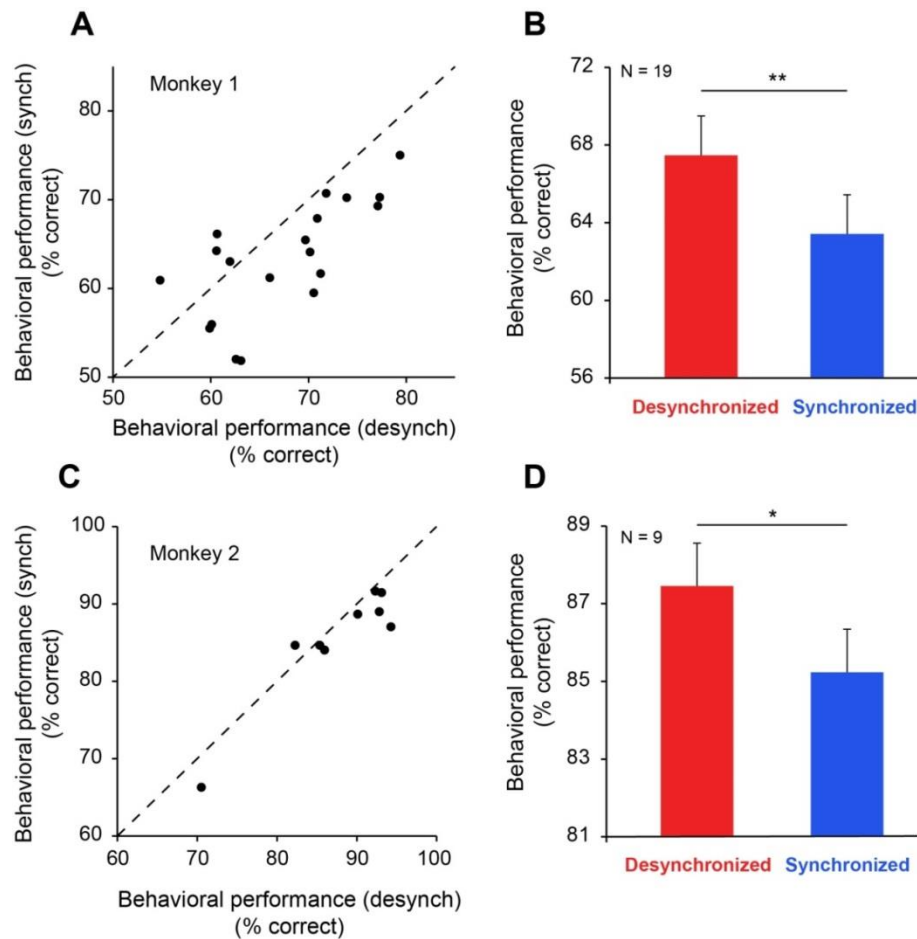


Figure III-5. Behavioral performance is higher in desynchronized trials for each monkey.

(A and C) Scatter plots showing the % correct responses in the synchronized vs. desynchronized trials for monkey 1 (panel A, N = 19 sessions) and monkey 2 (panel C, N = 9 sessions). **(B and D)** Behavioral discrimination performance was significantly greater in the desynchronized trials for monkey 1 (**P < 0.01) and monkey 2 (*P < 0.05).

Our measure of population synchrony (PSI) is based on the spiking activity of all the simultaneously recorded neurons within a session. Thus, we reasoned that the impact of PSI on network accuracy and behavioral performance would diminish if the

number of neurons pooled for the calculation of PSI is decreased – in this case, the PSI measure would not accurately reflect the ‘true’ state of the population of recorded neurons. We addressed this issue by sequentially dropping neurons from the population while recalculating the relative difference in behavioral and network performance in the two cortical states. The results confirmed our expectation – the difference between the effects associated with the two population synchrony states gradually diminished as more neurons were discarded from our sample (Fig. 4E, $P < 0.05$). This analysis raises the possibility that recording simultaneously from large ensembles of neurons – e.g., several thousands of cells – would provide even more accurate measures of network synchrony that may be used to explain an even larger fraction of the perceptual variability observed experimentally.

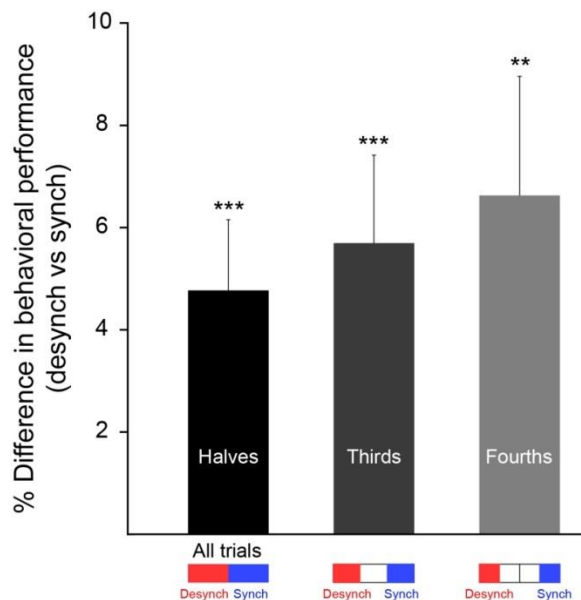


Figure III-6. Percent performance difference between desynchronized and synchronized trials using different trial separation criteria.

“Halves” represents the method implemented throughout the manuscript. That is, we separated all trials based on the median population synchrony index (PSI) value and then compared behavioral performance in the desynchronized vs. synchronized trials

(***P < 0.001). 'Red' represents the proportion of desynchronized trials, and 'blue' represents the proportion of synchronized trials chosen for the analysis. "Thirds" represents a classification scheme where we extracted the top 1/3 of the most synchronized trials and the bottom 1/3 of the most desynchronized trials, and then compared the two groups (***P < 0.001). "Fourths" represents a classification scheme where we extracted the top 1/4 of the most synchronized trials and the bottom 1/4 of the most desynchronized trials, and then compared the two groups (**P < 0.005).

Our results critically depend on the temporal resolution of the PSI measure. For instance, the results in **Figs. 1-3** were obtained using a bin size of 10 ms in order to capture rapid fluctuations in population synchrony. However, using larger time windows, e.g., 50 or 100 ms, still yields significant differences in behavioral performance between the synchronized and desynchronized cortical states (**Fig. 4F**, P < 0.05); decoder performance difference remained statistically significant for the 50 ms bin size (**Fig. 4F**, P < 0.001), but not for 100 ms (P = 0.078). The fact that the neural and behavioral effects induced by fluctuations in population synchrony are diminished when using larger time bins indicates that a low-resolution PSI fails to explain the variability in neuronal and behavioral performance during wakefulness. Lastly, we investigated whether our main results were being driven by a small subset of high-firing neurons which would dominate the population rate. To control for this possibility, we removed from the analysis those neurons with spontaneous firing rates three, or two, standard deviations above the mean. However, even in this case we found that behavioral and decoder performance were still significantly improved in the desynchronized state (**Fig. 4G**, P < 0.05).

Although we measured population synchrony based on the spiking activity of single neurons, another way to capture the fluctuations in network activity, ostensibly with less precision, is using local field potentials (LFPs)^{74,76,165,166}. The synchronous

state in this alternate classification scheme would be associated with high LFP power in the low frequency range (0.5-10 Hz) and low power in the high frequency range (10-100 Hz)^{76,151,165}. Thus, we reexamined the functional impact of fluctuations in population synchrony by computing the normalized LFP power in the synchronized and desynchronized trials (defined by the PSI measure, **Fig. 7A**) – we found that the synchronous cortical state is associated with an increase in low-frequency LFP power ($P < 0.0001$) and a decrease in high-frequency LFP power. Importantly, using the LFP power ratio – low frequency power (2-10 Hz) / high frequency power (10-100 Hz) – as a measure of population synchrony, we found that behavioral performance was higher in trials characterized by a desynchronized state ($P < 0.01$, **Fig. 7C-D**). Lastly, we selected the synchronized and desynchronized trials using both the PSI and LFP power ratio criteria. That is, trials were independently classified based on the median PSI and the median power ratio, and only the trials associated with the same state of synchrony in both classification schemes were analyzed. We found that combining multiple single-unit and LFP signals to define population synchrony leads to an improved definition of cortical state – there was an enhanced difference in behavioral performance ($P < 0.005$, **Fig. 7C-D**) in the synchronized vs. desynchronized trials relative to the case when power ratio alone or PSI alone were used to measure population synchrony ($P < 0.05$).

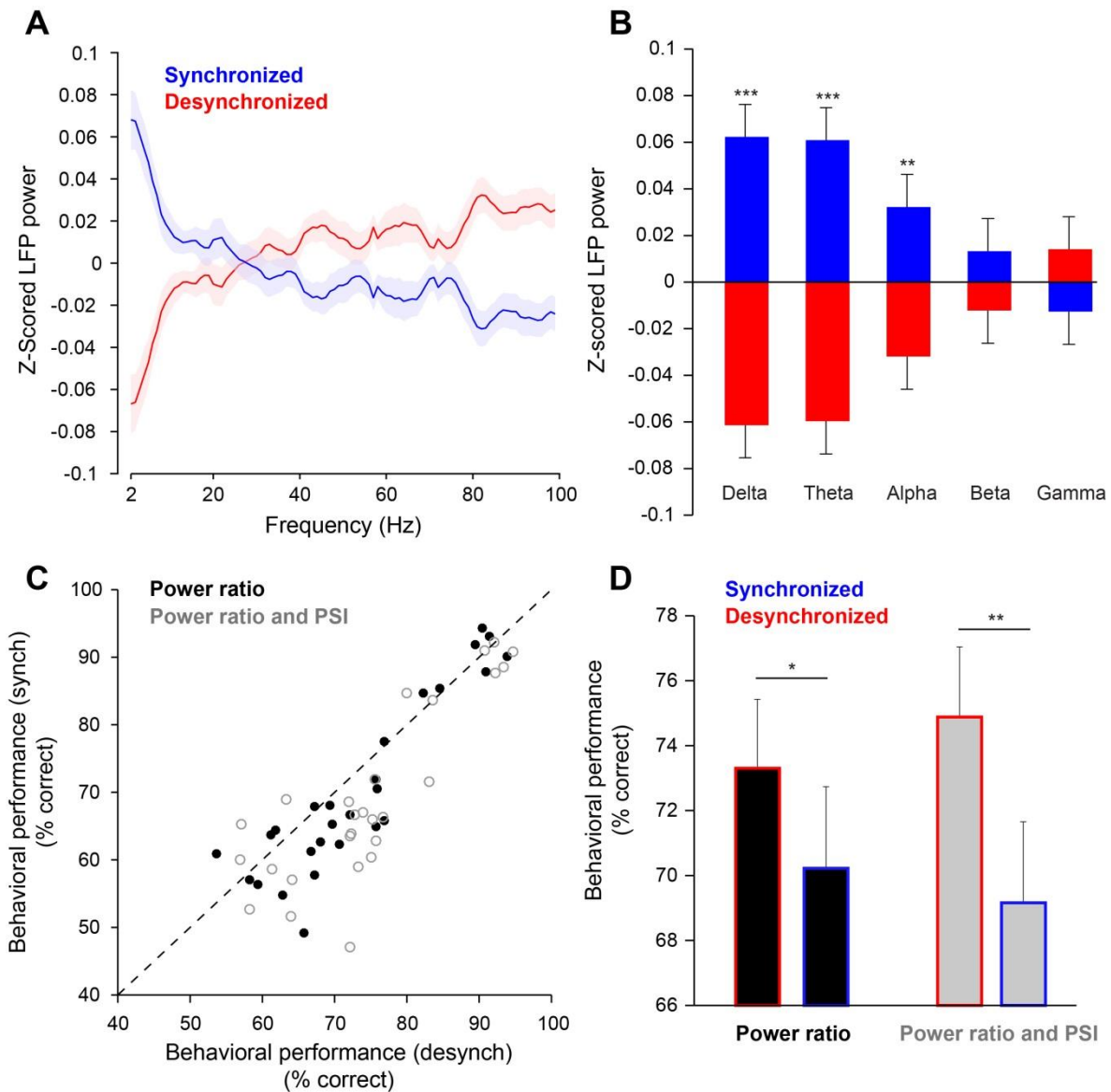


Figure III-7. Using LFP power to characterize the functional impact of population synchrony.

(A) z-scored LFP power in synchronized and desynchronized cortical states (defined by PSI). LFP power was calculated using a 5 Hz rolling window size with a step of 1 Hz. Shaded areas represent standard error. **(B)** z-scored LFP power in physiologic bands for synchronized and desynchronized trials (as defined by PSI) (Delta = 2-4 Hz, Theta = 4-8 Hz, Alpha = 8-12 Hz, Beta = 12-30 Hz, Gamma = 30-100 Hz) (** $P < 0.0001$, ** $P < 0.005$). **(C)** Black dots: Scatter plot of behavioral performance (% correct responses) in desynchronized/synchronized cortical states (defined by the LFP power ratio). Each point represents one session. Gray circles: Scatter plot of behavioral performance in desynchronized/synchronized cortical states. Trials were selected only if they shared the same state of synchrony using both the PSI and the power ratio methods. **(D)** Difference in average behavioral performance (% correct responses) between synchronized and desynchronized states was higher when cortical state was assessed

using both the PSI and power ratio methods (*P < 0.01; **P < 0.0005). Error bars represent standard error.

Discussion

In summary, our results demonstrate that rapid fluctuations in local population synchrony during wakefulness impact both the information encoded in network activity and behavioral performance. That is, synchronous fluctuations in population ongoing activity influence the strength of sensory responses and interneuronal correlations such as to decrease network discrimination performance and reduce perceptual accuracy even when the animal is seemingly alert and actively engaged in the task. The functional impact of cortical state has been previously examined in anesthetized animals^{76,78,126}, and recently using measures of arousal, such as pupil diameter, in awake mice^{123,151}. However, whether fluctuations in cortical population synchrony are able to influence the accuracy of sensory discriminations while the animal is awake and performing a task had been unknown.

Several mechanisms could be invoked to explain the rapid shift in cortical state from synchronized to desynchronized (and vice-versa), such as fluctuations in the strength of inputs to subcortical cholinergic nuclei or fluctuations in the glutamatergic inputs from thalamus and possibly other cortical regions. For instance, lesions of the basal forebrain, which provides cholinergic input to the cortex, have been shown to increase the low-frequency LFP power^{165,167}, and stimulation of the basal forebrain causes cortical desynchronization¹⁶⁷⁻¹⁷⁰. To further elucidate the functional role of fluctuations in population synchrony, future studies are needed to causally manipulate synchrony in the cortex and measure its impact on the trial-by-trial population code and

behavioral responses. Importantly, it remains to be seen whether the rapid fluctuations in population synchrony during wakefulness are coordinated across brain areas and whether the spatiotemporal pattern of population activity is relevant for behavior.

**CHAPTER IV: Rest Desynchronizes Cortical Networks and Improves Behavioral
Performance**

Introduction

Rest is a universal activity in animals¹⁷¹. It is known that neurons in the brain cannot fire eternally without intermixed periods of quiescence. However, the specific function of rest in the cortex remains elusive. Previous investigations have demonstrated that even brief periods of rest have a beneficial effect on cognitive and behavioral performance in a variety of tasks, including those involving visual stimuli^{79,81,87,172-174}. Importantly, it has been shown that human test subjects increase their perceptual performance following naps as short as 6 minutes in duration^{86,87}. In animal studies, it has been observed that cortical networks begin to oscillate between high and low firing states, primarily at frequencies between 0.5 and 4 Hz (delta waves), as animals begin to fall asleep^{67,68}. Thus, it is likely that high amplitude delta waves serve an important function for cortical networks. Yet, despite these previous studies, we still do not understand whether and how rest impacts the accuracy of neuronal network computations to improve behavioral performance.

Why is a network-based understanding of the function of rest important to study? Behavioral performance is more accurate than would be predicted from the responses of single neurons¹⁷⁵⁻¹⁷⁷. In addition, theoretical work has shown that population coding schemes encode more information than single cell coding schemes¹⁷⁸⁻¹⁸⁰. Unfortunately, despite the clear importance of understanding how populations of cells encode information, whether and how rest changes population coding accuracy remains unknown. Previous research from our lab (chapter III) has demonstrated that desynchronized networks are more optimal for neural coding and behavioral performance. Thus, we hypothesize that rest improves behavioral performance through cortical desynchronization that leads to enhanced accuracy of network coding in visual

area V4. To test this hypothesis, we recorded from populations of neuron in V4 while monkeys participate in a match-to-sample orientation discrimination task. After a 90 minute task period, we let the animals rest quietly in the experiment room, while electrophysiological recordings continue. After the rest period, we had the animals participate in a second task period. In this way, we tested if rest improves networks coding and behavioral performance in non-human primates.

Methods

All experiments described here were conducted in accordance with protocols approved by the National Institutes of Health and the Institutional Animal Care and Use Committee at The University of Texas Health Science Center at Houston. The surgical procedure was conducted as described in chapter III of this thesis.

Behavioral task:

Two male rhesus monkeys (*Macaca mulatta*) were trained to participate in a match-to-sample orientation discrimination task as described in chapter III of this thesis. Unique to this experiment, the animals participated in one of two separate block designs on each day (Fig. 1b). In the main experiment, called the 'rest' condition, the monkeys underwent between 200 and 300 trials of the orientation discrimination task, lasting approximately 90 minutes. They were then allowed to rest quietly in a dark room for 20-30 minutes. During the rest period, white noise was played to prevent outside noises from disturbing the animals. Eye tracking and video monitoring was conducted throughout the rest period (Fig. 1a). The daily experiments were timed such that the

rest period would fall at approximately 2pm, a time when monkeys naturally take daytime naps¹⁵⁴. Following the rest period, they engaged in a second task period of 200 to 300 trials, again lasting approximately 90 minutes.

In the control experiment, called the 'no rest' condition, animals also participated in the first and second task periods. In this condition, however, the animals were kept awake in a well-lit room for 20-30 minutes between the two task periods. One experimenter would stay in the room for the duration of the 'no rest' period to ensure that the animals remained awake. The animals participated in the main experiment and control experiment on randomized days so that they could not easily anticipate which condition they would experience on any given day.

Visual stimuli, eye movement, electrophysiology, synchrony index:

These methods were conducted as described in chapter III of this thesis.

Population d':

The discriminability between the target and test stimuli was computed using a multivariate generalization (due to many neurons being recorded simultaneously) of d^2 ^{35,130,131} given by:

$$d^2 = \Delta\mu^T Q^{-1} \Delta\mu;$$

Where $\Delta\mu$ is the vector difference in mean responses between the target and test orientation and Q is the pooled covariance matrix. The probability of correct classification was computed using a complementary error function:

$$\text{erfc}(-\sqrt{d^2})/2$$

Linear classifier:

A 50% train and test linear classifier was implemented as described in chapter III.

Statistics:

Neural data recorded in task 1 and task 2 from the same animal, and on the same day, were considered paired data. All other data was unpaired. For paired data, a Wilcoxon sign rank test was implemented. For unpaired data, a Wilcoxon rank sum test was used.

Results

To assess the impact of rest on perceptual performance, we recorded simultaneous spiking activity from populations of neurons in visual area V4. The animals participated in two natural image orientation discrimination tasks on each experimental day (Fig. 1C). In the main experimental condition, animals participated in task 1, which lasted approximately 90 minutes. Then, they were allowed to rest quietly for 20-30 minutes, and lastly, they participated in task 2, lasting another 90 minutes (Fig. 1A-B). In a separate control experiment, the animals were kept awake for 20-30 minutes in a brightly lit room between tasks 1 and 2 (Fig. 1B). To assess population synchrony on a trial-by-trial basis, we analyzed the spiking of neurons in the delay period between the target and test stimuli on each individual trial (Fig. 1D). Then, to quantify the level of synchrony on individual trials, we computed the coefficient of variation of the mean population firing rate, defined as the population synchrony index

(PSI), for the 1-sec delay period. Trials with more synchronous activity display a larger variance in the population rate compared the mean and thus a higher PSI. If neural firing is more desynchronized, the variance of the population rate is small compared the mean, leading to a smaller PSI. We observed that population activity was relatively desynchronized in awake, behaving animals (Fig. 2A and C). We continued our electrophysiological recordings throughout the 'rest' period. As the animals rested quietly in the room with their eyes closed, the network became more synchronized, as expected from decades of sleep literature (Fig. 2B and D)^{67,89,94}.

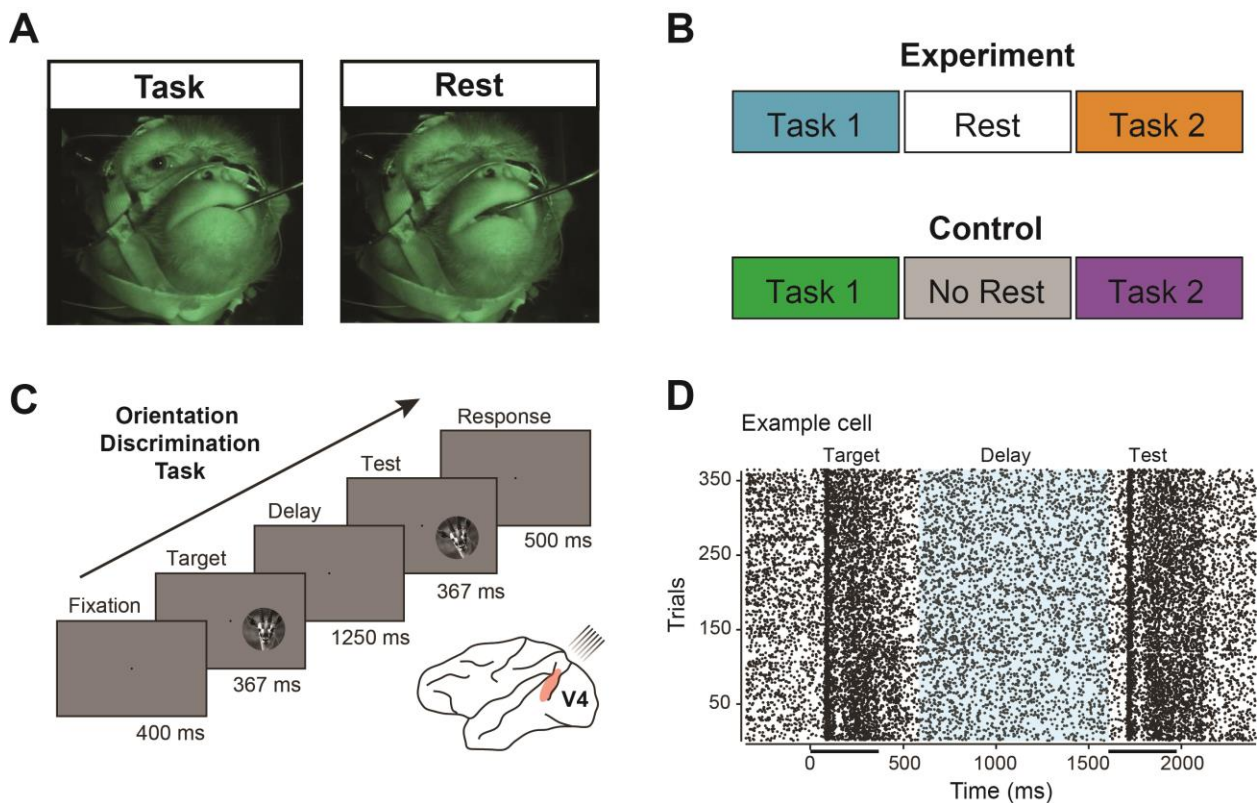


Figure IV-1. Design for rest experiment and orientation discrimination task.

(A) Night vision video of one monkey during the task and rest periods. **(B)** Top, the paradigm for the main experiment in task–rest–task block design. Bottom, the control paradigm consists of a task–no rest–task block design. **(C)** Schematic of the recording site and orientation discrimination task. Animals were trained to report whether two briefly flashed successive natural scenes (target and test) were identical or different. **(D)** Raster plot of one example neuron. The blue shaded delay period was used to

measure population synchrony on a trial-by-trial basis. The black bars under the x-axis mark the time intervals when the two stimuli, target and test, are presented.

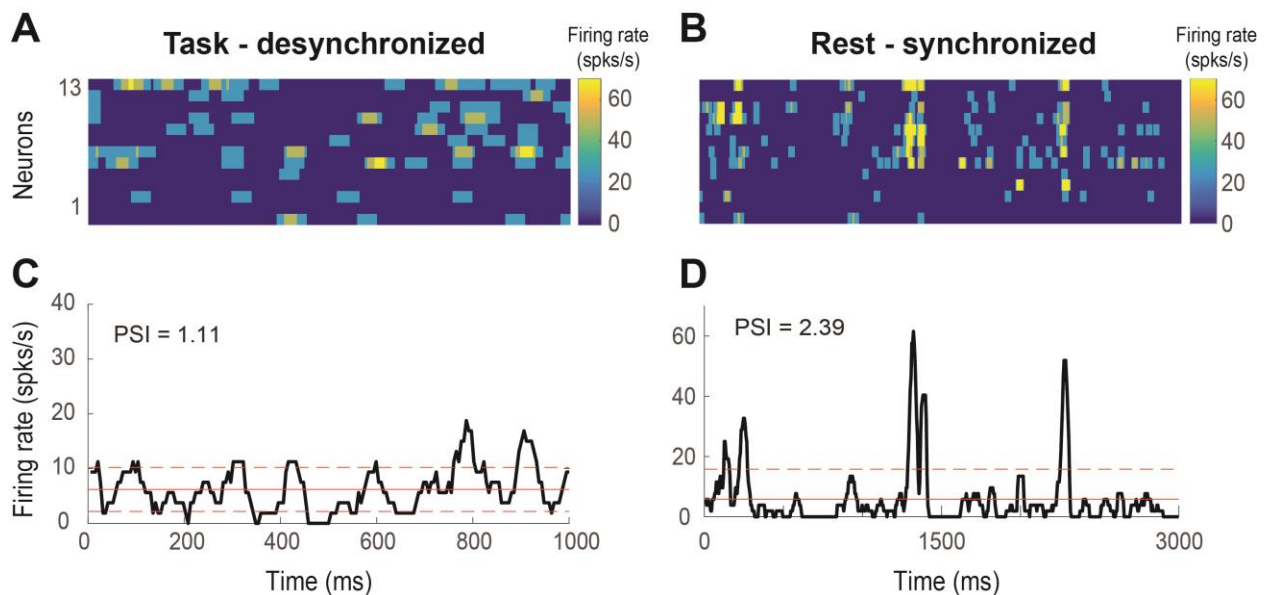


Figure IV-2. Single unit and population firing rates in two example time periods.

(A) Firing rates of 13 simultaneously recorded neurons from one example trial computed in a 40ms rolling window (step size 5 ms). The neurons fire in a desynchronized pattern. **(B)** Firing rates of the same 13 neurons during the rest period. Three synchronized up and down periods can be observed in this 3 second example. **(C)** Population firing rate for the desynchronized trial shown in A. The solid red line indicates the population mean and the dotted lines indicate 1 s.d. from the mean. PSI, population synchrony index (coefficient of variation of the population rate) **(D)** Same as figure C, but for the synchronized 3 second example depicted in B.

The implementation of population firing rate is a relatively new way to measure synchrony in networks that has only been available with the advent of recording from large numbers of individual neurons simultaneously^{78,126}. However, synchrony in cortical networks has been monitored for many years using field potentials (both EEG and local field potentials), which pool subthreshold and spiking activity from thousands of neurons in the vicinity of the recording electrode^{69,85}. The synchronized state defined by LFP is characterized by high power in the low frequency range (0.5 to 10 Hz) and

low power in the high frequency range (10 to 100 Hz). We computed the ratio of low LFP power to high LFP power (LFP power ratio) across the 'rest' period to compare the two different measures of population synchrony. As shown in Fig. 3, PSI and LFP power ratio track each other very closely across the eyes closed and eyes portion of the rest period in this example session (Fig. 3A – C). Thus, it is likely that the synchrony in local networks is related to the population synchrony of larger regions of the surrounding cortex.

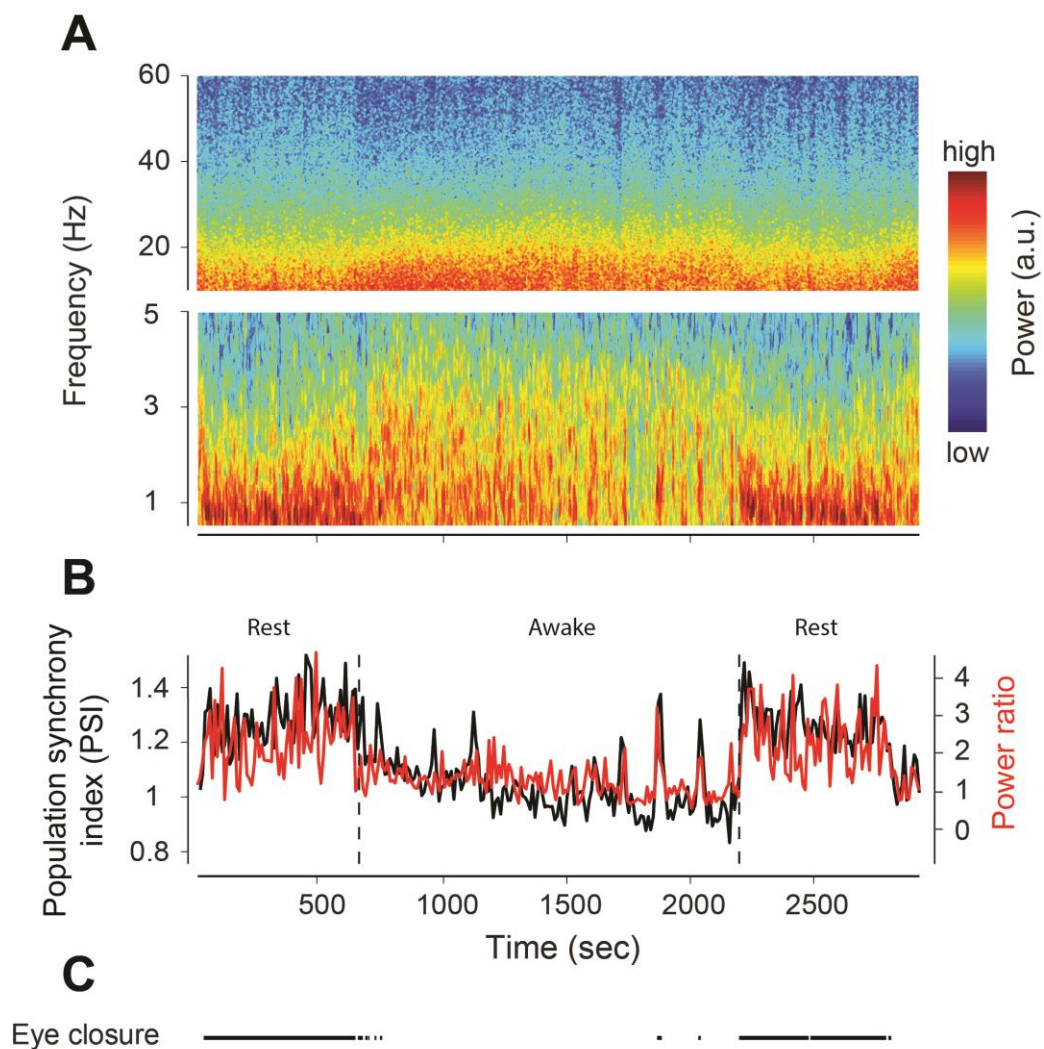


Figure IV-3. LFP Power Ratio and population synchrony rise during rest period.

This data represents an example resting period from 1 session. The monkey rested at the beginning of the rest period, then spontaneously awoke, then rested again at the

end of the period. **(A)** LFP power in low frequencies is higher and LFP power in high frequencies is lower during rest periods. **(B)** Population synchrony measured with the LFP Power Ratio (red) and Population Synchrony Index (PSI, black) are higher during rest periods. PSI and LFP Power Ratio were computed in contiguous 10 sec intervals throughout the rest period. **(C)** Eye closure corresponds to synchronized neural activity.

We next conducted analysis to answer our principal question in this study: does rest improve behavioral performance? As shown in figure 4, we found that behavioral performance was significantly improved in task 2 compared to task 1, when the monkeys were allowed to rest ($P < 0.0001$, Wilcoxon sign rank). In our control ‘no rest’ experiment, we found that task 2 behavioral performance was significantly worse than task 1 behavioral performance ($P < 0.005$, Wilcoxon sign rank). Importantly, we found that the percent difference in behavioral performance in task 2 vs. task 1 was significantly greater in the ‘rest’ condition compared to the ‘no rest’ condition ($P < 0.0001$, Wilcoxon rank sum) (Fig. 4).

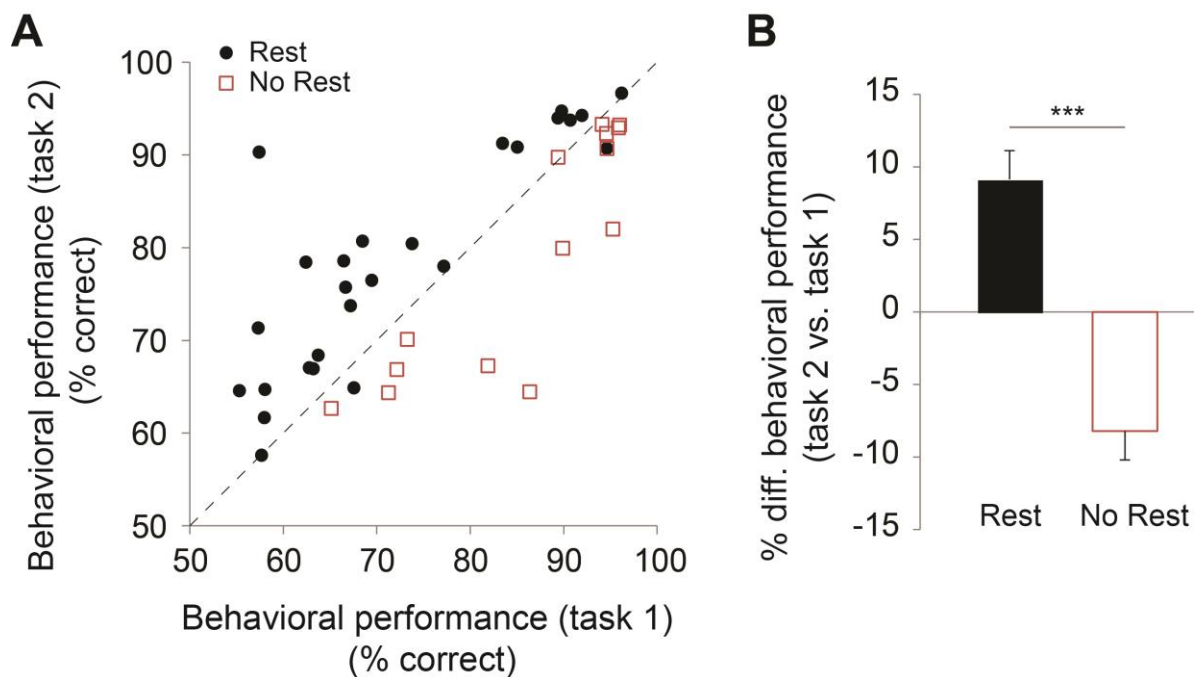


Figure IV-4. Behavioral performance is improved following rest.

(A) Behavioral performance of orientation discrimination in task 2 plotted as a function of behavioral performance in task 1 for the 'rest' (black circles) and 'no rest' (red squares) conditions. The dotted line represents unity. **(B)** The percent difference in behavioral performance of task 2 vs. task 1 is significantly greater in the 'rest' condition compared to the 'no rest' condition (** $P < 0.0001$, Wilcoxon rank sum). Error bars represent s.e.m.

These findings demonstrate that synchronized rest periods improve behavioral performance, but it is important to understand how cortical networks change from task 1 to task 2 following 'rest' compared to 'no rest'. Do neural properties change following synchronized rest in a way that reflects increased behavioral performance? We first set out to answer this question by comparing the mean PSI in task 1 and task 2 in both the 'rest' and 'no rest' experiments and found that following rest, cortical networks become significantly desynchronized ($P < 0.005$, Wilcoxon sign rank) (Fig. 5, left). In contrast, the mean synchrony did not significantly change when animals were not allowed to rest ($P > 0.05$, Wilcoxon sign rank) (Fig. 5, right). This indicates that synchronized rest periods have a causal effect to desynchronize the state of subsequent cortical networks.

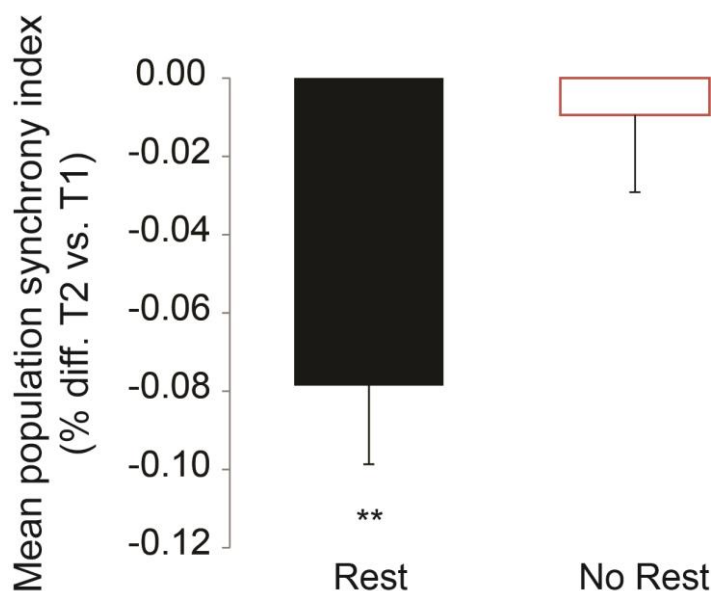


Figure IV-5. Population synchrony decreases following rest.

The % difference in mean PSI between task 1 and task 2 in the ‘rest’ and no rest’ conditions. PSI is significantly decreased in task 2 compared to task 1 in the ‘rest’ condition (** $P < 0.005$, Wilcoxon sign rank). There is no significant difference between task 1 and 2 in the ‘no rest’ condition.

As observed in chapter III of this thesis, desynchronized networks have been shown to be optimal for network coding, but whether neural properties change following rest has never been fully characterized. We first compared the spontaneous firing rates in both task 1 and task 2 in the ‘rest’ and ‘no rest’ condition. We found that spontaneous firing rates were significantly increased following rest but not following the ‘no rest’ condition ($P < 0.0001$, Wilcoxon sign rank) (Fig. 6). In previous work, it has been demonstrated that ongoing firing rates can impact evoked firing rates⁵⁷, thus, I set out to determine if test stimulus firing rates were similarly increased following resting periods. As shown in figure 7, the evoked firing rates were significantly increased in task 2 compared to task 1 in the ‘rest’ condition, but the evoked firing rates were slightly decreased in task 2 compared to task 1 in the ‘no rest’ condition ($P < 0.05$ and not significant, Wilcoxon sign rank). A difference in feedforward drive may be partly responsible for the increase in perceptual performance observed following rest.

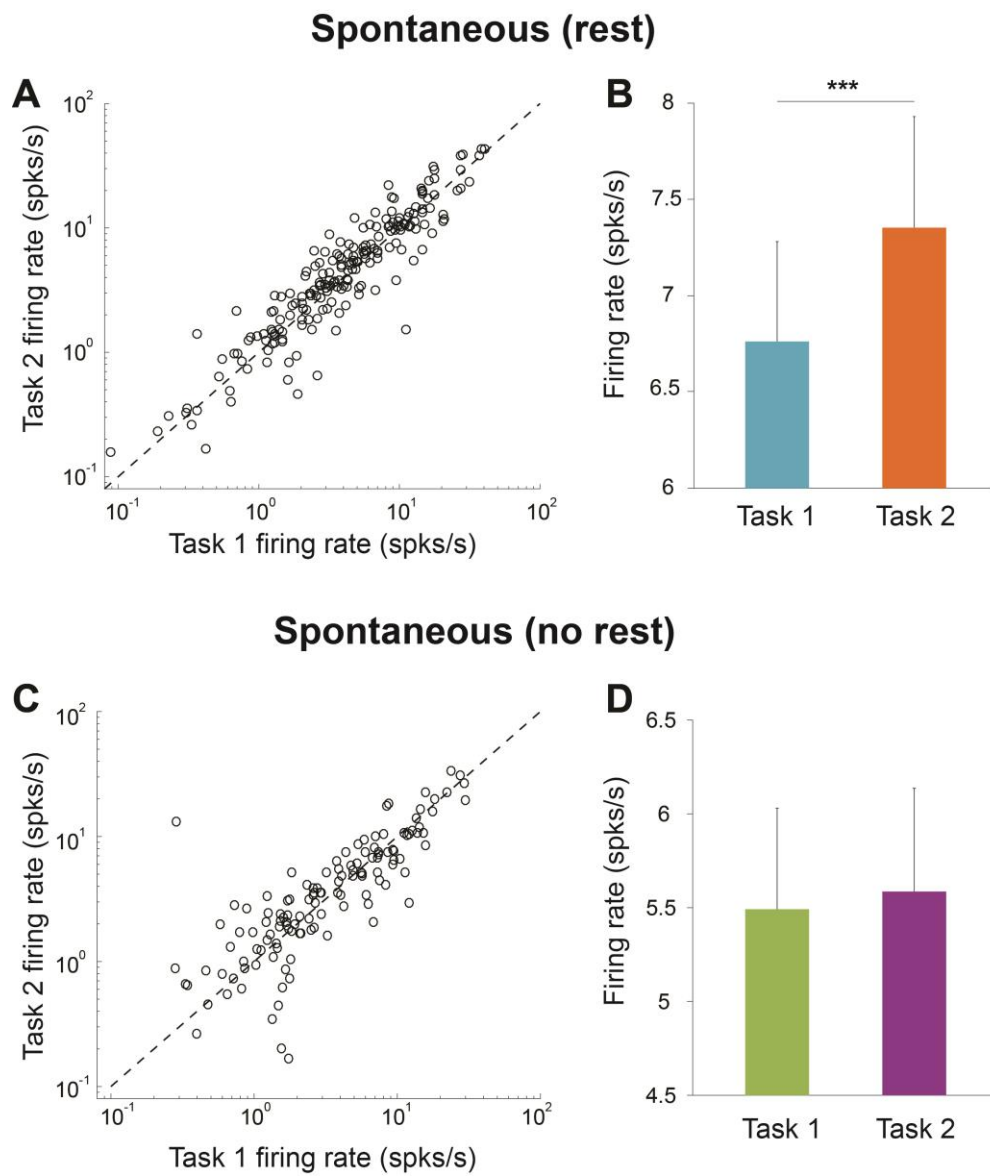


Figure IV-6. Spontaneous firing rates are increased following rest.

(A) Task 2 spontaneous firing rates plotted as a function of task 1 spontaneous firing rates in the 'rest' condition. Each circle represents one neuron in each condition. Spontaneous refers to the inter-stimulus delay period, as in figure 1. **(B)** The spontaneous firing rates are significantly increased in task 2 compared to task 1 (** $P < 0.005$, Wilcoxon sign rank). **(C-D)** Same as in A and B but for all the neurons recorded in the 'no rest' condition sessions. There is no significant difference in spontaneous firing rates between task 1 and task 2.

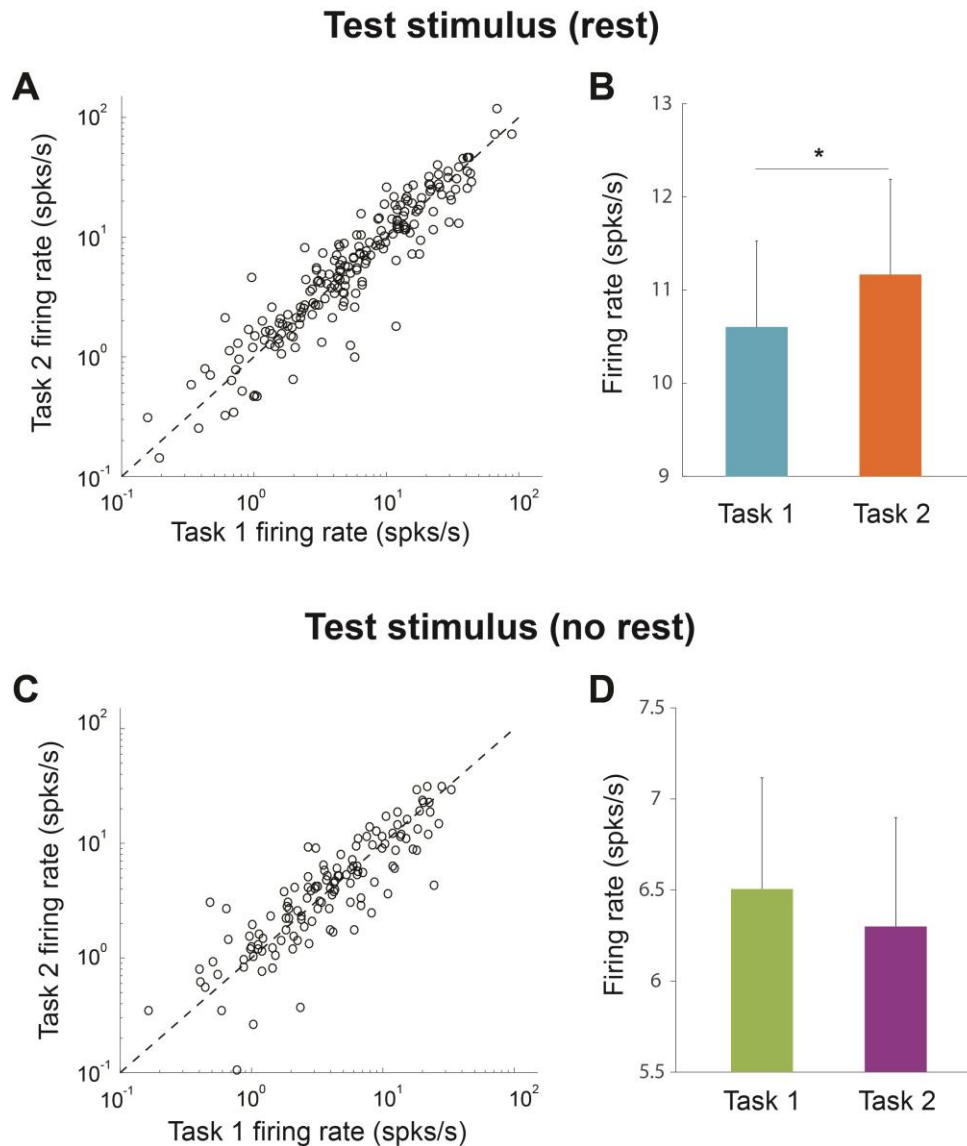


Figure IV-7. Evoked firing rates in the test period are increased following rest.

(A) Task 2 evoked firing rates plotted as a function of task 1 evoked firing rates in the 'rest' condition. Each circle represents one neuron in each condition. Test stimulus refers to evoked firing rates while the test stimulus was presented. **(B)** The evoked firing rates are significantly increased in task 2 compared to task 1 (** $P < 0.05$, Wilcoxon sign rank). **(C-D)** Same as in A and B but for all the neurons recorded in the 'no rest' condition sessions. There is no significant difference in evoked firing rates between task 1 and task 2.

Firing rates alone do not fully capture the ability of networks of neurons to process visual information. Another important coding property is how correlated pairs of neurons are in the network, a property which has previously been shown to influence the available information in a population of cells^{156,161,162}. We computed the correlated variability of all pairs of neurons in task 1 and task 2 of the 'rest' and 'no rest' conditions and found that correlations were significantly decreased in task 2 compared to task 1 in the 'rest' condition ($P < 0.05$, Wilcoxon sign rank) (Fig. 8, top). In contrast, there was trend toward increased spontaneous correlations in task 2 compared to task 1 in the 'no rest' condition (Fig. 8, bottom). While the magnitude of correlation difference is not drastically different between the two tasks, it is important to note that a small difference in correlations in the local network can theoretically have a great impact on neural coding of larger populations of neurons^{64,147}.

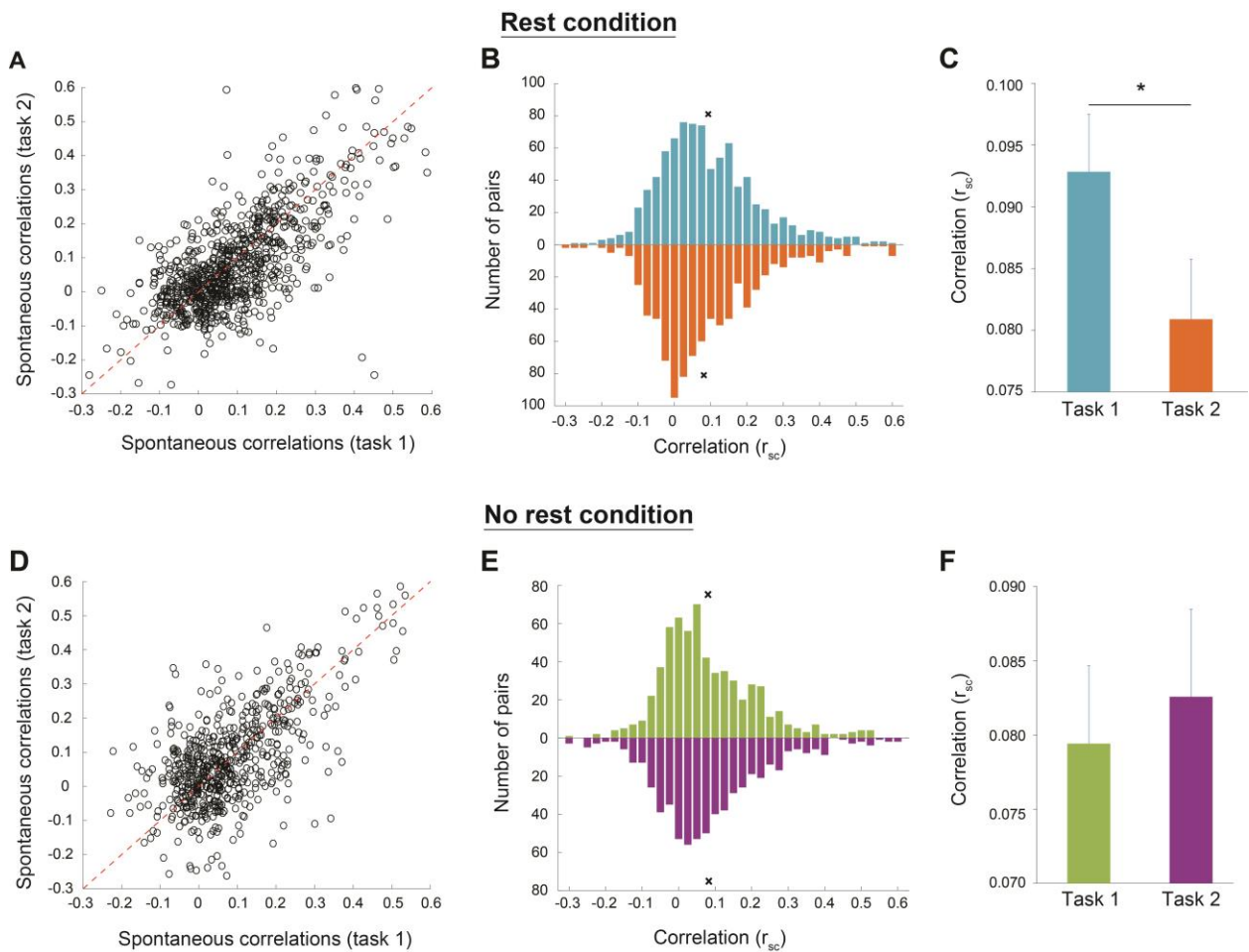


Figure IV-8. Spontaneous correlations are decreased following rest.

(A) Scatter plot of each cell pair for task 1 and task 2 in the ‘rest’ condition. The dotted red line represents unity. (B) Histogram of the task 1 spontaneous correlations plotted on top of the task 2 correlations in the ‘rest’ condition. The ‘x’ marks the mean correlation in task 1 and task 2. (C) The mean task 2 spontaneous correlation coefficient is significantly decreased compared to task 1 in the ‘rest’ condition (* $P < 0.05$, Wilcoxon sign rank). (D-F) Same as in A-C, but for the ‘no rest’ condition. There is no significant difference in spontaneous correlations between the task 1 and task 2.

Lastly, we computed two different measures of network discrimination in the ‘rest’ and ‘no rest’ conditions. First, we computed the population d' , a multivariate generalization of d' , for task 1 and task 2 in each condition. Using a complementary

error function, we were able to compute the probability of correct classification (PCC) between target and test stimuli for each set of data. We found that PCC was significantly greater in task 2 compared to task 1 following rest, but there was no significant difference between the two task periods when the animals were not allowed to rest ($P < 0.05$ and not significant, Wilcoxon sign rank) (Fig. 9, top). We next trained a linear classifier with 50% of our data in each condition and tested the classifier to compute decoder performance. We found that decoder performance was significantly greater in task 2 compared to task 1 when the animals were allowed to rest ($P < 0.005$, Wilcoxon sign rank), and there was no significant difference in decoder performance between the two tasks when the animals were not allowed to rest (Fig. 9, bottom). These results indicate that network discrimination is improved following a resting period, but there is no change in network discrimination when they are not allowed to rest.

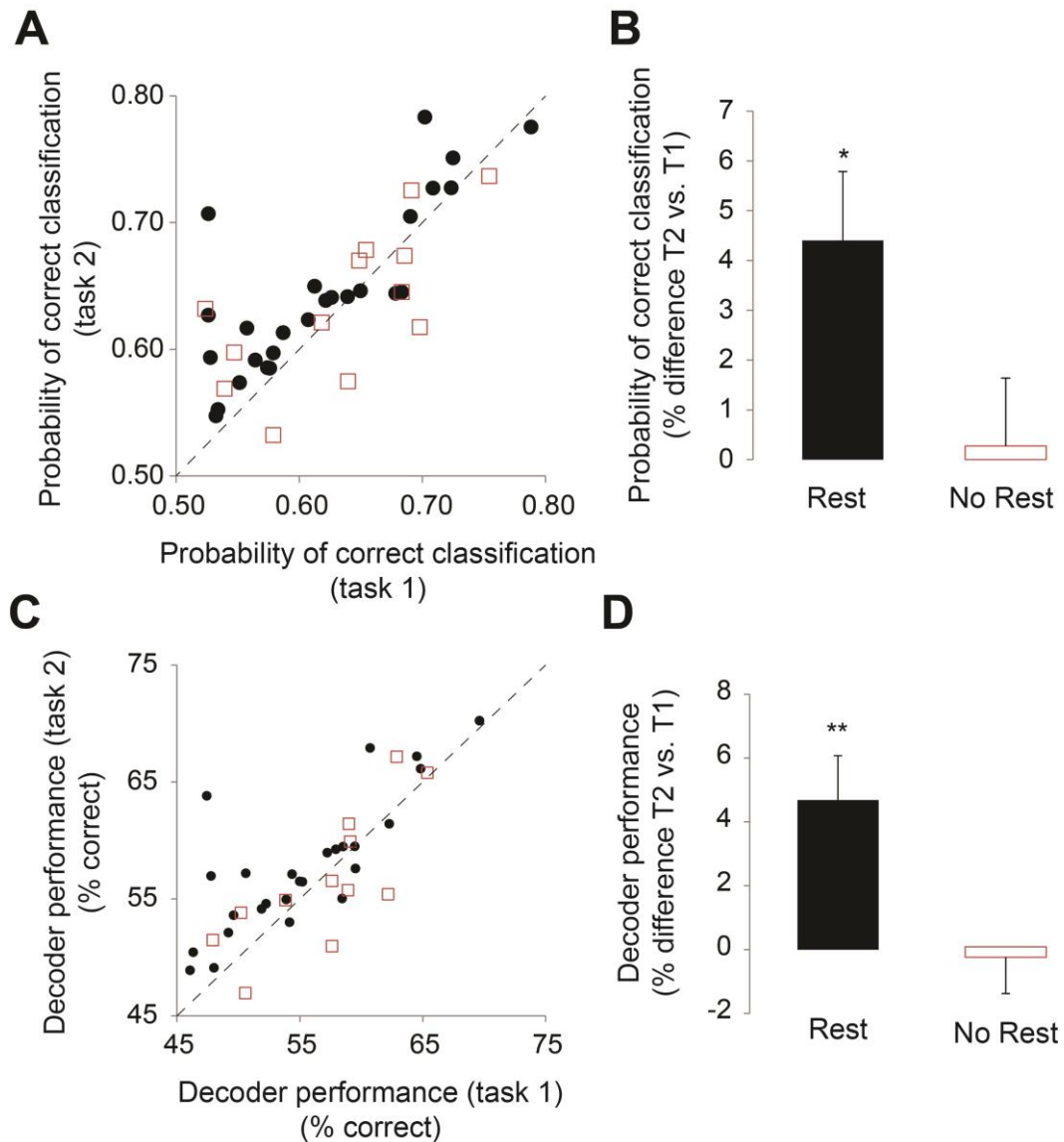


Figure IV-9. Neural discrimination performance is improved following rest.

(A) The probability of correct classification using a population d' analysis plotted for task 2 vs. task 1 in the 'rest' condition sessions (black circles) and 'no rest' condition sessions (red squares). **(B)** Classification performance is improved in task 2 compared to task 1 in the 'rest' condition (* $P < 0.05$, Wilcoxon sign rank). There is no difference between the classification performance of task 1 and task 2 in the 'no rest' condition. **(C)** Linear decoder performance using a train and test method for task 1 and task 2 in the 'rest' condition sessions (black circles) and 'no rest' condition sessions (red squares). **(D)** Linear decoder performance is increased in task 2 compared to task 1 in the 'rest' condition (** $P < 0.005$, Wilcoxon sign rank). There is no difference in decoder performance between task 1 and task 2 in the 'no rest' condition.

Discussion

Studies in humans have primarily focused on changes in *global brain activity* during rest. The existing methodology (e.g., EEG or fMRI) did not allow the spatial and temporal resolution required to examine changes at the single neuron or network level. For instance, a recent fMRI study examining activity in visual cortical area V1 during rest after perceptual learning, reported that subareas that were active during the task had enhanced activity during subsequent rest period¹⁷⁴. However, how neuronal activity across the network is modified at the single-cell resolution remains unknown. On the other hand, more invasive studies in small mammals, such as rats, using electrophysiological recordings mainly focused on a selective re-activation of memories. For instance, hippocampal place cells that were co-activated during a maze running task were more likely to be reactivated together during slow-wave sleep following the task¹⁸¹. This was the first evidence that the structure of correlations between neurons during a task was preserved even in the absence of further stimulation; similar findings were reported in motor, somatosensory, and parietal cortices¹⁸². Nonetheless, the question of why humans and higher mammals perform better after a period of rest had not been addressed. We conducted long recordings from population of spiking neurons and found that rest synchronizes cortical networks and leads to post-rest cortical desynchronization. We also observed an increase in firing rates and a decrease in correlated variability. Altogether, these findings represent first evidence of how rest alters networks to optimize neural coding and perceptual performance.

Although the idea that sensory inactivity or rest favors subsequent cognitive function has been around for a long time¹⁸³, the underlying neural mechanisms are still

poorly understood. Recently, it has been proposed that rest is critical to ensuring metabolic homeostasis¹⁸⁴, and that the restorative ability of sleep may be due to the enhanced removal of metabolic degradation products accumulating during wakefulness. Indeed, neurons are highly sensitive to their environment, and it is critical that waste products of metabolism are effectively removed from the brain's interstitial space, as waste products have been associated with adverse effects on synaptic transmission¹⁸⁵ and are believed to possibly trigger irreversible neuronal injury¹⁸⁶. However, while these findings suggest that the specific beneficial influence of rest is to remove the neurotoxic waste products, whether and how rest influences neuronal signaling and network processing, and how these changes influence behavioral and cognitive performance had never been previously explored. Our findings represent the first evidence that short periods of rest can alter neural properties to enhance network and behavioral performance. Future work will look at the full stages of sleep to determine how non-REM (non-rapid eye movement) and REM sleep work in concert to optimize the function of cortical networks.

CHAPTER V: Conclusions and Future Directions

The internal state of a racecar driver is putatively different from a student struggling to stay awake in math class. Indeed, it has always been subjectively understood that the function of an individual's brain may vary based on a variety of factors. The scientific study of spontaneous cortical activity has garnered significant interest in recent years through extensive research of sensory function in anesthetized and awake brains. From this work, it has become clear that neural responses result from the amalgamation of external stimuli and intrinsic cortical dynamics which vary along a continuum of states.

The goal of this research project has been to understand whether and how the spontaneous cortical state impacts neural coding and behavioral performance: 1) How do pre-stimulus firing rates impact networks and behavior? 2) How does the state of synchrony impact networks and behavior? 3) Do short period of daytime rest improve network coding and behavior? To address these questions, we studied single unit and population spiking and LFP data from the visual cortex of non-human primates as they performed orientation discrimination tasks (using gratings and natural stimuli).

In chapter II of this thesis, we discovered that the level of ongoing activity immediately preceding a test stimulus can influence the processing of sinusoidal grating stimuli in the primary visual cortex. In chapter III of this thesis, we demonstrated that trial-by-trial fluctuations in cortical synchrony can predict the efficiency of network discrimination and perceptual performance of natural stimuli in visual area V4. In chapter IV of this thesis, we showed that brief periods of rest can desynchronize subsequent cortical networks to improve network coding and behavioral performance in visual area V4. Altogether, our results demonstrate that the structure of spontaneous activity is critically important in visual processing and ultimately, in the behavioral

performance of animals. As a result of our work, we can better explain the fluctuations of spontaneous activity in cortical activity. What was previously called “noise” can be effectively reduced, indicating that the brain is more predictable than previously thought.

Implications of synchronous fluctuations in V4 impacting behavioral performance

It has been analytically demonstrated that synchronous fluctuations, alone, do not *limit* information in orientation discrimination tasks, but rather *reduce* the level at which information saturates in the presence of certain information-limiting correlations (information-limiting correlations, also referred to as differential correlations, represent a specific type of noise correlations that are proportional to the product of the derivatives of the tuning curves^{187,188}). In addition, synchronous fluctuations in V4 will not reduce information if downstream brain regions have access to the fluctuating gain factor caused by synchronous fluctuations. If downstream regions did have access, the downstream decoder could divide out the fluctuating gain, recover the full input information, and behavior would likely not be affected in any way¹⁸⁷. Our results suggest the alternative – that synchronous fluctuations in lower visual areas are not shared with decision areas and thus reduce information in a way that impacts behavior. Wavering attention is one possible explanation for the trial-by-trial fluctuations in synchrony observed in chapter III. It has been suggested that voluntary top-down attention is a mechanism that improves behavioral performance by desynchronizing networks^{187,189}. Prior studies have demonstrated that spatial attention reduces single-

unit normalized measures of spike count variance and pairwise correlations¹⁸⁹⁻¹⁹², similar to our results. Studies have also shown that attentional modulation leads to a decrease in evoked firing rate synchronization^{192,193}. In addition, many studies have found a relationship between local field potential (LFP) synchronization, particularly in the gamma band (35-70 Hz) frequency range, and attention^{194,195}.

Yet, we found no difference in evoked activity between states, contrasting results found by others studying attention in the extrastriate cortex¹⁹⁶⁻¹⁹⁸. Another more likely explanation (based on our findings from chapter IV) for the observed fluctuating states of synchrony is arousal. It has previously been shown that neurons in sleep-deprived rats can display synchronous activity that is detrimental to behavior¹⁴⁸. McGinley et al. also recently demonstrated that auditory detection performance was optimized at an *intermediate arousal state* as reflected by pupil size in mice¹²³. We found that the monkeys' performance was optimized in the *most desynchronized state* as measured by spiking activity in the simultaneously recorded population. However, it should be noted that our animals were likely not maximally, and as a result detrimentally, aroused under the calm, head-fixed experimental conditions.

In summary, we demonstrated in chapter III and IV that fluctuations in cortical synchrony can impact network and behavioral performance in the awake, behaving animal. That is, common fluctuations in population spiking activity decrease neural discrimination performance and gross behavioral performance even when the animal is seemingly alert and actively engaged in a task. Our investigations also indicate that downstream decoding regions do not have access to the fluctuating gain factor, suggesting that the synchronous activity is either locally generated or resulting from a top-down signal that is unavailable to decision areas.

Control of cortical states

The question of how and where cortical states are controlled in the brain has been pondered since the early twentieth century^{199,200}, and the question is still up for debate. It is clear that arousal varies grossly between waking and sleep states. In addition, my work demonstrated that arousal, as measured by neural spiking synchrony, can also fluctuate across trials in behaving animals. Several brain regions have been attributed to control of arousal including the basal forebrain, hypothalamus, and brainstem²⁰¹⁻²⁰³. Based on research using brain slices and neural track lesions, it is generally believed that the cerebral cortex requires excitatory stimulation from subcortical structures and the brainstem to persist in the waking state^{204,205}. Using a variety of anatomical and physiological techniques, important regulatory nuclei in the sleep-wake cycle have been identified and classified into a region collectively called the ascending reticular activating system²⁰⁶. Cholinergic neurons were found to project from the pedunculo pontine and laterodorsal tegmental nuclei (PPT-LDT) to the intralaminar nuclei of the thalamus and the reticular nucleus of the thalamus²⁰⁷⁻²⁰⁹. Monoaminergic cell groups in the locus coeruleus (noradrenaline), raphe nucleus (5-HT), and tuberomammillary nucleus (histamine) all characteristically fire in the waking state but not in NREM or REM sleep²¹⁰⁻²¹².

In addition, recent work has shown that the mammalian basal forebrain might be critical for controlling sleep and wakefulness. A recent optogenetic study by Xu et al.¹⁷⁰ demonstrated that basal forebrain glutamatergic neurons exhibited a strong wake-promoting effect on the cerebral cortex by direct excitation of both cholinergic and

parvalbumin+ GABAergic neurons. In agreement with this work, Kim et al.²¹³ used dual retrobead tracing and optogenetic stimulation to demonstrate that activation of cholinergic neurons in the basal forebrain induces desynchronization in specific sensory cortices. They also discovered that activation of noradrenergic locus coeruleus neurons induces broad desynchronization throughout the sensory cortices²¹³.

Future directions

The investigation of spontaneous cortical substates is certainly still in its infancy. The majority of current studies have employed an experimental method of partitioning data into discrete states of synchrony such as anesthetized vs. awake or quiet resting vs. active whisking in mice. Indeed, the strategy I employed in my own research similarly divided the data into two groups for comparison (low vs. high firing rates, synchronized vs. desynchronized trials, and 'rest' vs. 'no rest' conditions). While this strategy is practical in that it enables paired statistical comparisons between two groups, it surely fails to capture the full range and dimensionality of substates in the brain. In future work, it will be important to move beyond correlational analyses by causally controlling cortical substates to determine their impact on network coding and perceptual performance. Indeed, as mentioned in the previous section, several recent investigations have successfully demonstrated that it might be possible to control cortical substates through the use of electrical or pharmacological stimulators.

The nucleus basalis of the basal forebrain projects diffusely throughout the neocortex²¹⁴. Importantly, it is a region that has long been known to affect wakefulness and neural activity associated with cognition²¹⁵⁻²¹⁷. Previous work by Goard and Dan

demonstrated that microstimulation of the basal forebrain led to a decorrelation between neurons in the rat visual cortex along with an increase in reliability of evoked responses¹⁶⁵. One important future experiment will be to causally manipulate the level of synchrony in primary visual cortices in behaving animals. This could be achieved by either microstimulation of the basal forebrain in monkeys (adapted from the work previously conducted in rat¹⁶⁵) or alternatively, by means of optogenetic targeting of glutamatergic neurons in the basal forebrain. Using this procedure, we could first test if we can causally manipulate synchrony and neural properties in the visual cortex on trial-by-trial basis. At the same time, we could test perceptual performance and determine the true impact of basal forebrain contribution on network coding and behavior. Based on our previous findings, our hypothesis would be that causally desynchronizing the sensory cortex will optimize neural coding and behavioral performance.

Another question that emerges from our work is how does the spatial structure of spontaneous cortical activity vary across brain regions? For example, are cortical states, as measured by the level of ongoing activity or synchrony, shared across the visual cortex at any moment in time? Or alternatively, does each cortical area contain a local representation of state and efficiency in cortical processing in time? We could attempt to answer these questions by conducting simultaneous recordings in multiple visual cortices while the animals undergo orientation discrimination tasks. For instance, we could record from visual area V1 and V4 simultaneously and then investigate the dynamics of cortical state across visual areas.

This thesis represents a first step toward a greater understanding of how the brain dynamically processes external stimuli. The proposed ideas in this section

represent a possible next step in the scientific analysis. Certainly, there are still many unanswered questions about how fluctuations in spontaneous activity in the brain impact the processing of external information.

REFERENCES

- 1 Gibson, J. J. *The perception of the visual world*. (Houghton Mifflin, 1950).
- 2 Palmer, S. E. *Vision science: photons to phenomenology*. (The MIT Press, 1999).
- 3 Hubel, D. H. & Wiesel, T. N. Receptive fields of single neurones in the cat's striate cortex. *The Journal of physiology* **148**, 574-591 (1959).
- 4 Hubel, D. H. & Wiesel, T. N. Shape and arrangement of columns in cat's striate cortex. *The Journal of physiology* **165**, 559-568 (1963).
- 5 Hubel, D. H. & Wiesel, T. N. Receptive fields and functional architecture of monkey striate cortex. *The Journal of physiology* **195**, 215-243 (1968).
- 6 Hubel, D. H. & Wiesel, T. N. Receptive fields, binocular interaction and functional architecture in the cat's visual cortex. *The Journal of physiology* **160**, 106-154 (1962).
- 7 Tanaka, K. Cross-correlation analysis of geniculostriate neuronal relationships in cats. *Journal of neurophysiology* **49**, 1303-1318 (1983).
- 8 Jin, J., Wang, Y., Swadlow, H. A. & Alonso, J. M. Population receptive fields of ON and OFF thalamic inputs to an orientation column in visual cortex. *Nat Neurosci* **14**, 232-238, doi:10.1038/nn.2729 (2011).
- 9 Priebe, N. J. & Ferster, D. Mechanisms of neuronal computation in mammalian visual cortex. *Neuron* **75**, 194-208, doi:10.1016/j.neuron.2012.06.011 (2012).
- 10 Roe, A. W., Chelazzi, L., Connor, C. E., Conway, B. R., Fujita, I., Gallant, J. L., Lu, H. & Vanduffel, W. Toward a unified theory of visual area V4. *Neuron* **74**, 12-29, doi:10.1016/j.neuron.2012.03.011 (2012).

- 11 Tanigawa, H., Lu, H. D. & Roe, A. W. Functional organization for color and orientation in macaque V4. *Nat Neurosci* **13**, 1542-1548, doi:10.1038/nn.2676 (2010).
- 12 Ungerleider, L. G., Galkin, T. W., Desimone, R. & Gattass, R. Cortical connections of area V4 in the macaque. *Cerebral cortex* **18**, 477-499, doi:10.1093/cercor/bhm061 (2008).
- 13 Felleman, D. J. & Van Essen, D. C. Distributed hierarchical processing in the primate cerebral cortex. *Cerebral cortex* **1**, 1-47 (1991).
- 14 Fize, D., Vanduffel, W., Nelissen, K., Denys, K., Chef d'Hotel, C., Faugeras, O. & Orban, G. A. The retinotopic organization of primate dorsal V4 and surrounding areas: A functional magnetic resonance imaging study in awake monkeys. *The Journal of neuroscience : the official journal of the Society for Neuroscience* **23**, 7395-7406 (2003).
- 15 Sereno, M. I., Dale, A. M., Reppas, J. B., Kwong, K. K., Belliveau, J. W., Brady, T. J., Rosen, B. R. & Tootell, R. B. Borders of multiple visual areas in humans revealed by functional magnetic resonance imaging. *Science* **268**, 889-893 (1995).
- 16 Conway, B. R., Moeller, S. & Tsao, D. Y. Specialized color modules in macaque extrastriate cortex. *Neuron* **56**, 560-573, doi:10.1016/j.neuron.2007.10.008 (2007).
- 17 Conway, B. R. & Tsao, D. Y. Color architecture in alert macaque cortex revealed by fMRI. *Cerebral cortex* **16**, 1604-1613, doi:10.1093/cercor/bhj099 (2006).

- 18 Zeki, S. The distribution of wavelength and orientation selective cells in different areas of monkey visual cortex. *Proceedings of the Royal Society of London. Series B, Biological sciences* **217**, 449-470 (1983).
- 19 Zeki, S. M. Colour coding in rhesus monkey prestriate cortex. *Brain research* **53**, 422-427 (1973).
- 20 Hinkle, D. A. & Connor, C. E. Three-dimensional orientation tuning in macaque area V4. *Nat Neurosci* **5**, 665-670, doi:10.1038/nn875 (2002).
- 21 Hegde, J. & Van Essen, D. C. Stimulus dependence of disparity coding in primate visual area V4. *Journal of neurophysiology* **93**, 620-626, doi:10.1152/jn.00039.2004 (2005).
- 22 Watanabe, M., Tanaka, H., Uka, T. & Fujita, I. Disparity-selective neurons in area V4 of macaque monkeys. *Journal of neurophysiology* **87**, 1960-1973, doi:10.1152/jn.00780.2000 (2002).
- 23 Hinkle, D. A. & Connor, C. E. Disparity tuning in macaque area V4. *Neuroreport* **12**, 365-369 (2001).
- 24 Ferrera, V. P., Rudolph, K. K. & Maunsell, J. H. Responses of neurons in the parietal and temporal visual pathways during a motion task. *The Journal of neuroscience : the official journal of the Society for Neuroscience* **14**, 6171-6186 (1994).
- 25 Tolias, A. S., Keliris, G. A., Smirnakis, S. M. & Logothetis, N. K. Neurons in macaque area V4 acquire directional tuning after adaptation to motion stimuli. *Nat Neurosci* **8**, 591-593, doi:10.1038/nn1446 (2005).

- 26 Carlson, E. T., Rasquinha, R. J., Zhang, K. & Connor, C. E. A sparse object coding scheme in area V4. *Current biology : CB* **21**, 288-293, doi:10.1016/j.cub.2011.01.013 (2011).
- 27 Kobatake, E. & Tanaka, K. Neuronal selectivities to complex object features in the ventral visual pathway of the macaque cerebral cortex. *Journal of neurophysiology* **71**, 856-867 (1994).
- 28 Pasupathy, A. & Connor, C. E. Responses to contour features in macaque area V4. *Journal of neurophysiology* **82**, 2490-2502 (1999).
- 29 Essen, D. C. & Zeki, S. M. The topographic organization of rhesus monkey prestriate cortex. *The Journal of physiology* **277**, 193-226 (1978).
- 30 Mountcastle, V. B., Motter, B. C., Steinmetz, M. A. & Sestokas, A. K. Common and differential effects of attentive fixation on the excitability of parietal and prestriate (V4) cortical visual neurons in the macaque monkey. *The Journal of neuroscience : the official journal of the Society for Neuroscience* **7**, 2239-2255 (1987).
- 31 Steinmetz, N. A. & Moore, T. Eye movement preparation modulates neuronal responses in area V4 when dissociated from attentional demands. *Neuron* **83**, 496-506, doi:10.1016/j.neuron.2014.06.014 (2014).
- 32 Ghose, G. M. & Ts'o, D. Y. Form processing modules in primate area V4. *Journal of neurophysiology* **77**, 2191-2196 (1997).
- 33 McAdams, C. J. & Maunsell, J. H. Effects of attention on orientation-tuning functions of single neurons in macaque cortical area V4. *The Journal of neuroscience : the official journal of the Society for Neuroscience* **19**, 431-441 (1999).

- 34 Gallant, J. L., Braun, J. & Van Essen, D. C. Selectivity for polar, hyperbolic, and Cartesian gratings in macaque visual cortex. *Science* **259**, 100-103 (1993).
- 35 Averbeck, B. B. & Lee, D. Effects of noise correlations on information encoding and decoding. *Journal of neurophysiology* **95**, 3633-3644, doi:10.1152/jn.00919.2005 (2006).
- 36 Douglas, R. J. & Martin, K. A. Recurrent neuronal circuits in the neocortex. *Current biology : CB* **17**, R496-500, doi:10.1016/j.cub.2007.04.024 (2007).
- 37 Ahmed, B., Anderson, J. C., Douglas, R. J., Martin, K. A. & Nelson, J. C. Polynuclear innervation of spiny stellate neurons in cat visual cortex. *The Journal of comparative neurology* **341**, 39-49, doi:10.1002/cne.903410105 (1994).
- 38 Ringach, D. L. Spontaneous and driven cortical activity: implications for computation. *Current opinion in neurobiology* **19**, 439-444, doi:10.1016/j.conb.2009.07.005 (2009).
- 39 Shoham, D., Glaser, D. E., Arieli, A., Kenet, T., Wijnbergen, C., Toledo, Y., Hildesheim, R. & Grinvald, A. Imaging cortical dynamics at high spatial and temporal resolution with novel blue voltage-sensitive dyes. *Neuron* **24**, 791-802 (1999).
- 40 Slovin, H., Arieli, A., Hildesheim, R. & Grinvald, A. Long-term voltage-sensitive dye imaging reveals cortical dynamics in behaving monkeys. *Journal of neurophysiology* **88**, 3421-3438, doi:10.1152/jn.00194.2002 (2002).
- 41 Ohki, K., Chung, S., Ch'ng, Y. H., Kara, P. & Reid, R. C. Functional imaging with cellular resolution reveals precise micro-architecture in visual cortex. *Nature* **433**, 597-603, doi:10.1038/nature03274 (2005).

- 42 Arieli, A., Shoham, D., Hildesheim, R. & Grinvald, A. Coherent spatiotemporal patterns of ongoing activity revealed by real-time optical imaging coupled with single-unit recording in the cat visual cortex. *Journal of neurophysiology* **73**, 2072-2093 (1995).
- 43 Power, J. D., Cohen, A. L., Nelson, S. M., Wig, G. S., Barnes, K. A., Church, J. A., Vogel, A. C., Laumann, T. O., Miezin, F. M., Schlaggar, B. L. & Petersen, S. E. Functional network organization of the human brain. *Neuron* **72**, 665-678, doi:10.1016/j.neuron.2011.09.006 (2011).
- 44 Power, J. D., Schlaggar, B. L. & Petersen, S. E. Studying brain organization via spontaneous fMRI signal. *Neuron* **84**, 681-696, doi:10.1016/j.neuron.2014.09.007 (2014).
- 45 Yeo, B. T., Krienen, F. M., Sepulcre, J., Sabuncu, M. R., Lashkari, D., Hollinshead, M., Roffman, J. L., Smoller, J. W., Zollei, L., Polimeni, J. R., Fischl, B., Liu, H. & Buckner, R. L. The organization of the human cerebral cortex estimated by intrinsic functional connectivity. *Journal of neurophysiology* **106**, 1125-1165, doi:10.1152/jn.00338.2011 (2011).
- 46 Kohn, A. & Smith, M. A. Stimulus dependence of neuronal correlation in primary visual cortex of the macaque. *The Journal of neuroscience : the official journal of the Society for Neuroscience* **25**, 3661-3673 (2005).
- 47 Smith, M. A. & Kohn, A. Spatial and temporal scales of neuronal correlation in primary visual cortex. *The Journal of neuroscience : the official journal of the Society for Neuroscience* **28**, 12591-12603, doi:10.1523/JNEUROSCI.2929-08.2008 (2008).

- 48 Tsodyks, M., Kenet, T., Grinvald, A. & Arieli, A. Linking spontaneous activity of single cortical neurons and the underlying functional architecture. *Science* **286**, 1943-1946 (1999).
- 49 Chen, Y., Geisler, W. S. & Seidemann, E. Optimal decoding of correlated neural population responses in the primate visual cortex. *Nat Neurosci* **9**, 1412-1420, doi:10.1038/nn1792 (2006).
- 50 Kenet, T., Bibitchkov, D., Tsodyks, M., Grinvald, A. & Arieli, A. Spontaneously emerging cortical representations of visual attributes. *Nature* **425**, 954-956, doi:10.1038/nature02078 (2003).
- 51 Luczak, A., Bartho, P. & Harris, K. D. Spontaneous events outline the realm of possible sensory responses in neocortical populations. *Neuron* **62**, 413-425, doi:10.1016/j.neuron.2009.03.014 (2009).
- 52 Luczak, A., Bartho, P. & Harris, K. D. Gating of sensory input by spontaneous cortical activity. *The Journal of neuroscience : the official journal of the Society for Neuroscience* **33**, 1684-1695, doi:10.1523/JNEUROSCI.2928-12.2013 (2013).
- 53 Fiser, J., Chiu, C. & Weliky, M. Small modulation of ongoing cortical dynamics by sensory input during natural vision. *Nature* **431**, 573-578, doi:10.1038/nature02907 (2004).
- 54 Destexhe, A. Intracellular and computational evidence for a dominant role of internal network activity in cortical computations. *Current opinion in neurobiology* **21**, 717-725, doi:10.1016/j.conb.2011.06.002 (2011).

- 55 Abeles, M., Bergman, H., Gat, I., Meilijson, I., Seidemann, E., Tishby, N. & Vaadia, E. Cortical activity flips among quasi-stationary states. *Proc Natl Acad Sci U S A* **92**, 8616-8620 (1995).
- 56 Rabinovich, M., Huerta, R. & Laurent, G. Neuroscience. Transient dynamics for neural processing. *Science* **321**, 48-50, doi:10.1126/science.1155564 (2008).
- 57 Arieli, A., Sterkin, A., Grinvald, A. & Aertsen, A. Dynamics of ongoing activity: explanation of the large variability in evoked cortical responses. *Science* **273**, 1868-1871 (1996).
- 58 MacLean, J. N., Watson, B. O., Aaron, G. B. & Yuste, R. Internal dynamics determine the cortical response to thalamic stimulation. *Neuron* **48**, 811-823, doi:10.1016/j.neuron.2005.09.035 (2005).
- 59 Nauhaus, I., Busse, L., Carandini, M. & Ringach, D. L. Stimulus contrast modulates functional connectivity in visual cortex. *Nat Neurosci* **12**, 70-76, doi:10.1038/nn.2232 (2009).
- 60 Chawla, D., Rees, G. & Friston, K. J. The physiological basis of attentional modulation in extrastriate visual areas. *Nat Neurosci* **2**, 671-676, doi:10.1038/10230 (1999).
- 61 Kastner, S., Pinsk, M. A., De Weerd, P., Desimone, R. & Ungerleider, L. G. Increased activity in human visual cortex during directed attention in the absence of visual stimulation. *Neuron* **22**, 751-761 (1999).
- 62 Fries, P., Womelsdorf, T., Oostenveld, R. & Desimone, R. The effects of visual stimulation and selective visual attention on rhythmic neuronal synchronization in macaque area V4. *The Journal of neuroscience : the official journal of the*

- Society for Neuroscience* **28**, 4823-4835, doi:10.1523/JNEUROSCI.4499-07.2008 (2008).
- 63 Super, H., van der Togt, C., Spekreijse, H. & Lamme, V. A. Internal state of monkey primary visual cortex (V1) predicts figure-ground perception. *The Journal of neuroscience : the official journal of the Society for Neuroscience* **23**, 3407-3414 (2003).
- 64 Gutnisky, D. A., Beaman, C. B., Lew, S. E. & Dragoi, V. Spontaneous Fluctuations in Visual Cortical Responses Influence Population Coding Accuracy. *Cerebral cortex*, doi:10.1093/cercor/bhv312 (2016).
- 65 Gervasoni, D., Lin, S. C., Ribeiro, S., Soares, E. S., Pantoja, J. & Nicolelis, M. A. Global forebrain dynamics predict rat behavioral states and their transitions. *The Journal of neuroscience : the official journal of the Society for Neuroscience* **24**, 11137-11147, doi:10.1523/JNEUROSCI.3524-04.2004 (2004).
- 66 Steriade, M., McCormick, D. A. & Sejnowski, T. J. Thalamocortical oscillations in the sleeping and aroused brain. *Science* **262**, 679-685 (1993).
- 67 Steriade, M., Timofeev, I. & Grenier, F. Natural waking and sleep states: a view from inside neocortical neurons. *Journal of neurophysiology* **85**, 1969-1985 (2001).
- 68 Vyazovskiy, V. V., Olcese, U., Lazimy, Y. M., Faraguna, U., Esser, S. K., Williams, J. C., Cirelli, C. & Tononi, G. Cortical firing and sleep homeostasis. *Neuron* **63**, 865-878, doi:10.1016/j.neuron.2009.08.024 (2009).
- 69 Buzsaki, G., Anastassiou, C. A. & Koch, C. The origin of extracellular fields and currents--EEG, ECoG, LFP and spikes. *Nature reviews. Neuroscience* **13**, 407-420, doi:10.1038/nrn3241 (2012).

- 70 Kryger, M. H., Roth, T. & Demet, W. C. *Principles and Practice of Sleep Medicine*. (Saunders, 2010).
- 71 Harris, K. D. & Thiele, A. Cortical state and attention. *Nat. Rev. Neurosci.* **12**, 509-523, doi:10.1038/nrn3084 (2011).
- 72 Crochet, S. & Petersen, C. C. Correlating whisker behavior with membrane potential in barrel cortex of awake mice. *Nature Neuroscience* **9**, 608-610, doi:10.1038/nn1690 (2006).
- 73 Greenberg, D. S., Houweling, A. R. & Kerr, J. N. Population imaging of ongoing neuronal activity in the visual cortex of awake rats. *Nature Neuroscience* **11**, 749-751, doi:10.1038/nn.2140 (2008).
- 74 Poulet, J. F. & Petersen, C. C. Internal brain state regulates membrane potential synchrony in barrel cortex of behaving mice. *Nature* **454**, 881-885, doi:10.1038/nature07150 (2008).
- 75 Reimer, J., Froudarakis, E., Cadwell, C. R., Yatsenko, D., Denfield, G. H. & Tolias, A. S. Pupil fluctuations track fast switching of cortical states during quiet wakefulness. *Neuron* **84**, 355-362, doi:10.1016/j.neuron.2014.09.033 (2014).
- 76 Ecker, A. S., Berens, P., Cotton, R. J., Subramanian, M., Denfield, G. H., Cadwell, C. R., Smirnakis, S. M., Bethge, M. & Tolias, A. S. State dependence of noise correlations in macaque primary visual cortex. *Neuron* **82**, 235-248, doi:10.1016/j.neuron.2014.02.006 (2014).
- 77 Luczak, A., Bartho, P., Marguet, S. L., Buzsaki, G. & Harris, K. D. Sequential structure of neocortical spontaneous activity in vivo. *Proc Natl Acad Sci U S A* **104**, 347-352, doi:10.1073/pnas.0605643104 (2007).

- 78 Scholvinck, M. L., Saleem, A. B., Benucci, A., Harris, K. D. & Carandini, M. Cortical state determines global variability and correlations in visual cortex. *The Journal of Neuroscience* **35**, 170-178, doi:10.1523/JNEUROSCI.4994-13.2015 (2015).
- 79 Mednick, S., Nakayama, K. & Stickgold, R. Sleep-dependent learning: a nap is as good as a night. *Nat Neurosci* **6**, 697-698, doi:10.1038/nn1078 (2003).
- 80 Mednick, S. C., Drummond, S. P., Boynton, G. M., Awh, E. & Serences, J. Sleep-dependent learning and practice-dependent deterioration in an orientation discrimination task. *Behavioral neuroscience* **122**, 267-272, doi:10.1037/0735-7044.122.2.267 (2008).
- 81 Mednick, S. C., Nakayama, K., Cantero, J. L., Atienza, M., Levin, A. A., Pathak, N. & Stickgold, R. The restorative effect of naps on perceptual deterioration. *Nat Neurosci* **5**, 677-681, doi:10.1038/nn864 (2002).
- 82 Tietzel, A. J. & Lack, L. C. The short-term benefits of brief and long naps following nocturnal sleep restriction. *Sleep* **24**, 293-300 (2001).
- 83 Tietzel, A. J. & Lack, L. C. The recuperative value of brief and ultra-brief naps on alertness and cognitive performance. *Journal of sleep research* **11**, 213-218 (2002).
- 84 Tucker, M. A., Hirota, Y., Wamsley, E. J., Lau, H., Chaklader, A. & Fishbein, W. A daytime nap containing solely non-REM sleep enhances declarative but not procedural memory. *Neurobiology of learning and memory* **86**, 241-247, doi:10.1016/j.nlm.2006.03.005 (2006).
- 85 Wamsley, E. J., Tucker, M. A., Payne, J. D. & Stickgold, R. A brief nap is beneficial for human route-learning: The role of navigation experience and EEG

- spectral power. *Learning & memory* **17**, 332-336, doi:10.1101/lm.1828310 (2010).
- 86 Tucker, M. A. & Fishbein, W. Enhancement of declarative memory performance following a daytime nap is contingent on strength of initial task acquisition. *Sleep* **31**, 197-203 (2008).
- 87 Lahl, O., Wispel, C., Willigens, B. & Pietrowsky, R. An ultra short episode of sleep is sufficient to promote declarative memory performance. *Journal of sleep research* **17**, 3-10, doi:10.1111/j.1365-2869.2008.00622.x (2008).
- 88 Genzel, L., Kroes, M. C., Dresler, M. & Battaglia, F. P. Light sleep versus slow wave sleep in memory consolidation: a question of global versus local processes? *Trends in neurosciences* **37**, 10-19, doi:10.1016/j.tins.2013.10.002 (2014).
- 89 Campbell, S. S. & Tobler, I. Animal sleep: a review of sleep duration across phylogeny. *Neuroscience and biobehavioral reviews* **8**, 269-300 (1984).
- 90 Phillips, A. J., Robinson, P. A., Kedziora, D. J. & Abeyesuriya, R. G. Mammalian sleep dynamics: how diverse features arise from a common physiological framework. *PLoS computational biology* **6**, e1000826, doi:10.1371/journal.pcbi.1000826 (2010).
- 91 Balzamo, E., Santucci, V., Seri, B., Vuillon-Cacciuttolo, G. & Bert, J. Nonhuman primates: laboratory animals of choice for neurophysiologic studies of sleep. *Laboratory animal science* **27**, 879-886 (1977).
- 92 Hsieh, K. C., Robinson, E. L. & Fuller, C. A. Sleep architecture in unrestrained rhesus monkeys (*Macaca mulatta*) synchronized to 24-hour light-dark cycles. *Sleep* **31**, 1239-1250 (2008).

- 93 Fogel, S. M. & Smith, C. T. Learning-dependent changes in sleep spindles and Stage 2 sleep. *Journal of sleep research* **15**, 250-255, doi:10.1111/j.1365-2869.2006.00522.x (2006).
- 94 Sejnowski, T. J. & Destexhe, A. Why do we sleep? *Brain research* **886**, 208-223 (2000).
- 95 Sirota, A., Csicsvari, J., Buhl, D. & Buzsaki, G. Communication between neocortex and hippocampus during sleep in rodents. *Proc Natl Acad Sci U S A* **100**, 2065-2069, doi:10.1073/pnas.0437938100 (2003).
- 96 Genzel, L., Dresler, M., Wehrle, R., Grozinger, M. & Steiger, A. Slow wave sleep and REM sleep awakenings do not affect sleep dependent memory consolidation. *Sleep* **32**, 302-310 (2009).
- 97 Chow, H. M., Horovitz, S. G., Carr, W. S., Picchioni, D., Coddington, N., Fukunaga, M., Xu, Y., Balkin, T. J., Duyn, J. H. & Braun, A. R. Rhythmic alternating patterns of brain activity distinguish rapid eye movement sleep from other states of consciousness. *Proc Natl Acad Sci U S A* **110**, 10300-10305, doi:10.1073/pnas.1217691110 (2013).
- 98 Nir, Y., Staba, R. J., Andrillon, T., Vyazovskiy, V. V., Cirelli, C., Fried, I. & Tononi, G. Regional slow waves and spindles in human sleep. *Neuron* **70**, 153-169, doi:10.1016/j.neuron.2011.02.043 (2011).
- 99 Spoormaker, V. I., Schroter, M. S., Gleiser, P. M., Andrade, K. C., Dresler, M., Wehrle, R., Samann, P. G. & Czeisler, M. Development of a large-scale functional brain network during human non-rapid eye movement sleep. *The Journal of neuroscience : the official journal of the Society for Neuroscience* **30**, 11379-11387, doi:10.1523/JNEUROSCI.2015-10.2010 (2010).

- 100 Tononi, G. & Cirelli, C. Sleep function and synaptic homeostasis. *Sleep medicine reviews* **10**, 49-62, doi:10.1016/j.smrv.2005.05.002 (2006).
- 101 Tononi, G. & Cirelli, C. Time to be SHY? Some comments on sleep and synaptic homeostasis. *Neural plasticity* **2012**, 415250, doi:10.1155/2012/415250 (2012).
- 102 Van Der Werf, Y. D., Altena, E., Vis, J. C., Koene, T. & Van Someren, E. J. Reduction of nocturnal slow-wave activity affects daytime vigilance lapses and memory encoding but not reaction time or implicit learning. *Progress in brain research* **193**, 245-255, doi:10.1016/B978-0-444-53839-0.00016-8 (2011).
- 103 Yoo, S. S., Hu, P. T., Gujar, N., Jolesz, F. A. & Walker, M. P. A deficit in the ability to form new human memories without sleep. *Nat Neurosci* **10**, 385-392, doi:10.1038/nn1851 (2007).
- 104 Takashima, A., Nieuwenhuis, I. L., Jensen, O., Talamini, L. M., Rijpkema, M. & Fernandez, G. Shift from hippocampal to neocortical centered retrieval network with consolidation. *The Journal of neuroscience : the official journal of the Society for Neuroscience* **29**, 10087-10093, doi:10.1523/JNEUROSCI.0799-09.2009 (2009).
- 105 Haider, B., Duque, A., Hasenstaub, A. R., Yu, Y. & McCormick, D. A. Enhancement of visual responsiveness by spontaneous local network activity in vivo. *Journal of neurophysiology* **97**, 4186-4202 (2007).
- 106 Smith, A. J., Blumenfeld, H., Behar, K. L., Rothman, D. L., Shulman, R. G. & Hyder, F. Cerebral energetics and spiking frequency: the neurophysiological basis of fMRI. *Proc Natl Acad Sci U S A* **99**, 10765-10770, doi:10.1073/pnas.132272199 (2002).

- 107 Curto, C., Sakata, S., Marguet, S., Itskov, V. & Harris, K. D. A simple model of cortical dynamics explains variability and state dependence of sensory responses in urethane-anesthetized auditory cortex. *The Journal of Neuroscience* **29**, 10600-10612, doi:10.1523/JNEUROSCI.2053-09.2009 (2009).
- 108 Hyder, F., Rothman, D. L. & Shulman, R. G. Total neuroenergetics support localized brain activity: implications for the interpretation of fMRI. *Proc Natl Acad Sci U S A* **99**, 10771-10776, doi:10.1073/pnas.132272299 (2002).
- 109 Leske, S., Ruhnau, P., Frey, J., Lithari, C., Muller, N., Hartmann, T. & Weisz, N. Prestimulus Network Integration of Auditory Cortex Predisposes Near-Threshold Perception Independently of Local Excitability. *Cerebral cortex* **25**, 4898-4907, doi:10.1093/cercor/bhv212 (2015).
- 110 Sadaghiani, S., Poline, J. B., Kleinschmidt, A. & D'Esposito, M. Ongoing dynamics in large-scale functional connectivity predict perception. *Proc Natl Acad Sci U S A* **112**, 8463-8468, doi:10.1073/pnas.1420687112 (2015).
- 111 Busch, N. A., Dubois, J. & VanRullen, R. The phase of ongoing EEG oscillations predicts visual perception. *The Journal of neuroscience : the official journal of the Society for Neuroscience* **29**, 7869-7876, doi:29/24/7869 [pii] 10.1523/JNEUROSCI.0113-09.2009 (2009).
- 112 Hanslmayr, S., Aslan, A., Staudigl, T., Klimesch, W., Herrmann, C. S. & Bauml, K. H. Prestimulus oscillations predict visual perception performance between and within subjects. *Neuroimage* **37**, 1465-1473, doi:S1053-8119(07)00603-9 [pii] 10.1016/j.neuroimage.2007.07.011 (2007).

- 113 Hesselmann, G., Kell, C. A., Eger, E. & Kleinschmidt, A. Spontaneous local variations in ongoing neural activity bias perceptual decisions. *Proc Natl Acad Sci U S A* **105**, 10984-10989, doi:0712043105 [pii]
10.1073/pnas.0712043105 (2008).
- 114 Linkenkaer-Hansen, K., Nikulin, V. V., Palva, S., Ilmoniemi, R. J. & Palva, J. M. Prestimulus oscillations enhance psychophysical performance in humans. *The Journal of neuroscience : the official journal of the Society for Neuroscience* **24**, 10186-10190 (2004).
- 115 Mathewson, K. E., Gratton, G., Fabiani, M., Beck, D. M. & Ro, T. To see or not to see: prestimulus alpha phase predicts visual awareness. *The Journal of neuroscience : the official journal of the Society for Neuroscience* **29**, 2725-2732, doi:29/9/2725 [pii]
10.1523/JNEUROSCI.3963-08.2009 (2009).
- 116 van Dijk, H., Schoffelen, J. M., Oostenveld, R. & Jensen, O. Prestimulus oscillatory activity in the alpha band predicts visual discrimination ability. *The Journal of neuroscience : the official journal of the Society for Neuroscience* **28**, 1816-1823, doi:28/8/1816 [pii]
10.1523/JNEUROSCI.1853-07.2008 (2008).
- 117 Ergenoglu, T., Demiralp, T., Bayraktaroglu, Z., Ergen, M., Beydagi, H. & Uresin, Y. Alpha rhythm of the EEG modulates visual detection performance in humans. *Brain Res Cogn Brain Res* **20**, 376-383, doi:10.1016/j.cogbrainres.2004.03.009
S0926641004000941 [pii] (2004).

- 118 Hanslmayr, S., Klimesch, W., Sauseng, P., Gruber, W., Doppelmayr, M., Freunberger, R. & Pecherstorfer, T. Visual discrimination performance is related to decreased alpha amplitude but increased phase locking. *Neurosci Lett* **375**, 64-68, doi:S0304-3940(04)01359-X [pii]
10.1016/j.neulet.2004.10.092 (2005).
- 119 Romei, V., Brodbeck, V., Michel, C., Amedi, A., Pascual-Leone, A. & Thut, G. Spontaneous fluctuations in posterior alpha-band EEG activity reflect variability in excitability of human visual areas. *Cerebral cortex* **18**, 2010-2018, doi:bhm229 [pii]
10.1093/cercor/bhm229 (2008).
- 120 Bompas, A., Sumner, P., Muthumumaraswamy, S. D., Singh, K. D. & Gilchrist, I. D. The contribution of pre-stimulus neural oscillatory activity to spontaneous response time variability. *Neuroimage* **107**, 34-45, doi:10.1016/j.neuroimage.2014.11.057 (2015).
- 121 Baumgarten, T. J., Schnitzler, A. & Lange, J. Beta oscillations define discrete perceptual cycles in the somatosensory domain. *Proc Natl Acad Sci U S A* **112**, 12187-12192, doi:10.1073/pnas.1501438112 (2015).
- 122 Tan, A. Y., Chen, Y., Scholl, B., Seidemann, E. & Priebe, N. J. Sensory stimulation shifts visual cortex from synchronous to asynchronous states. *Nature* **509**, 226-229, doi:10.1038/nature13159 (2014).
- 123 McGinley, M. J., David, S. V. & McCormick, D. A. Cortical Membrane Potential Signature of Optimal States for Sensory Signal Detection. *Neuron* **87**, 179-192, doi:10.1016/j.neuron.2015.05.038 (2015).

- 124 Pachitariu, M., Lyamzin, D. R., Sahani, M. & Lesica, N. A. State-dependent population coding in primary auditory cortex. *The Journal of Neuroscience* **35**, 2058-2073, doi:10.1523/JNEUROSCI.3318-14.2015 (2015).
- 125 Niell, C. M. & Stryker, M. P. Modulation of visual responses by behavioral state in mouse visual cortex. *Neuron* **65**, 472-479, doi:10.1016/j.neuron.2010.01.033 (2010).
- 126 Renart, A., de la Rocha, J., Bartho, P., Hollender, L., Parga, N., Reyes, A. & Harris, K. D. The asynchronous state in cortical circuits. *Science* **327**, 587-590, doi:10.1126/science.1179850 (2010).
- 127 Azouz, R. & Gray, C. M. Adaptive coincidence detection and dynamic gain control in visual cortical neurons in vivo. *Neuron* **37**, 513-523 (2003).
- 128 Chance, F. S., Abbott, L. F. & Reyes, A. D. Gain modulation from background synaptic input. *Neuron* **35**, 773-782 (2002).
- 129 Han, F., Caporale, N. & Dan, Y. Reverberation of recent visual experience in spontaneous cortical waves. *Neuron* **60**, 321-327, doi:10.1016/j.neuron.2008.08.026 (2008).
- 130 Averbeck, B. B. & Lee, D. Coding and transmission of information by neural ensembles. *Trends in neurosciences* **27**, 225-230, doi:10.1016/j.tins.2004.02.006 (2004).
- 131 Poor, H. *An Introduction to Signal Detection and Estimation*. (Springer, 1994).
- 132 Hansen, B. J., Eagleman, S. & Dragoi, V. Examining local network processing using multi-contact laminar electrode recording. *Journal of visualized experiments : JoVE*, doi:10.3791/2806 (2011).

- 133 Okun, M., Steinmetz, N. A., Cossell, L., Iacaruso, M. F., Ko, H., Bartho, P., Moore, T., Hofer, S. B., Mrcic-Flogel, T. D., Carandini, M. & Harris, K. D. Diverse coupling of neurons to populations in sensory cortex. *Nature* **521**, 511-515, doi:10.1038/nature14273 (2015).
- 134 Luck, S. J., Chelazzi, L., Hillyard, S. A. & Desimone, R. Neural mechanisms of spatial selective attention in areas V1, V2, and V4 of macaque visual cortex. *Journal of neurophysiology* **77**, 24-42 (1997).
- 135 Yoshor, D., Ghose, G. M., Bosking, W. H., Sun, P. & Maunsell, J. H. Spatial attention does not strongly modulate neuronal responses in early human visual cortex. *The Journal of neuroscience : the official journal of the Society for Neuroscience* **27**, 13205-13209, doi:27/48/13205 [pii] 10.1523/JNEUROSCI.2944-07.2007 (2007).
- 136 Poort, J. & Roelfsema, P. R. Noise correlations have little influence on the coding of selective attention in area V1. *Cerebral cortex* **19**, 543-553, doi:10.1093/cercor/bhn103 (2009).
- 137 Singer, J. & Kreiman, G. in *Visual population codes: toward a common multivariate framework for cell recording and functional imaging* (eds N. Kriegeskorte & G. Kreiman) Ch. 18, (The MIT Press, 2011).
- 138 de la Rocha, J., Doiron, B., Shea-Brown, E., Josic, K. & Reyes, A. Correlation between neural spike trains increases with firing rate. *Nature* **448**, 802-806, doi:10.1038/nature06028 (2007).
- 139 Ecker, A. S., Berens, P., Keliris, G. A., Bethge, M., Logothetis, N. K. & Tolias, A. S. Decorrelated neuronal firing in cortical microcircuits. *Science* **327**, 584-587, doi:10.1126/science.1179867 (2010).

- 140 Shadlen, M. N. & Newsome, W. T. The variable discharge of cortical neurons: implications for connectivity, computation, and information coding. *The Journal of neuroscience : the official journal of the Society for Neuroscience* **18**, 3870-3896 (1998).
- 141 Babiloni, C., Vecchio, F., Bultrini, A., Luca Romani, G. & Rossini, P. M. Pre- and poststimulus alpha rhythms are related to conscious visual perception: a high-resolution EEG study. *Cerebral cortex* **16**, 1690-1700, doi:bhj104 [pii] 10.1093/cercor/bhj104 (2006).
- 142 Wyart, V. & Tallon-Baudry, C. How ongoing fluctuations in human visual cortex predict perceptual awareness: baseline shift versus decision bias. *The Journal of neuroscience : the official journal of the Society for Neuroscience* **29**, 8715-8725, doi:29/27/8715 [pii] 10.1523/JNEUROSCI.0962-09.2009 (2009).
- 143 Ress, D., Backus, B. T. & Heeger, D. J. Activity in primary visual cortex predicts performance in a visual detection task. *Nat Neurosci* **3**, 940-945 (2000).
- 144 Hesselmann, G., Kell, C. A. & Kleinschmidt, A. Ongoing activity fluctuations in hMT+ bias the perception of coherent visual motion. *The Journal of neuroscience : the official journal of the Society for Neuroscience* **28**, 14481-14485, doi:28/53/14481 [pii] 10.1523/JNEUROSCI.4398-08.2008 (2008).
- 145 Ahissar, E., Vaadia, E., Ahissar, M., Bergman, H., Arieli, A. & Abeles, M. Dependence of cortical plasticity on correlated activity of single neurons and on behavioral context. *Science* **257**, 1412-1415 (1992).

- 146 Cohen, M. R. & Newsome, W. T. Context-dependent changes in functional circuitry in visual area MT. *Neuron* **60**, 162-173, doi:10.1016/j.neuron.2008.08.007 (2008).
- 147 Gutnisky, D. A. & Dragoi, V. Adaptive coding of visual information in neural populations. *Nature* **452**, 220-224, doi:10.1038/nature06563 (2008).
- 148 Vyazovskiy, V. V., Olcese, U., Hanlon, E. C., Nir, Y., Cirelli, C. & Tononi, G. Local sleep in awake rats. *Nature* **472**, 443-447, doi:10.1038/nature10009 (2011).
- 149 Polack, P. O., Friedman, J. & Golshani, P. Cellular mechanisms of brain state-dependent gain modulation in visual cortex. *Nature Neuroscience* **16**, 1331-1339, doi:10.1038/nn.3464 (2013).
- 150 Bennett, C., Arroyo, S. & Hestrin, S. Subthreshold mechanisms underlying state-dependent modulation of visual responses. *Neuron* **80**, 350-357, doi:10.1016/j.neuron.2013.08.007 (2013).
- 151 Vinck, M., Batista-Brito, R., Knoblich, U. & Cardin, J. A. Arousal and locomotion make distinct contributions to cortical activity patterns and visual encoding. *Neuron* **86**, 740-754, doi:10.1016/j.neuron.2015.03.028 (2015).
- 152 Gervasoni, D., Lin, S. C., Ribeiro, S., Soares, E. S., Pantoja, J. & Nicolelis, M. A. Global forebrain dynamics predict rat behavioral states and their transitions. *The Journal of Neuroscience* **24**, 11137-11147, doi:10.1523/JNEUROSCI.3524-04.2004 (2004).
- 153 McGinley, M. J., Vinck, M., Reimer, J., Batista-Brito, R., Zagha, E., Cadwell, C. R., Tolias, A. S., Cardin, J. A. & McCormick, D. A. Waking State: Rapid

- Variations Modulate Neural and Behavioral Responses. *Neuron* **87**, 1143-1161, doi:10.1016/j.neuron.2015.09.012 (2015).
- 154 Daley, J. T., Turner, R. S., Freeman, A., Bliwise, D. L. & Rye, D. B. Prolonged assessment of sleep and daytime sleepiness in unrestrained *Macaca mulatta*. *Sleep* **29**, 221-231 (2006).
- 155 Churchland, M. M., Yu, B. M., Cunningham, J. P., Sugrue, L. P., Cohen, M. R., Corrado, G. S., Newsome, W. T., Clark, A. M., Hosseini, P., Scott, B. B., Bradley, D. C., Smith, M. A., Kohn, A., Movshon, J. A., Armstrong, K. M., Moore, T., Chang, S. W., Snyder, L. H., Lisberger, S. G., Priebe, N. J., Finn, I. M., Ferster, D., Ryu, S. I., Santhanam, G., Sahani, M. & Shenoy, K. V. Stimulus onset quenches neural variability: a widespread cortical phenomenon. *Nature Neuroscience* **13**, 369-378, doi:10.1038/nn.2501 (2010).
- 156 Hansen, B. J., Chelaru, M. I. & Dragoi, V. Correlated variability in laminar cortical circuits. *Neuron* **76**, 590-602, doi:10.1016/j.neuron.2012.08.029 (2012).
- 157 Bair, W., Zohary, E. & Newsome, W. T. Correlated firing in macaque visual area MT: time scales and relationship to behavior. *The Journal of Neuroscience* **21**, 1676-1697 (2001).
- 158 Gutnisky, D. A., Hansen, B. J., Iliescu, B. F. & Dragoi, V. Attention alters visual plasticity during exposure-based learning. *Curr. Biol.* **19**, 555-560, doi:10.1016/j.cub.2009.01.063 (2009).
- 159 Benjamini, Y. & Yekutieli, D. The control of the false discovery rate in multiple testing under dependency. *The Annals of Statistics* **29**, 1165-1188 (2001).

- 160 Glickman, M. E., Rao, S. R. & Schultz, M. R. False discovery rate control is a recommended alternative to Bonferroni-type adjustments in health studies. *J. Clin. Epidemiol.* **67**, 850-857, doi:10.1016/j.jclinepi.2014.03.012 (2014).
- 161 Abbott, L. F. & Dayan, P. The effect of correlated variability on the accuracy of a population code. *Neural Comput.* **11**, 91-101 (1999).
- 162 Cafaro, J. & Rieke, F. Noise correlations improve response fidelity and stimulus encoding. *Nature* **468**, 964-967, doi:10.1038/nature09570 (2010).
- 163 Goris, R. L., Movshon, J. A. & Simoncelli, E. P. Partitioning neuronal variability. *Nature Neuroscience* **17**, 858-865, doi:10.1038/nn.3711 (2014).
- 164 Churchland, A. K., Kiani, R., Chaudhuri, R., Wang, X. J., Pouget, A. & Shadlen, M. N. Variance as a signature of neural computations during decision making. *Neuron* **69**, 818-831, doi:10.1016/j.neuron.2010.12.037 (2011).
- 165 Goard, M. & Dan, Y. Basal forebrain activation enhances cortical coding of natural scenes. *Nature Neuroscience* **12**, 1444-1449, doi:10.1038/nn.2402 (2009).
- 166 Kelly, R. C., Smith, M. A., Kass, R. E. & Lee, T. S. Local field potentials indicate network state and account for neuronal response variability. *Journal of computational neuroscience* **29**, 567-579, doi:10.1007/s10827-009-0208-9 (2010).
- 167 Buzsaki, G., Bickford, R. G., Ponomareff, G., Thal, L. J., Mandel, R. & Gage, F. H. Nucleus basalis and thalamic control of neocortical activity in the freely moving rat. *The Journal of Neuroscience* **8**, 4007-4026 (1988).

- 168 Munk, M. H., Roelfsema, P. R., Konig, P., Engel, A. K. & Singer, W. Role of reticular activation in the modulation of intracortical synchronization. *Science* **272**, 271-274 (1996).
- 169 Mena-Segovia, J., Sims, H. M., Magill, P. J. & Bolam, J. P. Cholinergic brainstem neurons modulate cortical gamma activity during slow oscillations. *J. Physiol.* **586**, 2947-2960, doi:10.1113/jphysiol.2008.153874 (2008).
- 170 Xu, M., Chung, S., Zhang, S., Zhong, P., Ma, C., Chang, W. C., Weissbourd, B., Sakai, N., Luo, L., Nishino, S. & Dan, Y. Basal forebrain circuit for sleep-wake control. *Nature Neuroscience* **18**, 1641-1647, doi:10.1038/nn.4143 (2015).
- 171 Cirelli, C. & Tononi, G. Is sleep essential? *PLoS biology* **6**, e216, doi:10.1371/journal.pbio.0060216 (2008).
- 172 Karni, A., Tanne, D., Rubenstein, B. S., Askenasy, J. J. & Sagi, D. Dependence on REM sleep of overnight improvement of a perceptual skill. *Science* **265**, 679-682 (1994).
- 173 Stickgold, R., Whidbee, D., Schirmer, B., Patel, V. & Hobson, J. A. Visual discrimination task improvement: A multi-step process occurring during sleep. *Journal of cognitive neuroscience* **12**, 246-254 (2000).
- 174 Yotsumoto, Y., Sasaki, Y., Chan, P., Vasios, C. E., Bonmassar, G., Ito, N., Nanez, J. E., Sr., Shimojo, S. & Watanabe, T. Location-specific cortical activation changes during sleep after training for perceptual learning. *Current biology : CB* **19**, 1278-1282, doi:10.1016/j.cub.2009.06.011 (2009).
- 175 Georgopoulos, A. P., Schwartz, A. B. & Kettner, R. E. Neuronal population coding of movement direction. *Science* **233**, 1416-1419 (1986).

- 176 Paradiso, M. A. & Carney, T. Orientation discrimination as a function of stimulus eccentricity and size: nasal/temporal retinal asymmetry. *Vision research* **28**, 867-874 (1988).
- 177 Sparks, D. L., Holland, R. & Guthrie, B. L. Size and distribution of movement fields in the monkey superior colliculus. *Brain research* **113**, 21-34 (1976).
- 178 Abbott, L. F. & Dayan, P. The effect of correlated variability on the accuracy of a population code. *Neural computation* **11**, 91-101 (1999).
- 179 Pouget, A., Dayan, P. & Zemel, R. Information processing with population codes. *Nature reviews. Neuroscience* **1**, 125-132, doi:10.1038/35039062 (2000).
- 180 Sompolinsky, H., Yoon, H., Kang, K. & Shamir, M. Population coding in neuronal systems with correlated noise. *Physical review. E, Statistical, nonlinear, and soft matter physics* **64**, 051904, doi:10.1103/PhysRevE.64.051904 (2001).
- 181 Wilson, M. A. & McNaughton, B. L. Reactivation of hippocampal ensemble memories during sleep. *Science* **265**, 676-679 (1994).
- 182 Hoffman, K. L. & McNaughton, B. L. Coordinated reactivation of distributed memory traces in primate neocortex. *Science* **297**, 2070-2073, doi:10.1126/science.1073538 (2002).
- 183 Jenkins, J. & Dallenback, K. Obliviscence during sleep and waking. *Am. J. Pyschol.*, 605–612 (1924).
- 184 Xie, L., Kang, H., Xu, Q., Chen, M. J., Liao, Y., Thiyagarajan, M., O'Donnell, J., Christensen, D. J., Nicholson, C., Iliff, J. J., Takano, T., Deane, R. & Nedergaard, M. Sleep drives metabolite clearance from the adult brain. *Science* **342**, 373-377, doi:10.1126/science.1241224 (2013).

- 185 Parameshwaran, K., Dhanasekaran, M. & Suppiramaniam, V. Amyloid beta peptides and glutamatergic synaptic dysregulation. *Experimental neurology* **210**, 7-13, doi:10.1016/j.expneurol.2007.10.008 (2008).
- 186 Mattson, M. P. Mechanism of neuronal degeneration and preventative approaches: quickening the pace of AD research. *Neurobiology of aging* **15 Suppl 2**, S121-125 (1994).
- 187 Kanitscheider, I., Coen-Cagli, R. & Pouget, A. Origin of information-limiting noise correlations. *Proc Natl Acad Sci U S A* **112**, E6973-6982, doi:10.1073/pnas.1508738112 (2015).
- 188 Moreno-Bote, R., Beck, J., Kanitscheider, I., Pitkow, X., Latham, P. & Pouget, A. Information-limiting correlations. *Nature Neuroscience* **17**, 1410-1417, doi:10.1038/nn.3807 (2014).
- 189 Rabinowitz, N. C., Goris, R. L., Cohen, M. & Simoncelli, E. Attention stabilizes the shared gain of V4 populations. *eLife* **4**, doi:10.7554/eLife.08998 (2015).
- 190 Cohen, M. R. & Maunsell, J. H. Attention improves performance primarily by reducing interneuronal correlations. *Nature Neuroscience* **12**, 1594-1600, doi:10.1038/nn.2439 (2009).
- 191 Herrero, J. L., Gieselmann, M. A., Sanayei, M. & Thiele, A. Attention-induced variance and noise correlation reduction in macaque V1 is mediated by NMDA receptors. *Neuron* **78**, 729-739, doi:10.1016/j.neuron.2013.03.029 (2013).
- 192 Mitchell, J. F., Sundberg, K. A. & Reynolds, J. H. Spatial attention decorrelates intrinsic activity fluctuations in macaque area V4. *Neuron* **63**, 879-888, doi:10.1016/j.neuron.2009.09.013 (2009).

- 193 Cohen, M. R. & Maunsell, J. H. Attention improves performance primarily by reducing interneuronal correlations. *Nat Neurosci* **12**, 1594-1600, doi:10.1038/nn.2439 (2009).
- 194 Taylor, K., Mandon, S., Freiwald, W. A. & Kreiter, A. K. Coherent oscillatory activity in monkey area v4 predicts successful allocation of attention. *Cerebral cortex* **15**, 1424-1437, doi:10.1093/cercor/bhi023 (2005).
- 195 Womelsdorf, T. & Fries, P. The role of neuronal synchronization in selective attention. *Current opinion in neurobiology* **17**, 154-160, doi:10.1016/j.conb.2007.02.002 (2007).
- 196 McAdams, C. J. & Maunsell, J. H. Effects of attention on the reliability of individual neurons in monkey visual cortex. *Neuron* **23**, 765-773 (1999).
- 197 Moran, J. & Desimone, R. Selective attention gates visual processing in the extrastriate cortex. *Science* **229**, 782-784 (1985).
- 198 Treue, S. & Maunsell, J. H. Attentional modulation of visual motion processing in cortical areas MT and MST. *Nature* **382**, 539-541, doi:10.1038/382539a0 (1996).
- 199 Von Economo, C. Sleep as a problem of localization. *The Journal of Nervous and Mental Disease* **71**, 249-259 (1930).
- 200 Nauta, W. J. Hypothalamic regulation of sleep in rats; an experimental study. *Journal of neurophysiology* **9**, 285-316 (1946).
- 201 Brown, R. E., Basheer, R., McKenna, J. T., Strecker, R. E. & McCarley, R. W. Control of sleep and wakefulness. *Physiological reviews* **92**, 1087-1187, doi:10.1152/physrev.00032.2011 (2012).
- 202 Jones, B. E. Neurobiology of waking and sleeping. *Handbook of clinical neurology* **98**, 131-149, doi:10.1016/B978-0-444-52006-7.00009-5 (2011).

- 203 Saper, C. B., Fuller, P. M., Pedersen, N. P., Lu, J. & Scammell, T. E. Sleep state switching. *Neuron* **68**, 1023-1042, doi:10.1016/j.neuron.2010.11.032 (2010).
- 204 Moruzzi, G. & Magoun, H. W. Brain stem reticular formation and activation of the EEG. *Electroencephalography and clinical neurophysiology* **1**, 455-473 (1949).
- 205 Lin, J. S. Brain structures and mechanisms involved in the control of cortical activation and wakefulness, with emphasis on the posterior hypothalamus and histaminergic neurons. *Sleep medicine reviews* **4**, 471-503, doi:10.1053/smrv.2000.0116 (2000).
- 206 Saper, C. B., Chou, T. C. & Scammell, T. E. The sleep switch: hypothalamic control of sleep and wakefulness. *Trends in neurosciences* **24**, 726-731 (2001).
- 207 Rye, D. B., Saper, C. B., Lee, H. J. & Wainer, B. H. Pedunculo pontine tegmental nucleus of the rat: cytoarchitecture, cytochemistry, and some extrapyramidal connections of the mesopontine tegmentum. *The Journal of comparative neurology* **259**, 483-528, doi:10.1002/cne.902590403 (1987).
- 208 Berendse, H. W. & Groenewegen, H. J. Organization of the thalamostriatal projections in the rat, with special emphasis on the ventral striatum. *The Journal of comparative neurology* **299**, 187-228, doi:10.1002/cne.902990206 (1990).
- 209 Hallanger, A. E. & Wainer, B. H. Ascending projections from the pedunculo pontine tegmental nucleus and the adjacent mesopontine tegmentum in the rat. *The Journal of comparative neurology* **274**, 483-515, doi:10.1002/cne.902740403 (1988).
- 210 Vanni-Mercier, G., Sakai, K. & Jouvet, M. [Specific neurons for wakefulness in the posterior hypothalamus in the cat]. *Comptes rendus de l'Academie des sciences. Serie III, Sciences de la vie* **298**, 195-200 (1984).

- 211 McGinty, D. J. & Harper, R. M. Dorsal raphe neurons: depression of firing during sleep in cats. *Brain research* **101**, 569-575 (1976).
- 212 Aston-Jones, G., Chiang, C. & Alexinsky, T. Discharge of noradrenergic locus coeruleus neurons in behaving rats and monkeys suggests a role in vigilance. *Progress in brain research* **88**, 501-520 (1991).
- 213 Kim, J. H., Jung, A. H., Jeong, D., Choi, I., Kim, K., Shin, S., Kim, S. J. & Lee, S. H. Selectivity of Neuromodulatory Projections from the Basal Forebrain and Locus Ceruleus to Primary Sensory Cortices. *The Journal of neuroscience : the official journal of the Society for Neuroscience* **36**, 5314-5327, doi:10.1523/JNEUROSCI.4333-15.2016 (2016).
- 214 Lehmann, J., Nagy, J. I., Atmadia, S. & Fibiger, H. C. The nucleus basalis magnocellularis: the origin of a cholinergic projection to the neocortex of the rat. *Neuroscience* **5**, 1161-1174 (1980).
- 215 Everitt, B. J. & Robbins, T. W. Central cholinergic systems and cognition. *Annual review of psychology* **48**, 649-684, doi:10.1146/annurev.psych.48.1.649 (1997).
- 216 Hasselmo, M. E. Neuromodulation and cortical function: modeling the physiological basis of behavior. *Behavioural brain research* **67**, 1-27 (1995).
- 217 Pinto, L., Goard, M. J., Estandian, D., Xu, M., Kwan, A. C., Lee, S. H., Harrison, T. C., Feng, G. & Dan, Y. Fast modulation of visual perception by basal forebrain cholinergic neurons. *Nat Neurosci* **16**, 1857-1863, doi:10.1038/nn.3552 (2013).

Copyright © 2016 Charles Bradford Beaman. All rights reserved.

VITA

Charles Bradford Beaman was born in Austin, TX on August 29, 1984, the son of Joseph Beaman and Lisa Beaman. After completing high school at Phillips Academy, Andover, MA, in 2003, he entered The University of Texas in Austin, TX. He became sick with cancer for one year and a half and was treated at MD Anderson Cancer Center. He received the degree of Bachelor of Science in Mechanical Engineering with a minor in Spanish, graduating with special honors in May 2009. In May of 2009, he entered the MD/PhD program at The University of Texas Health Science Center and MD Anderson Cancer Center.

Permanent address:

700 Texas Avenue

Austin, TX 78705